Ph.D. DISSERTATION

Performance Analysis and Optimization for a Multi-hop Network and Cognitive Radio Network

다중 홉 네트워크와 무선 인지 네트워크의 성능 분석 및 최적화 기법

BY

Chulhee Jang

AUGUST 2013

DEPARTMENT OF ELECTRICAL AND
COMPUTER ENGINEERING
COLLEGE OF ENGINEERING
SEOUL NATIONAL UNIVERSITY

Performance Analysis and Optimization for a Multi-hop Network and Cognitive Radio Network

Doctoral Dissertation
Submitted in May of 2013 to the Graduate School
of Seoul National University
in Partial Fulfillment of the Requirements
for the Degree of Doctor of Philosophy

in

Electrical and Computer Engineering

by

Chulhee Jang

Department of Electrical and Computer Engineering
College of Engineering
Seoul National University

Abstract

Relay communication is one of the most promising technologies for the next-generation wireless systems which support enhanced quality of service such as data rate and reliability. Thanks to its advantage, the relay communication has been drawing a lot of interest and adopted in wireless standards such as IEEE 802.16j. However, there are still many challenges to be addressed such as multi-hop protocols and applications to cognitive radio networks.

The dissertation contains two main results. First, we propose a novel decode-and-forward protocol for a multi-hop network. In the proposed protocol, multiple terminals transmit simultaneously to minimize the outage probability. We analyze the outage probability of the proposed protocol in a closed-form. Also, we propose an optimization algorithm that minimizes the outage probability. The optimization algorithm includes the power allocation and the selection of the number of hops and phases. Also, we propose the reduced complexity selection of the selection of the number of hops and phases by using some approximations and mathematical manipulations. We show that the computational complexity is reduced significantly. Numerical results verify the validity of our theoretical analysis by comparison with Monte Carlo simulations results. It is shown that the proposed multi-hop protocol provides lower outage probability than the conventional multi-hop protocol as well as

single-hop protocol, especially in the case of low signal-to-noise ratio (SNR) and that of high path-loss exponent. It is also shown that the reduced complexity selection provides similar outage probability to the exhaustive search in most regions. In addition, we extend the concept of the proposed DF protocol to the AF protocol.

Second, we investigate a spectrum-sharing cognitive radio network. We consider three network scenarios according to the relation of the primary network and secondary network: one that the primary network and secondary network are synchronized, one that the primary network and secondary network are not synchronized with same frame length, and one that the frame lengths of the primary network and secondary network are different. For each scenario, we propose an power allocation and relay selection. Also, we analyze the outage probability. Numerical results verify the validity of our theoretical analysis by comparison with Monte Carlo simulation results. It is shown that the interference to the primary network causes a floor of outage probability curve. It is also shown that the slopes of outage probability curves are similar for all network scenarios. However, the floor levels vary and that of the first network scenario is the lowest. We investigate the effect of various system parameters on the outage probability. As the system parameters, we consider the number of relays, the transmit SNR of the primary users, the interference threshold, the tolerable probability threshold, and the distance between the primary network and secondary network.

Keywords: Relay communication, multi-hop network, cognitive radio network, spectrum-sharing, outage probability, optimization, wireless communications.

Student ID: 2008-30241

Contents

Abstract i

1 Introduction **1**

1.1 Background and Related Works 2

1.1.1 Relay Communication 2

1.1.2 Protocol for the Multi-hop Network 3

1.1.3 Cognitive Radio Network 4

1.2 Outline of Dissertation 6

1.3 Notations 8

2 A Novel DF Protocol for Multi-hop Network **12**

2.1 System Model 14

2.2 Outage Probability 18

2.3 Optimization 21

2.3.1 Optimization Problem 22

2.3.2 Power Allocation 22

2.3.3 Selection of M and K 23

2.3.4 Reduced Complexity Selection of M and K 24

2.3.5 Complexity Comparison 35

2.3.6 Minimization of the total power 36
2.4 Numerical Results 38
2.5 Extension to an AF protocol 66
2.6 Summary 67

3 Spectrum Sharing Cognitive Radio Network 71
3.1 System Model and Network Scenarios 74
3.2 Power Allocation and Relay Selection 80
3.2.1 Scenario 1 80
3.2.2 Scenarios 2 and 3 81
3.3 Outage Probability 83
3.3.1 Scenario 1 83
3.3.2 Scenario 2 84
3.3.3 Scenario 3 88
3.4 Numerical Results 88
3.5 Single-hop Spectrum Sharing Cognitive Radio Network 107
3.6 Summary 117

4 Conclusions 119

A Proof of Theorem 2 122

B Proof of Theorem 3 124

C Proof of Theorem 4 127

D Proof of Theorem 5 129

E Proof of Theorem 6 132

F Proof of Corollary 3 **135**

G Proof of Theorem 8 **137**

Bibliography **139**

Korean Abstract **150**

Acknowledgments **152**

List of Tables

1.1 Lists of abbreviations 9

2.1 Example of computational complexity 37

List of Figures

2.1 System model of the multi-hop network. The solid, dotted, and dashed lines stand for the desired transmission, the removable interfered transmission, and irremovable interfered transmission, respectively. 15

2.2 Transmission protocol of the single-hop, conventional multi-hop, and proposed multi-hop networks. 16

2.3 Flow chart of optimization based on (2.37). 25

2.4 Graph of the function $g_3(K)$. 29

2.5 Graph of the function $g_1(K)$ in the range $K \geq M$. 30

2.6 Flow chart of optimization based on (2.82). 34

2.7 Flow chart of the optimization algorithm that minimizes the total power for given target outage probability. 40

2.8 Optimal number of hops for the conventional multi-hop network according to the path-loss exponent for the target rate R=1b/s/Hz. . . 41

2.9 Optimal number of hops for the conventional multi-hop network according to the path-loss exponent for the target rate R=0.5, 1, and 2 b/s/Hz. 43

2.10 Outage probability of the multi-hop network applying the power allocation for various values of M and K with the target rate R=1, the path-loss exponent $\alpha = 6$, and the distance between the source and the destination $d_{0,K}$=1. 44

2.11 Outage probability of the multi-hop network applying the power allocation for various values of M and K with the target rate R=1, the path-loss exponent $\alpha = 6$, and the distance between the source and the destination $d_{0,K}$=10. 45

2.12 Outage probability for various target rates R and path-loss exponents α with the distance between the source and the destination $d_{0,K}$=10. 58

2.13 Outage probability according to the path-loss exponent for the multi-hop network with the target rate $R = 1$ b/s/Hz and the distance between the source and the destination $d_{0,K}$=10. 62

2.14 Required transmission SNR versus the target outage probability for the multi-hop network with the target rate $R = 1$ b/s/Hz and the distance between the source and the destination $d_{0,K}$=10. 65

2.15 Outage probability for various path-loss exponents α with the target rate R=1 and the distance between the source and the destination $d_{0,K}$=10. 69

3.1 System model of the cognitive radio network where the primary network and the secondary network co-exist. Solid lines and dashed lines represent the desired transmission and the interfered transmission, respectively. 75

3.2 Transmission protocol of the cognitive radio network for three network scenarios according to the relation of the primary and secondary networks. 78
3.3 Transmission protocol of the cognitive radio network for one frame of secondary network. 79
3.4 Outage probability of the secondary network with the interference threshold $\bar{I}/N_0 = 5$dB, the transmit SNR of the PUs P_{PS}/N_0=20dB, the distance between the primary network and secondary network $d = 3$, the tolerable probability threshold $\epsilon = 0.1$, and various numbers of relays. 91
3.5 Outage probability of the secondary network with the number of relays $K = 5$, the transmit SNR of the PUs P_{PS}/N_0=20dB, the distance between the primary network and secondary network $d = 3$, the tolerable probability threshold $\epsilon = 0.1$, and various interference thresholds. . . 95
3.6 Outage probability of the secondary network with the number of relays $K = 5$, the interference threshold $\bar{I}/N_0 = 5$dB, the distance between the primary network and secondary network $d = 3$, the tolerable probability threshold $\epsilon = 0.1$, and various transmit SNRs of the PUs. . . . 98
3.7 Outage probability of the secondary network with the number of relays $K = 5$, the interference threshold $\bar{I}/N_0 = 5$dB, the transmit SNR of the PUs P_{PS}/N_0=20dB, the tolerable probability threshold $\epsilon = 0.1$, and various distances between the primary network and secondary network. 102

3.8 Outage probability of the secondary network with the number of relays $K = 5$, the interference threshold $\bar{I}/N_0 = 5$dB, the transmit SNR of the PUs P_{PS}/N_0=20dB, the distance between the primary network and secondary network $d = 3$, and various tolerable probability thresholds. 104

3.9 Outage probability of the secondary network according to β with the interference threshold $\bar{I}/N_0 = 5$dB, the transmit SNR of the PSs P_{PS}/N_0=20dB, the maximum transmit SNR of the SU $P_S^{\max}/N_0 = 10$dB the tolerable probability threshold $\epsilon = 0.1$, and the distance between the primary network and secondary network $d = 3$. 106

3.10 Outage probability of the secondary network with the number of relays $K = 5$, the interference threshold $\bar{I}/N_0 = 5$dB, the transmit SNR of the PUs P_{PS}/N_0=20dB, the tolerable probability threshold $\epsilon = 0.1$, and the distance between the primary network and secondary network $d = 3$. 108

3.11 Outage probability of the single-hop secondary network with the transmit SNR of the PUs P_{PS}/N_0=20dB, the distance between the primary network and secondary network $d = 3$, the tolerable probability threshold $\epsilon = 0.1$, and various interference thresholds. 111

3.12 Outage probability of the single-hop secondary network with the interference threshold $\bar{I}/N_0 = 5$dB, the distance between the primary network and secondary network $d = 3$, the tolerable probability threshold $\epsilon = 0.1$, and various transmit SNRs of the PUs. 112

3.13 Outage probability of the single-hop secondary network with the interference threshold $\bar{I}/N_0 = 5$dB, the transmit SNR of the PUs P_{PS}/N_0=20dB, the tolerable probability threshold $\epsilon = 0.1$, and various distances between the primary network and secondary network. 113

3.14 Outage probability of the single-hop secondary network with the interference threshold $\bar{I}/N_0 = 5$dB, the transmit SNR of the PUs P_{PS}/N_0=20dB, the distance between the primary network and secondary network $d = 3$, and various tolerable probability thresholds. 114

3.15 Outage probability of the single-hop secondary network according to β with the interference threshold $\bar{I}/N_0 = 5$dB, the transmit SNR of the PSs P_{PS}/N_0=20dB, the maximum transmit SNR of the SU $P_S^{\max}/N_0 =$ 10dB the tolerable probability threshold $\epsilon = 0.1$, and the distance between the primary network and secondary network $d = 3$. 115

Chapter 1

Introduction

As the demands for wireless services are growing rapidly, the next-generation wireless systems are required to support enhanced the quality of service (QoS) such as data rate and reliability. Due to the limitation of wireless channels and the lack of wireless resources, it needs to enhance the QoS with few excessive loads such as the complexity, cost, and power consumption. As one of the attractive approach, the relay communication has been studied widely. In the relay communication, the transmission between the source and destination becomes more reliable with the support of relays with few excessive network loads. Thanks to its advantage, the relay communication has been drawing a lot of interest from both academia and industry. Also, the applications to the wireless systems have been studied widely.

In this chapter, Section 1.1 provides the background of the relay communication. Section 1.2 describes the outline of this dissertation. In Section 1.3, we provide the notations, the list of the abbreviations, and some mathematical definitions and functions used throughout the dissertation.

1.1 Background and Related Works

1.1.1 Relay Communication

The relay communication is regarded as one of the key technologies for next-generation wireless systems [1]-[7]. In the relay communication, several terminals located between the source and destination acts as relays that deliver source data to the destination [8]. As the distance between adjacent terminals shortens the effect of channel impairments such as path-loss is reduced. This enables to support improved QoS such as enhanced capacity and extended coverage [9].

The basic idea of the relay communication was firstly introduced by Van der Meulen in 1971 by analyzing the capacity of the three-node network which consists of the source, destination, and relay [10]. In 1979, Cover and El Gamal analyzed the capacity of more various relay channels such as degraded, reversely degraded, and feedback relay [11].

After these early works, the relay communication was not an attractive subject for a long time because it was regarded as an theoretical approach which is hard to implement [12]. However, it finally have been drawing a lot of interest with review of its significant performance gain and discussion about the possibility and methods of implementation. Sendonaris *et al.* introduced the concepts and practical implementations of two user cooperation in a code-division multiple-access (CDMA) system [13]-[15]. Gastpar and Vetterli investigated the advantage of multiple relays by analyzing the capacity in terms of the number of relays [16]. Laneman and Wornell introduced the space-time coded protocol that provides lower outage probability compared to the repetition based protocol [17]. Laneman *et al.* developed the relaying protocols such as decode-and-forward (DF) and amplify-and-forward (AF) [18].

Also, they developed various relaying strategies such as the fixed relaying, selection relaying, and incremental relaying.

As well as these works, there have been numerous studies on the relay communication. Also, it has been an attractive subject to apply the relay communication to various communication networks, e.g., the vehicular network [19]-[22], the IDMA network [23]-[25], and the cognitive radio (CR) network. Recently, it has been adopted in wireless standards such as IEEE 802.16j [26].

1.1.2 Protocol for the Multi-hop Network

Many works on the relay communication focused on the new protocol to provide the enhanced QoS. In [27], Boyer *et al.* developed the multi-hop protocols that achieve the diversity gain. In [28], Stefanov and Erkip introduced the concept of cooperative space-time coding for the cooperating terminals with multiple antennas. In [29] and [30], Bletsas *et al.* introduced the relay selection based protocols for multiple-relay dual-hop network. In [31] and [32], Hossain *et al.* introduced the multi-hop protocols based on the automatic repeat-request (ARQ). In [33], Gui *et al.* introduced the relay selection based protocol for multiple-relay multi-hop network. In [34], Yi *et al.* developed the multi-hop protocol with the relay ordering.

In most conventional multi-hop protocols, the relays operate in half-duplex mode and all hops use the orthogonal channels by dividing the channel into multiple phases to prevent the inter-relay interference. Mostly, the number of phases is same to the number of hops. The mutual information between adjacent two terminals is inversely proportional to the number of phases [35], [36]. As a result, the mutual information decrease as the number of hops increases.

In another aspect, the signal-to-interference plus noise ratio (SINR) increases as

the number of hops increases. The signal is attenuated due to wireless channels impairments. The signal attenuation is mainly affected by the transmission distance. As the number of hops increases, the transmission distance per hop shortens, and thereby, the signal attenuation becomes relaxed. As a result, the SINR increases and the mutual information increases.

Since there is a tradeoff as discussed above, the number of hops should be selected carefully to improve the performance. Moreover, if it is possible to decrease the number of phases and increase the number of hops at the same time, the performance can be increased dramatically. With this idea, Y. Hu *et al.* developed the successive relaying protocols for a dual-hop multiple-relay network [37]. Also, A. Ikhlef *et al.* developed asymptotic full-duplex relaying protocols for a dual-hop multiple-relay network where the relays have buffers [38]. However, they do not consider the inter-relay interference and only consider the dual-hop network. In [39]-[42], the full-duplex relays are studied. However, since SINR is not fully considered, the increase of performance is not guaranteed compared to the half-duplex relays. Moreover, full-duplex relays are not considered to be impractical [43].

1.1.3 Cognitive Radio Network

As the demands for wireless services are growing rapidly, the demands for spectrum resources are also growing rapidly. In the conventional policy, most of spectrum bands are exclusively allocated and only the primary users (PUs), the users in the primary network (licensed network), are allowed to utilize the spectrum bands. According to some surveys of spectrum utilization, it is found that the spectrum occupancy is very low and it needs to improve the spectrum utilization efficiency [45]-[47]. For example, the spectrum occupancy is 13.1% in New York City and 35% in Washington,

D.C., at the spectrum bands below 3GHz [48]. Also, the spectrum occupancy varies significantly in time, spectrum bands, and locations.

As the residual spectrum resources are deficient and the additional demands for spectrum resources are growing, a new approach called the CR network is introduced [49], [50]. In the CR network, the secondary users (SUs), the users in the secondary network (unlicensed network), are allowed to utilize the unlicensed spectrum according to its surrounding environment [51]. Generally, the performance of the secondary network is worse than the primary network due to its essential utilization property. As an attractive approach to improve the performance of the secondary network, the relay communication is drawing a lot of interest.

There are mainly two approaches in the CR network: spectrum sensing and spectrum sharing. In the spectrum sensing CR network, the SUs are allowed to utilize the unlicensed spectrum if and only if the PUs do not utilize the spectrum bands [52]. The relay communication is applied in the spectrum sensing CR network in two different ways. First way is so-called cooperative spectrum sensing. For the utilization of the unlicensed network, the SUs should observe the signal from the PUs carefully. In the cooperative spectrum sensing, multiple SUs act as the relays by forwarding the observed signal to the fusion center [48]. The performance of cooperative spectrum sensing is investigated in terms of the missed-detection probability and the false alarm probability [53]-[57]. Second way is the dual-hop communication between the source and destination in the secondary network. The performance of the dual-hop communication in the secondary network is investigated in terms of the outage probability [58]-[60].

In the spectrum sharing CR network, the SUs are allowed to utilize the unlicensed spectrum if the QoS of PUs is guaranteed though the PUs utilize the spectrum bands

[61]. The SUs in the spectrum sharing CR network is more probable to utilize the unlicensed spectrum compared to the spectrum sensing CR network. However, the signal from PUs becomes the interference in the SUs and vice versa as both PUs and SUs utilize the same spectrum simultaneously. The relay communication in the spectrum sharing CR network has been studied as follows. In [62], Y. Zou *et al.* analyze the outage probability of the best relay selection for the secondary network interfered by the signal from PUs. However, they did not consider the interference at the PUs by the SUs. In [63] and [64], J. Lee and D. Li *et al.* analyze the outage probability of the best relay selection for the secondary network where the transmission power is limited by the interference to the PUs. However, they did not consider the interference from the PUs. In [65], W. Xu *et al.* analyze the outage probability of the secondary network considering both interference. However, they consider one relay. Also, most of works on the spectrum sharing CR network assumed the perfect synchronization and perfect channel state information (CSI) between the primary network and the secondary network. However, since the primary network the secondary network can not controlled by one central unit simultaneously, this is impractical.

1.2 Outline of Dissertation

In this dissertation, we consider the wireless relay networks.

In Chapter 2, we propose a novel decode-and-forward protocol for a multi-hop network. We analyze the outage probability of the proposed protocol. Also, we propose an optimization algorithm that minimizes the outage probability. The optimization algorithm includes the power allocation and the selection of the number of hops and

phases. Numerical results verify the validity of our theoretical analysis by comparison with Monte Carlo simulations results. It is shown that the proposed multi-hop protocol provides lower outage probability than the conventional multi-hop protocol as well as single-hop protocol, especially in the case of low signal-to-noise ratio (SNR) and that of high path-loss exponent. It is also shown that the reduced complexity selection provides similar outage probability to the exhaustive search in most regions. In addition, we extend the concept of the proposed DF protocol to the AF protocol.

In Chapter 3, we investigate a spectrum-sharing CR network. We suppose multiple relays and the both interference interacted between the primary network and the secondary network. We consider three network scenarios according to the relation of the primary network and secondary network: first, one that the primary network and secondary network are synchronized, second, one that the primary network and secondary network are not synchronized with same frame length, and third, one that the frame lengths of the primary network and secondary network are different. For each scenario, we propose an power allocation and relay selection. Also, we analyze the outage probability. Numerical results verify the validity of our theoretical analysis by comparison with Monte Carlo simulation results. We investigate the effect of various system parameters on the outage probability. As the system parameters, we consider the number of relays, the transmit SNR of the primary users, the interference threshold, the tolerable probability threshold, and the distance between the primary network and secondary network.

Finally, in Chapter 4, the conclusions and future works are drawn.

1.3 Notations

We use the following notations: $Re[x]$ denotes the real part of x. $Im[x]$ denotes the imaginary part of x. $\lfloor x \rfloor$ denotes the largest integer not larger than x. $\lceil x \rceil$ denotes the smallest integer not smaller than x. $(x)^+$ is defined as

$$(x)^+ = \begin{cases} x, & x > 0, \\ 0 & x \leq 0. \end{cases} \tag{1.1}$$

$\mathbb{E}[x]$ denotes the expectation of x. For a set $\mathcal{S}$, $|\mathcal{S}|$ denotes the cardinality of $\mathcal{S}$.

Table 1.1 lists the abbreviations used throughout the dissertation.

Also, we review some mathematical definitions and functions used throughout the dissertation.

Definition 1 (Lambert W Function [66], [67])**.** *The Lambert W function is defined to be the inverse of the function*

$$f(\omega) = \omega e^{\omega}. \tag{1.2}$$

Thus, this function verifies

$$W(z)e^{W(z)} = z. \tag{1.3}$$

The Lambert W function is also called the ***omega function*** *or* ***product logarithm****.*

Definition 2 (Exponential Integral [68], [69])**.** *The exponential integral is defined as*

$$Ei(x) = -\int_{-x}^{\infty} \frac{e^{-t}}{t} dt. \tag{1.4}$$

The alternative notation is also used as

$$E_1(x) = \int_{x}^{\infty} \frac{e^{-t}}{t} dt. \tag{1.5}$$

Table 1.1. Lists of abbreviations

AF	amplify-and-forward
ARQ	automatic repeat-request
AWGN	additive white Gaussian noise
CDF	cumulative distribution function
CDMA	code-division multiple access
CR	cognitive radio
CSI	channel state information
DF	decode-and-forward
PDF	probability density function
PU	primary user
SINR	signal-to-interference plus noise ratio
SNR	signal-to-noise ratio
SU	secondary user
QoS	quality of service

From (1.4) and (1.5), the relation of two notations is given by

$$E_1(x) = -Ei(-x). \tag{1.6}$$

The exponential integral $E_1(z)$ is generalized to

$$E_n(x) = \int_1^\infty \frac{e^{-xt}}{t^n} dt. \tag{1.7}$$

In addition, if $-3\pi/2 \leq \arg x \leq 3\pi/2$ and $|x|$ is large, the exponential integral $E_1(z)$ is approximated as

$$E_1(x) = \frac{e^{-x}}{x} \sum_{m=0}^{\infty} \frac{m!}{(-x)^m}. \tag{1.8}$$

Definition 3 (Gamma Function [68], [70])**.** *The Gamma function is defined as*

$$\Gamma(x) = \int_0^\infty e^{-t} t^{x-1} dt \tag{1.9}$$

for $Re[x] > 0$.

Definition 4 (Beta Function [68], [70])**.** *The Beta function is defined as*

$$B(x, y) = \int_0^1 t^{x-1} (1-t)^{y-1} dt \tag{1.10}$$

for $Re[x] > 0$ and $Re[y] > 0$. The Beta function is expressed in terms of the Gamma function as

$$B(x, y) = \frac{\Gamma(x)\Gamma(y)}{\Gamma(x+y)}. \tag{1.11}$$

If $y > 0$, the Beta function is represented in the closed-form as

$$B(x, y) = \frac{1}{y} \sum_{n=0}^{\infty} (-1)^n \frac{y(y-1)\cdots(y-n)}{n!(x+n)}. \tag{1.12}$$

Definition 5 (Hypergeometric Function [68], [70])**.** *For nonnegative integers p and q, the Hypergeometric Function is defined as*

$${}_pF_q(\alpha_1, \alpha_2, \cdots, \alpha_p; \beta_1, \beta_2, \cdots, \beta_q; z) = \sum_{k=0}^{\infty} \frac{(\alpha_1)_k (\alpha_2)_k \cdots (\alpha_p)_k}{(\beta_1)_k (\beta_2)_k \cdots (\beta_q)_k} \frac{z^k}{k!} \tag{1.13}$$

where $(a)_k$ *is the Pochhammer symbol defined as*

$$(a)_k = a\,(a+1)\cdots(a+k-1) = \frac{\Gamma\,(a+k)}{\Gamma\,(a)}. \tag{1.14}$$

As a special case of the Hypergeometric function, the Gauss Hypergeometric function is given by

$$\begin{aligned} {}_2F_1\,(\alpha_1,\alpha_2;\beta;z) &= \sum_{k=0}^{\infty} \frac{(\alpha_1)_k(\alpha_2)_k}{(\beta)_k}\frac{z^k}{k!} \\ &= \frac{\Gamma\,(\beta)}{\Gamma\,(\alpha_1)\,\Gamma\,(\alpha_2)} \sum_{k=0}^{\infty} \frac{\Gamma\,(\alpha_1+k)\,\Gamma\,(\alpha_2+k)}{\Gamma\,(\beta+k)}\frac{z^k}{k!}. \end{aligned} \tag{1.15}$$

Definition 6 (Incomplete Beta Function [68], [70])**.** *The incomplete Beta function is defined as*

$$B_x\,(p,q) = \int_0^x t^{p-1}(1-t)^{q-1}dt. \tag{1.16}$$

The Incomplete Beta function is expressed in terms of the Hypergeometric function as

$$B_x\,(p,q) = \frac{x^p}{p}{}_2F_1\,(p,1-q;p+1;x)\,. \tag{1.17}$$

Chapter 2

A Novel DF Protocol for Multi-hop Network

In the multi-hop network, the mutual information between adjacent two terminals is generally given by

$$I = \frac{1}{M} \min_k \log_2(1 + SINR_k) \tag{2.1}$$

where M is the number of phases, K is the number of hops, and $SINR_k$ is the SINR of k-th hop. There are two aspects of the effect of the number of hops on the performance of the multi-hop network.

First, the pre-log factor decreases as the number of hops increases. In most conventional multi-hop protocols, the relays operate in half-duplex mode and all hops use the orthogonal channels by dividing the channel into multiple phases to prevent the inter-relay interference. Mostly, the number of phases is same to the number of hops. The mutual information between adjacent two terminals is inversely proportional to the number of phases [35], [36]. As a result, the mutual information decrease as the number of hops increases.

Second, the SINR increases as the number of hops increases. The signal is attenuated due to wireless channels impairments. The signal attenuation is mainly affected by the transmission distance. As the number of hops increases, the transmission distance per hop shortens, and thereby, the signal attenuation becomes relaxed. As a result, the SINR increases and the mutual information increases.

Since there is a tradeoff between the SINR and the pre-log factor, the number of hops should be selected carefully to improve the performance. Moreover, if it is possible to decrease the number of phases and increase the number of hops at the same time, the performance can be increased dramatically. With this idea, Y. Hu *et al.* developed the successive relaying protocols for a dual-hop multiple-relay network [37]. Also, A. Ikhlef *et al.* developed asymptotic full-duplex relaying protocols for a dual-hop multiple-relay network where the relays have buffers [38]. However, they do not consider the inter-relay interference and only consider the dual-hop network. In [39]-[42], the full-duplex relays are studied. However, since SINR is not fully considered, the increase of performance is not guaranteed compared to the half-duplex relays. Moreover, full-duplex relays are not considered to be impractical [43].

In this chapter, we propose a novel class of the multi-hop protocol. We consider a DF relaying scheme and the half-duplex relays which are the practical considerations. In the proposed protocol, the number of phases can be different to the number of hops and several terminals can transmit data simultaneously. If several terminals transmit data simultaneously, i.e., fewer phases are used, the pre-log factor increases but SINR decreases due to the interferences from other terminals. By considering this tradeoff, the proposed protocol selects the number of hops and the number of phases carefully.

The remainder of this chapter is organized as follows. Section 2.1 introduces the system model and the novel class of DF-based protocol for the multi-hop network. In

Section 2.2, we derive the closed-form expression of the outage probability. In Section 2.3, we propose an algorithm to optimize the proposed protocol. The optimization of the proposed protocols includes the power allocation and the selection of the number of hops and phases. Also, we propose the reduced complexity selection of the number of hops and phases by using some approximations and mathematical manipulations. Complexity comparison of the proposed selection algorithms is shown. In Section 2.3, numerical results verify the validity of the performance analysis by comparison with Monte Carlo simulation results. Also, we compare the performance of the proposed multi-hop protocol with the conventional multi-hop protocol and single-hop protocol. In Section 2.5, we extend the concept of the proposed DF protocol to the AF protocol. Finally, this Chapter is summarized in Section 2.6.

2.1 System Model

Consider the DF-based multi-hop network where a single source T_0 communicating with a single destination T_K through K-hop transmission with the help of $K-1$ relays $T_k, k = 1, 2, \cdots, K-1$, as shown in Figure 2.1. Assume that there are a lot of potential relays. Therefore, we can always find the relays that the distance per hop is same and the relays are on a line between the source and the destination. Then, the distance between T_i and T_j is given by

$$d_{i,j} = \frac{|j-i| \cdot d_{0,K}}{K} \tag{2.2}$$

for arbitrary K. Also, assume each terminal has a single antenna and cannot transmit and receive simultaneously, i.e., half duplex.

Assume that the channel between the terminal i and the terminal j has the channel coefficient $h_{i,j}$ which is a zero-mean circularly symmetric complex Gaussian random

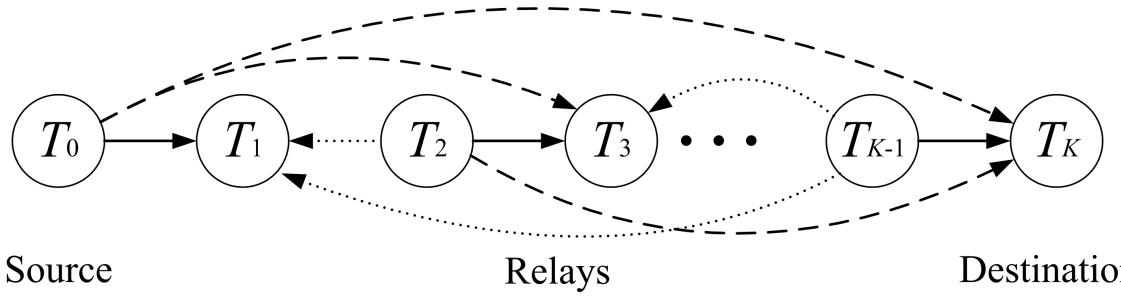

Figure 2.1. System model of the multi-hop network. The solid, dotted, and dashed lines stand for the desired transmission, the removable interfered transmission, and irremovable interfered transmission, respectively.

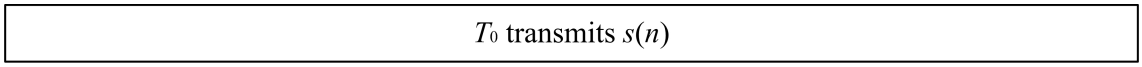

(a) Single-hop network

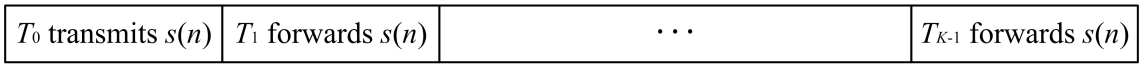

(b) Conventional multi-hop network

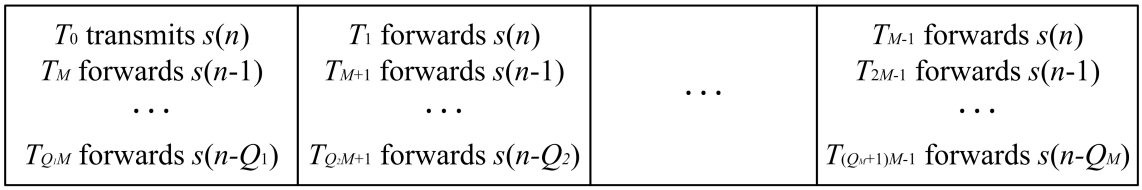

(c) Proposed multi-hop network

Figure 2.2. Transmission protocol of the single-hop, conventional multi-hop, and proposed multi-hop networks.

variable with the variance $\lambda_{i,j}$. The channel variance is given by

$$\lambda_{i,j} = (d_{i,j})^{-\alpha} \tag{2.3}$$

where α is the path-loss exponent.

Figure 2.2 illustrates the protocols of the single-hop, conventional multi-hop, and proposed multi-hop networks. Different to the conventional multi-hop protocol, in our model, one time slot is divided into M phases in the time-domain where M is not larger than K. The time slot is divided in the time-domain and all terminals use same spectrum bands. Assume all terminals are synchronized by adopting some synchronization techniques such as [71], [72]. Aslo, assume each terminal knows the channel coefficients from and to all other terminals by transmitting pilot signals at the beginning of each time slot using orthogonal channels. As the the transmission of pilot signal requires very small amount of time, the time fraction of pilot signal is ignorable.

In the m-th phase, the terminals T_k with $k = qM + m - 1, q = 0, 1, \cdots, Q_m$ transmit the information signal and/or forward the signal received in the previous phase simultaneously where $Q_m = \left\lfloor \frac{K-m}{M} \right\rfloor$. In the m-th phase of the n-th frame, the received signal at T_k with $k = qM + m, q = 0, 1, \cdots, Q_m$ is given by

$$y_k = h_{k-1,k} s_{k-1} \left(n - \frac{k-m}{M} \right) + \sum_{\substack{i=0 \\ i \neq \frac{k-m}{M}}}^{Q_m} h_{k_i,k} s_{k_i} (n-i) + \omega_k \tag{2.4}$$

where $s_{k-1}(n-i)$ is the source data at the $(n-i)$-th frame forwarded from T_{k-1}, T_{k_i} is i-th terminal transmitting with T_{k-1} simultaneously, i.e., $k_i = iM + m - 1$, and ω_k is an additive white Gaussian noise (AWGN) at T_k with zero-mean and variance N_0. For convenience, suppose $N_0 = 1$

In Figure 2.1, solid lines represent desired transmissions and dotted and dashed lines represent interfered transmissions. Since the interfering signals represented with

the dotted lines are already known at the terminals, they are removable. Assume there is no interference except the interference from other relays. After the interference cancelation, the received signal is given by

$$y_k = h_{k-1,k} s_{k-1} \left(n - \frac{k-m}{M} \right) + \sum_{i=0}^{\frac{k-m-M}{M}} h_{k_i,k} s_{k_i} (n-i) + \omega_k. \tag{2.5}$$

2.2 Outage Probability

Consider k larger than M. From (2.5), the received SINR at T_k is given by

$$\gamma_{k-1,k} = \frac{P_{k-1}|h_{k-1,k}|^2}{\sum_{i=0}^{\lfloor \frac{k-M-1}{M} \rfloor} P_{k_i}|h_{k_i,k}|^2 + 1} \tag{2.6}$$

where P_i is the transmission power of T_i.

Denote the received power of the signal from T_i at T_j as $X_{i,j}$. Then, $X_{i,j}$ is given by

$$X_{i,i} = P_i |h_{i,j}|^2. \tag{2.7}$$

Since $|h_{i,j}|^2$ is exponentially distributed, the cumulative distribution function (CDF) of $X_{i,i}$ is given by [73]

$$F_{X_{i,j}}(x) = 1 - \exp\left(-\frac{x}{P_i \lambda_{i,j}} \right). \tag{2.8}$$

Also, denote the power of the interference at T_k as Z_k. Then, Z_k is given by

$$Z_k = \sum_{i=0}^{\lfloor \frac{k-M-1}{M} \rfloor} P_{k_i}|h_{k_i,k}|^2. \tag{2.9}$$

Theorem 1 (Distribution of sum of exponential random variables [30])**.** *Let $Y_i, i = 1, \cdots, N$, be N statistically independent and not necessarily identically distributed*

exponential random variables with mean λ_i. *Then, the probability density function (PDF) of a sum* $Z = \sum_{i=1}^{N} Y_i$ *is given by*

$$f_Z(z) = \sum_{i=1}^{\rho(\mathcal{A})} \sum_{j=1}^{\tau_i(\mathcal{A})} \chi_{i,j}(\mathcal{A}) \frac{\lambda_{<i>}^{-j}}{(j-1)!} z^{j-1} e^{-z/\lambda_{<i>}} \tag{2.10}$$

where $\mathcal{A} = \operatorname{diag}(\lambda_1, \lambda_2, \cdots, \lambda_N)$, $\rho(\mathcal{A})$ *is the number of distinct diagonal elements of* $\mathcal{A}$, $\lambda_{<i>}, i = 1, 2, \cdots, \rho(\mathcal{A})$ *are the distinct diagonal elements in decreasing order, i.e.,* $\lambda_{<1>} > \lambda_{<2>} > \cdots > \lambda_{<N>}$, *and* $\chi_{i,j}(\mathcal{A})$ *is the* (i,j)*-th characteristic coefficient of* $\mathcal{A}$ *[74]. The CDF of* Z *is given by*

$$F_Z(z) = \sum_{i=1}^{\rho(\mathcal{A})} \sum_{j=1}^{\tau_i(\mathcal{A})} \sum_{k=0}^{j-1} \frac{\chi_{i,j}(\mathcal{A})}{k!} \left(\frac{z}{\lambda_{<i>}}\right)^k e^{-z/\lambda_{<i>}}. \tag{2.11}$$

Proof. See [30]. □

Corollary 1. *If all of* λ_i *are distinct in* Theorem *1, the PDF and the CDF are given by*

$$f_Z(z) = \sum_{i=1}^{N} \left\{ \prod_{\substack{j=1 \\ j \neq i}}^{N} \left(1 - \frac{\lambda_j}{\lambda_i}\right)^{-1} \right\} \frac{e^{-z/\lambda_i}}{\lambda_i}, \tag{2.12}$$

$$F_Z(z) = 1 - \sum_{i=1}^{N} \left\{ \prod_{\substack{j=1 \\ j \neq i}}^{N} \left(1 - \frac{\lambda_j}{\lambda_i}\right)^{-1} \right\} e^{-z/\lambda_i}. \tag{2.13}$$

Corollary 2. *If* $\lambda_i = \lambda$ *for all* i *in* Theorem *1, the PDF and the CDF are given by*

$$f_Z(z) = \frac{\lambda^{-N}}{(N-1)!} z^{N-1} e^{-z/\lambda}, \tag{2.14}$$

$$F_Z(z) = 1 - \sum_{k=0}^{N-1} \frac{1}{k!} \left(\frac{x}{\lambda}\right)^k e^{-z/\lambda}. \tag{2.15}$$

Using *Corollary* 1, the PDF of Z_k is given by

$$f_{Z_k}(x) = \sum_{i=0}^{\left\lfloor \frac{k-M-1}{M} \right\rfloor} \prod_{\substack{j=0 \\ j\neq i}}^{\left\lfloor \frac{k-M-1}{M} \right\rfloor} \left(1 - \frac{P_{k_j}\lambda_{k_j,k}}{P_{k_i}\lambda_{k_i,k}}\right)^{-1} \frac{1}{P_{k_i}\lambda_{k_i,k}} \exp\left(-\frac{x}{P_{k_i}\lambda_{k_i,k}}\right). \quad (2.16)$$

Then, the CDF of $\gamma_{k-1,k}$ is given by [75],

$$\begin{aligned} F_{\gamma_{k-1,k}}(\gamma) &= \Pr\left[\frac{X_{k-1,k}}{1+Z_k} < \gamma\right] \\ &= \int_0^\infty F_{X_{k-1,k}}(\gamma(1+x)) f_{Z_k}(x) dx \\ &= 1 - \sum_{i=0}^{\left\lfloor \frac{k-M-1}{M} \right\rfloor} \prod_{\substack{j=0 \\ j\neq i}}^{\left\lfloor \frac{k-M-1}{M} \right\rfloor} \left(1 - \frac{P_{k_j}\lambda_{k_j,k}}{P_{k_i}\lambda_{k_i,k}}\right)^{-1} \frac{1}{P_{k_i}\lambda_{k_i,k}} \\ &\quad \times \int_0^\infty \exp\left(-\frac{x}{P_{k_i}\lambda_{k_i,k}} - \frac{\gamma(1+x)}{P_{k-1}\lambda_{k-1,k}}\right) dx \\ &= 1 - \exp\left(-\frac{\gamma}{P_{k-1}\lambda_{k-1,k}}\right) \\ &\quad \times \sum_{i=0}^{\left\lfloor \frac{k-M-1}{M} \right\rfloor} \prod_{\substack{j=0 \\ j\neq i}}^{\left\lfloor \frac{k-M-1}{M} \right\rfloor} \left(1 - \frac{P_{k_j}\lambda_{k_j,k}}{P_{k_i}\lambda_{k_i,k}}\right)^{-1} \left(1 + \frac{P_{k_i}\lambda_{k_i,k}}{P_{k-1}\lambda_{k-1,k}}\gamma\right)^{-1}. \end{aligned} \quad (2.17)$$

For k not larger than M, the CDF of $\gamma_{k-1,k}$ is given by

$$F_{\gamma_{k-1,k}}(\gamma) = 1 - \exp\left(-\frac{\gamma}{P_{k-1}\lambda_{k-1,k}}\right). \quad (2.18)$$

In the proposed protocol, $N + \left\lfloor \frac{K-1}{M} \right\rfloor$ time slots are necessary to transmit N frames. Then, the pre-log factor is given by $1/\tilde{M}$ rather than $1/K$ where $\tilde{M} = M + \frac{M}{N}\left\lfloor \frac{K-1}{M} \right\rfloor$. The mutual information between T_{k-1} and T_k is given by

$$I_{T_{k-1},T_k} = \frac{1}{\tilde{M}} \log_2(1 + \gamma_{k-1,k}). \quad (2.19)$$

Also, the mutual information between the source and the destination is given by

$$I = \min\left\{I_{T_0,T_1}, I_{T_1,T_2}, \cdots, I_{T_{K-1},T_K}\right\}. \quad (2.20)$$

The outage event occurs when the mutual information is less than the certain target rate R. The outage probability is given by

$$\begin{aligned}
P_{out}(R) &= \Pr\left[I < R\right] \\
&= \Pr\left[\min\left\{I_{T_0,T_1}, I_{T_1,T_2}, \cdots, I_{T_{K-1},T_K}\right\} < R\right] \\
&= 1 - \prod_{k=1}^{K} \Pr\left[I_{T_{k-1},T_k} \geq R\right] \\
&= 1 - \prod_{k=1}^{K} \left\{1 - F_{\gamma_{k-1,k}}\left(2^{\tilde{M}R} - 1\right)\right\} \\
&= 1 - \prod_{k=1}^{K} \exp\left(-\frac{2^{\tilde{M}R} - 1}{P_{k-1}\lambda_{k-1,k}}\right) \\
&\quad \times \prod_{k=M+1}^{K} \sum_{i=0}^{\lfloor \frac{k-M-1}{M} \rfloor} \prod_{\substack{j=0 \\ j \neq i}}^{\lfloor \frac{k-M-1}{M} \rfloor} \left(1 - \frac{P_{k_j}\lambda_{k_j,k}}{P_{k_i}\lambda_{k_i,k}}\right)^{-1} \\
&\quad \times \left\{1 + \frac{P_{k_i}\lambda_{k_i,k}}{P_{k-1}\lambda_{k-1,k}}\left(2^{\tilde{M}R} - 1\right)\right\}^{-1}. \qquad (2.21)
\end{aligned}$$

2.3 Optimization

As shown in (2.21), the transmission power P_k, the number of phases M, the number of hops K have a decisive effect on the outage probability. Assume only the statistical CSI is available. In this section, we propose the optimization algorithms related to the above parameters with the statistical CSI. Throughout the section, suppose K is larger than 3.

2.3.1 Optimization Problem

Denote the power of T_i for given M and K as $P_i^{(M,K)}$ instead of P_i. Let P_{tot} bet the total available power of the network. Then, the optimization problem to minimize the outage probability is formulated as

$$\left\{M^*, K^*, P_k^{(M^*,K^*)^*}\right\} = \arg\max_{\left\{M,K,P_k^{(M,K)}\right\}} \min P_{out}(R) \tag{2.22}$$

$$\text{subject to}: \sum_{k=0}^{K-1} P_k^{(M,K)} \leq P_{tot} \tag{2.23}$$

$$P_k^{(M,K)} \geq 0, \forall k \tag{2.24}$$

$$K_{\min} \leq K \leq K_{\max} \tag{2.25}$$

$$M_{\min} \leq M \leq K. \tag{2.26}$$

This problem is decoupled into two separate problems: first, the power allocation and second, the selection of M and K.

2.3.2 Power Allocation

When M and K are given, the power allocation problem is formulated as

$$\left\{P_k^{(M,K)^*}\right\} = \arg\min_{\left\{P_k^{(M,K)}\right\}} P_{out}(R) \tag{2.27}$$

$$\text{subject to}: \sum_{k=0}^{K-1} P_k^{(M,K)} \leq P_{tot} \tag{2.28}$$

$$P_k^{(M,K)} \geq 0, \forall k. \tag{2.29}$$

The power allocation problem (2.27) is identical to

$$\left\{P_k^{(M,K)^*}\right\} = \arg\min_{\left\{P_k^{(M,K)}\right\}} \left\{I_{T_0,T_1}, \cdots, I_{T_{K-1},T_K}\right\}. \tag{2.30}$$

This problem has a solution when $I_{T_0,T_1} = I_{T_1,T_2} = \cdots = I_{T_{K-1},T_K}$ [76]. From $I_{T_0,T_1} = I_{T_1,T_2}$ and $I_{T_0,T_1} = I_{T_2,T_3}$, the power of T_1 and T_2 are given by

$$P_1^{(M,K)} = \frac{P_0^{(M,K)}\lambda_{0,1}}{\lambda_{1,2}}, \tag{2.31}$$

$$P_2^{(M,K)} = \begin{cases} \frac{P_0^{(M,K)}\lambda_{0,1}}{\lambda_{2,3}}, & M > 2, \\ \frac{P_0^{(M,K)}\lambda_{0,1}\left(P_0^{(M,K)}\lambda_{0,3}+1\right)}{\lambda_{2,3}}, & M = 2. \end{cases} \tag{2.32}$$

Similarly, by solving $I_{T_0,T_1} = I_{T_k,T_{k+1}}$ sequentially, $P_k^{(M,K)}, k = 3, \cdots, K-1$, can be represented as a function of $P_0^{(M,K)}$. Let $P_k^{(M,K)} = f_k\left(P_0^{(M,K)}\right)$. Since (2.27) is maximized when the equality of (2.28) holds, P_0 is determined as a solution of the following:

$$\sum_{k=0}^{K-1} f_k\left(P_0^{(M,K)}\right) = P_{tot}. \tag{2.33}$$

Note that this is a $\left\lfloor \frac{K-1}{M} + 1 \right\rfloor$-th order polynomial equation. If $\left\lfloor \frac{K-1}{M} + 1 \right\rfloor > 4$, it is intractable to find the closed-form expressions of the solution. Thus, it is solved using a numerical method [77].

2.3.3 Selection of M and K

The problem of selecting M and K is formulated as

$$(M^*, K^*) = \arg\min_{(M,K)} P_{out}(R) \tag{2.34}$$

$$\text{subject to :} \quad K_{\min} \leq K \leq K_{\max} \tag{2.35}$$

$$M_{\min} \leq M \leq K. \tag{2.36}$$

Since $P_0^{(M,K)}$ is not given in the closed-form, (2.34) is intractable to solve algebraically. The optimal values of M and K are found by an exhaustive search as

$$(M^*, K^*) = \arg\min_{(M,K)\in\Omega_1} P_{out}(R) \tag{2.37}$$

where

$$\Omega_1 = \{(M, K) : M_{\min} \leq M \leq K, K_{\min} \leq K \leq K_{\max}\}. \tag{2.38}$$

Since the variables should be positive integers, the complexity of the exhaustive search is not high.

The flow chart of optimization based on (2.37) is shown in Figure 2.3.

2.3.4 Reduced Complexity Selection of M and K

To reduce the complexity of (2.37), we solve the problem in (2.34) by categorizing according to the range of K as follows.

1) $M = K$

Note that this is the optimization of the conventional multi-hop network. In this case, we have $\tilde{M} = K$ and the outage probability in (2.21) is simplified to

$$P_{out}(R) = 1 - \prod_{k=1}^{K} \exp\left(-\frac{2^{KR} - 1}{P_{k-1}\lambda_{k-1,k}}\right). \tag{2.39}$$

Also, the optimization problem in (2.34) is given by

$$K^*_{\text{conv}} = \arg\min_{K} P_{out}(R). \tag{2.40}$$

The solution of the power allocation is given by

$$P_k = \frac{P_{tot}}{K}, \forall k. \tag{2.41}$$

Using (2.3), (2.4), and (2.41), after some manipulations, (2.40) is simplified to

$$K^*_{\text{conv}} = \arg\min_{K} \frac{2^{KR} - 1}{K^{\alpha-2}}. \tag{2.42}$$

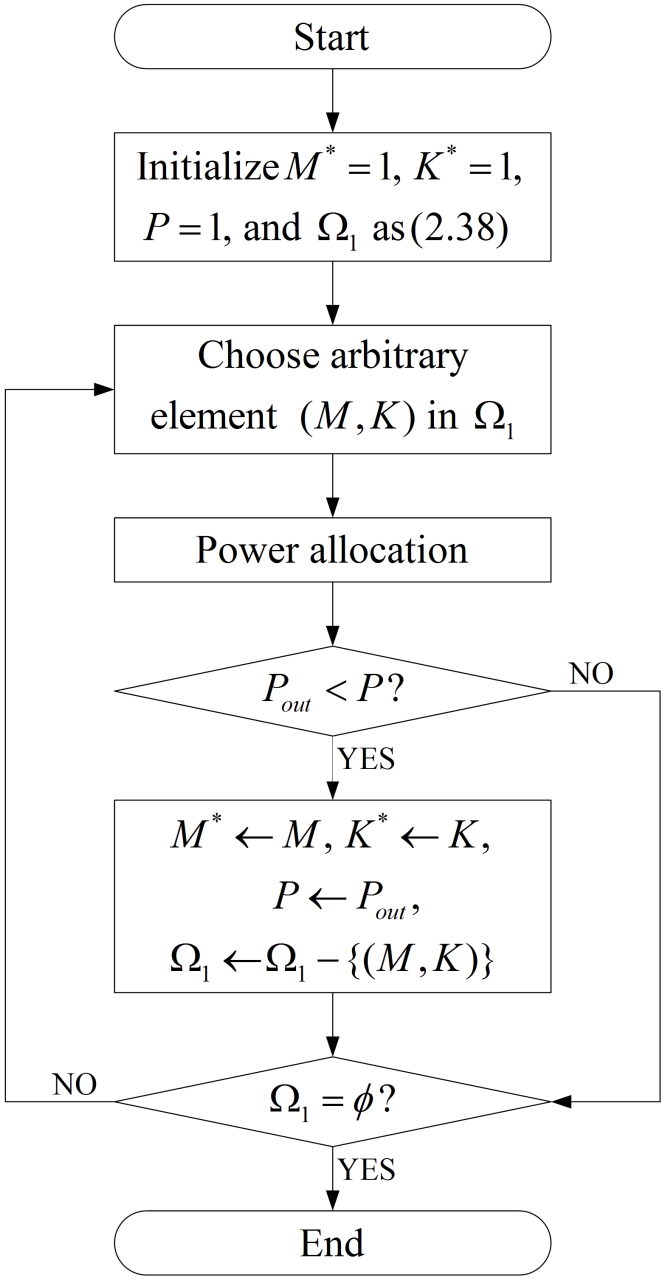

Figure 2.3. Flow chart of optimization based on (2.37).

By setting

$$\frac{d}{dK}\frac{2^{KR}-1}{K^{\alpha-2}}=0 \tag{2.43}$$

and solving for K, we obtain

$$K_{\mathrm{conv,opt}}=\frac{\alpha-2+W\left[(2-\alpha)\exp\left(2-\alpha\right)\right]}{R\ln 2}. \tag{2.44}$$

Since K should be the positive integer, K^*_{conv} is determined as

$$K^*_{\mathrm{conv}}=\begin{cases}\arg\min\limits_{K\in\{\lfloor K_{\mathrm{conv,opt}}\rfloor,\atop \lceil K_{\mathrm{conv,opt}}\rceil\}} \frac{2^{KR}-1}{K^{\alpha-2}}, & K_{\mathrm{conv,opt}}>1,\\ 1, & K_{\mathrm{conv,opt}}\leq 1.\end{cases} \tag{2.45}$$

Note that K^*_{conv} is related not to the distance between the source and the destination but to the target rate and the path-loss exponent.

2) $M<K\leq 2M$

The optimization problem (2.34) is approximated as

$$\begin{aligned}(M^*,K^*)&\approx\arg\min_{(M,K)}1-\Pr\left[I_{T_0,T_1}\geq R\right]^K\\&=\arg\min_{(M,K)}\frac{2^{MR}-1}{P_0^{(M,K)}K^{\alpha-1}}.\end{aligned} \tag{2.46}$$

This approximation comes from the property that I_{T_k,T_k+1} becomes same for all k after the power allocation.

The solution of (2.33) is given by

$$P_0^{(M,K)}=\frac{-K+\sqrt{K^2+4(K-M)\lambda_{0,M+1}P_{tot}}}{2(K-M)\lambda_{0,M+1}}. \tag{2.47}$$

Then, substituting (2.47) into (2.46), it becomes

$$(M^*,K^*)=\arg\min_{(M,K)}\frac{(2^{MR}-1)(K-M)(M+1)^{-\alpha}}{-1+\sqrt{1+\frac{4K^{\alpha-2}(K-M)}{\left((M+1)d_{0,K}\right)^{\alpha}}P_{tot}}}. \tag{2.48}$$

Solve the above problem with respect to K for given M. For given M, (2.48) is simplified to

$$K^* = \arg\min_K g_1(K) \tag{2.49}$$

where

$$g_1(K) \triangleq \frac{K-M}{-1+\sqrt{1+\frac{4K^{\alpha-2}(K-M)}{\left((M+1)d_{0,K}\right)^{\alpha}}P_{tot}}}. \tag{2.50}$$

Taking the derivative of $g_1(K)$ with respect to K, we obtain

$$\begin{aligned}\frac{\partial g_1(K)}{\partial K} = &-\frac{(K-M)\,2K^{\alpha-3}\left((\alpha-1)\,K-(\alpha-2)\,M\right)\left((M+1)\,d_{0,K}\right)^{-\alpha}P_{tot}}{\sqrt{g_2(K)}\left(-1+\sqrt{g_2(K)}\right)^2} \\ &+\frac{1}{-1+\sqrt{g_2(K)}}\end{aligned} \tag{2.51}$$

where

$$g_2(K) \triangleq 1+4K^{\alpha-2}(K-M)((M+1)d)^{-\alpha}P_{tot}. \tag{2.52}$$

Then, the condition that $g_1(K)$ decreases is given by

$$\begin{aligned}\frac{\partial g_1(K)}{\partial K} < 0 \Leftrightarrow g_3(K) &< \frac{\alpha-2}{4}\left\{\frac{\left((M+1)\,d_{0,K}\right)^{\alpha}}{P_{tot}}\right\}^2 \\ &\text{or } \ (3-\alpha)\,K+(\alpha-2)\,M<0\end{aligned} \tag{2.53}$$

where

$$g_3(K) \triangleq \ K^{\alpha-3}((3-\alpha)\,K+(\alpha-2)\,M)^2. \tag{2.54}$$

Taking the derivative of $g_3(K)$ with respect to K, the condition that $g_3(K)$ decreases is given by

$$\begin{aligned}\frac{\partial g_3(K)}{\partial K} < 0 &\Leftrightarrow \{(3-\alpha)\,K+(\alpha-2)\,M\}\,\{(1-\alpha)\,K+(\alpha-2)\,M\}<0 \\ &\Leftrightarrow \frac{\alpha-2}{\alpha-1}M<K<\frac{\alpha-2}{\alpha-3}M.\end{aligned} \tag{2.55}$$

Therefore, the function $g_3(K)$ is plotted as shown in Figure 2.4. The case 1, case 2, and case 3 stand for the cases that satisfy

$$g_3\left(\frac{\alpha-2}{\alpha-3}\right) \geq \frac{\alpha-2}{4}\left\{\frac{\left((M+1)\,d_{0,K}\right)^{\alpha}}{P_{tot}}\right\}^2, \tag{2.56}$$

$$g_3\left(\frac{\alpha-2}{\alpha-3}\right) < \frac{\alpha-2}{4}\left\{\frac{\left((M+1)\,d_{0,K}\right)^{\alpha}}{P_{tot}}\right\}^2 < g_3\left(\frac{\alpha-2}{\alpha-1}\right), \tag{2.57}$$

$$g_3\left(\frac{\alpha-2}{\alpha-1}\right) \leq \frac{\alpha-2}{4}\left\{\frac{\left((M+1)\,d_{0,K}\right)^{\alpha}}{P_{tot}}\right\}^2, \tag{2.58}$$

respectively. For each case, the first condition in right-hand side of (2.53) has one of the following forms

$$K < c_1, \tag{2.59}$$

$$K < c_1 \text{ or } c_2 < K < c_3, \tag{2.60}$$

$$K < c_3 \tag{2.61}$$

where c_1, c_2, and c_3 are constants that satisfy

$$c_1 \leq \frac{\alpha-2}{\alpha-1}M \leq c_2 \leq \frac{\alpha-2}{\alpha-3}M \leq c_3. \tag{2.62}$$

Since $\frac{\alpha-2}{\alpha-1}M < M$, the function $g_1(K)$ is plotted in the range $K \geq M$ as shown in Figure 2.5. The ranges shown with vertical and perpendicular lines are the range that $g_1(K)$ decreases. The ranges shown with vertical lines comes from (2.59)-(2.61). The ranges shown with perpendicular lines comes from the second condition in right-hand side of (2.53). Since $M < K \leq 2M$ and K is a positive integer, $g_1(K)$ has a minimum value when $K = M+1$ or $K = 2M$.

Consider the case $K = M+1$. Then, (2.48) is rewritten as

$$M^* = \arg\min_{M} h_1(K) \tag{2.63}$$

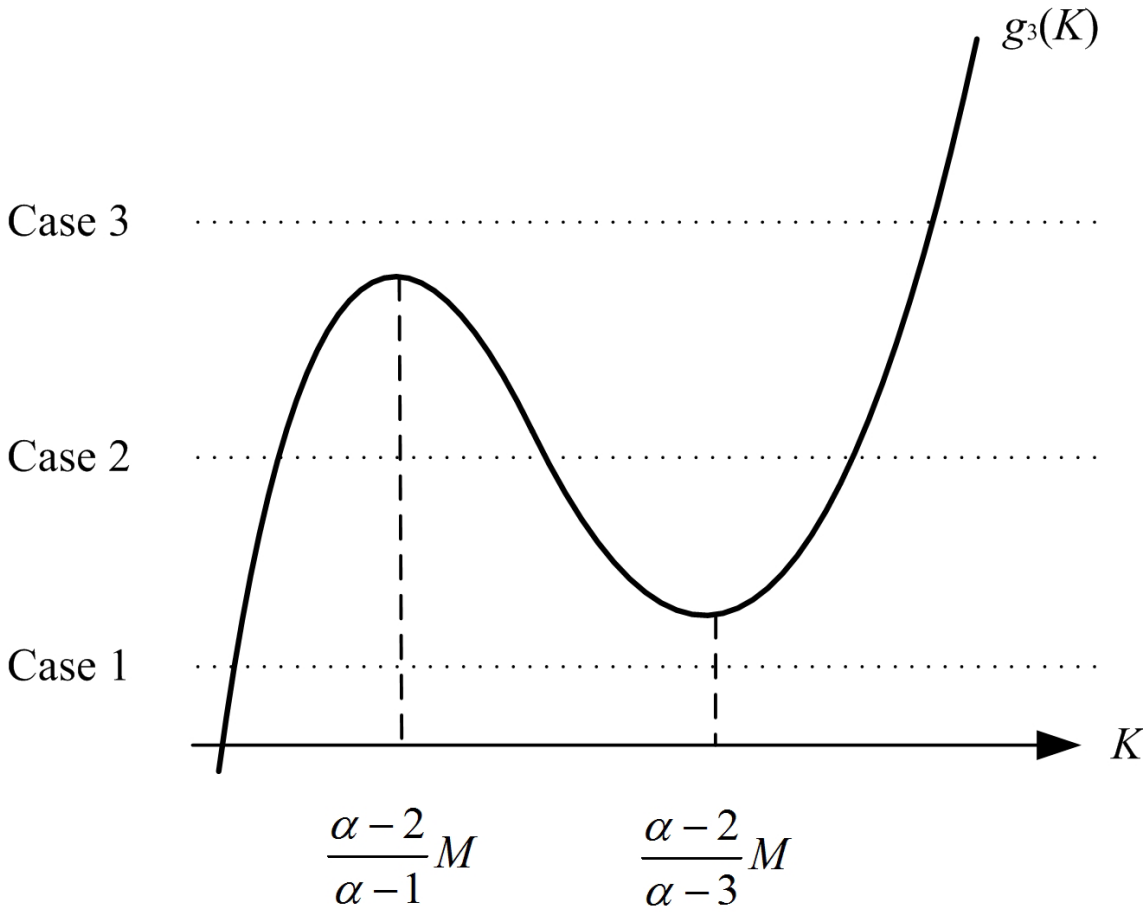

Figure 2.4. Graph of the function $g_3(K)$.

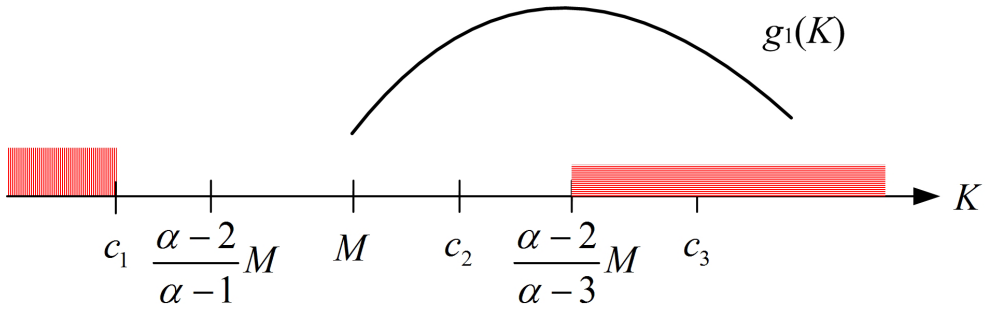

(a) Case 1

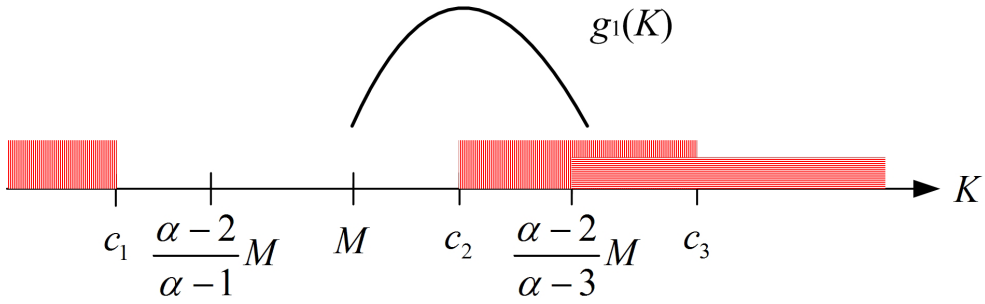

(b) Case 2

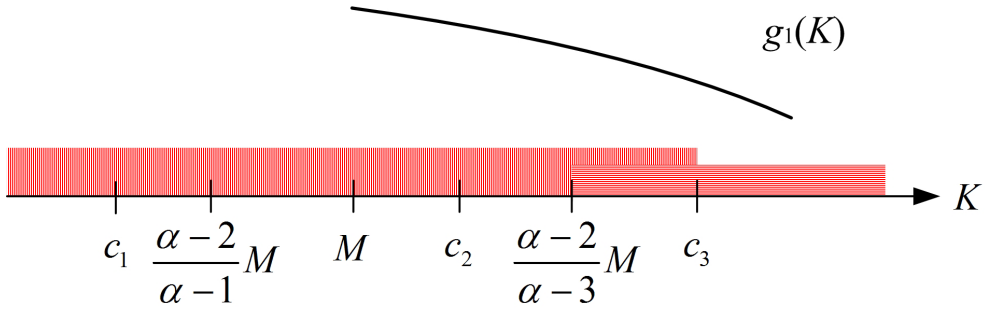

(c) Case 3

Figure 2.5. Graph of the function $g_1(K)$ in the range $K \geq M$.

where

$$h_1(M) = \frac{(2^{MR}-1)(M+1)^{-\alpha}}{-1+\sqrt{1+\frac{4}{(M+1)^2 d_{0,K}^{\alpha}} P_{tot}}}. \tag{2.64}$$

Taking the derivative of $h_1(K)$, we obtain

$$\operatorname{sgn}\left(\frac{dh_1(M)}{dM}\right) = \operatorname{sgn}\left(h_2(M)\right) \tag{2.65}$$

where $\operatorname{sgn}(x)$ is the sign of x and

$$\begin{aligned} h_2(M) = &\left\{2^{MR}(M+1)R\ln 2 - \alpha\left(2^{MR}-1\right)\right\} \times \left\{h_3(M) - \sqrt{h_3(M)}\right\} \\ &+ \left(2^{MR}-1\right)\left(h_3(M)-1\right) \end{aligned} \tag{2.66}$$

in which

$$h_3(M) = 1 + 4(M+1)^{-2} d_{0,K}^{-\alpha} P_{tot}. \tag{2.67}$$

Define

$$c_4 = 1 + \left(1 + \frac{4P_{tot}}{9d_{0,K}^{\alpha}}\right)^{-\frac{1}{2}}, \tag{2.68}$$

$$\begin{aligned} h_l(M) = &\left\{2^{MR}(M+1)R\ln 2 + \left(2^{MR}-1\right)(1-\alpha)\right\} \\ &\times \left\{h_3(M) - \sqrt{h_3(M)}\right\}, \end{aligned} \tag{2.69}$$

$$\begin{aligned} h_u(M) = &\left\{2^{MR}(M+1)R\ln 2 + \left(2^{MR}-1\right)(c_4-\alpha)\right\} \\ &\times \left\{h_3(M) - \sqrt{h_3(M)}\right\}. \end{aligned} \tag{2.70}$$

Since

$$h_l(M) < h_2(M) \le h_u(M), \tag{2.71}$$

$h_l(M)$ and $h_u(M)$ are the lower bound and upper bound of $h_2(M)$, respectively. Solving $h_l(M) \ge 0$ and $h_u(M) \ge 0$ for M, we obtain

$$h_l(M) \ge 0 \Leftrightarrow M \ge M_1, \tag{2.72}$$

$$h_u(M) \ge 0 \Leftrightarrow M \ge M_2 \tag{2.73}$$

where

$$M_1 = \frac{(\alpha-1) + W\left[2^R(1-\alpha)\exp(1-\alpha)\right]}{R\ln 2} - 1, \tag{2.74}$$

$$M_2 = \frac{(\alpha-c_4) + W\left[2^R(c_4-\alpha)\exp(c_4-\alpha)\right]}{R\ln 2} - 1. \tag{2.75}$$

Therefore, the solution of (2.63) is in the range $\lfloor M_2 \rfloor \leq M^* \leq \lceil M_1 \rceil$.

Similarly, for the case $K = 2M$, the solution of (2.46) is in the range $\lfloor M_4 \rfloor \leq M^* \leq \lceil M_3 \rceil$ where

$$M_3 = \frac{\frac{2\alpha-3}{2} + W\left[\frac{3-2\alpha}{2}\exp\left(\frac{3-2\alpha}{2}\right)\right]}{R\ln 2}, \tag{2.76}$$

$$M_4 = \frac{\alpha - 1 - \frac{c_5}{2} + W\left[\left(1-\alpha+\frac{c_5}{2}\right)\exp\left(1-\alpha+\frac{c_5}{2}\right)\right]}{R\ln 2} - 1 \tag{2.77}$$

in which

$$c_5 = 1 + \left(1 + \frac{2P_{tot}}{3^\alpha d_{0,K}^\alpha}\right)^{-\frac{1}{2}}. \tag{2.78}$$

3) $K > 2M$

Recall the approximation in (2.46).

Consider that K is not the multiple of M. Since the order of the polynomial equation in (2.33) and $P_k^{(M,K)}$ and $P_k^{(M,K+1)}$ have identical function of $P_k^{(M,K)}$ and $P_k^{(M,K+1)}$, we have the following approximation:

$$\frac{P_0^{(M,K)}}{P_k^{(M,K)}} \approx \frac{P_0^{(M,K+1)}}{P_k^{(M,K+1)}} \approx \frac{1}{\beta_k} (= \text{constant}). \tag{2.79}$$

Since $P_0^{(M,K)} = \frac{P_{tot}}{\sum_{k=0}^{K-1} \beta_k}$ and $P_0^{(M,K+1)} = \frac{P_{tot}}{\sum_{k=0}^{K} \beta_k}$, we obtain

$$\begin{aligned}\frac{P_0^{(M,K+1)}(K+1)}{P_0^{(M,K)}K} &\approx \frac{(K+1)\sum_{k=0}^{K-1}\beta_k}{K\sum_{k=0}^{K}\beta_k} \\ &= \frac{K\sum_{k=0}^{K-1}\beta_k + \sum_{k=0}^{K-1}\beta_k}{K\sum_{k=0}^{K-1}\beta_k + K\beta_K}. \end{aligned} \tag{2.80}$$

Since β_{K-1} is equal to β_K and much larger than $\beta_k, k = 1, \cdots, M$, $K\sum_{k=0}^{K-1}\beta_k$ is sufficiently larger than $\sum_{k=0}^{K-1}\beta_k$ and $K\beta_K$, and thus (2.80) is approximated to 1. Therefore, we obtain

$$\frac{P_0^{(K+1,M)}(K+1)^{\alpha-1}}{P_0^{(K,M)}K^{\alpha-1}} \approx \left(\frac{K+1}{K}\right)^{\alpha-2} > 1. \tag{2.81}$$

Then, $P_0^{(K,M)}K^{\alpha-1}$ is maximized when K is the multiple of M for given M.

Finally, the problem of selecting M and K is reformulated as

$$(M^*, K^*) = \arg \min_{(M,K)\in\Omega_2} P_{out}(R) \tag{2.82}$$

where

$$\begin{aligned}\Omega_2 = (\{(K,K) : K = K^*_{\text{conv}}\} \cup \{(M, M+1) : \lfloor M_2 \rfloor \le M \le \lceil M_1 \rceil\} \\ \cup \{(M, 2M) : \lfloor M_4 \rfloor \le M \le \lceil M_3 \rceil\} \cup \{(M, lM) : l \in \mathbb{N}\}) \cap \Omega_1 \end{aligned} \tag{2.83}$$

in which $\mathbb{N}$ is a set of integers larger than 2.

The flow chart of optimization based on (2.82) is shown in Figure 2.6.

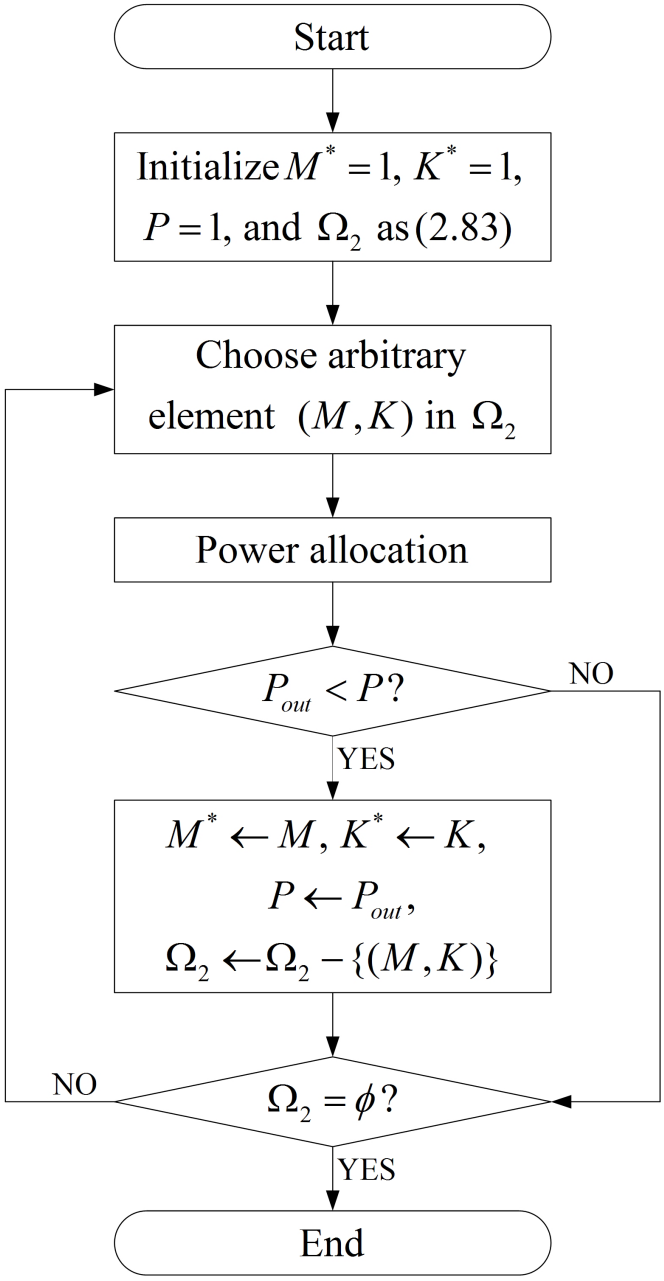

Figure 2.6. Flow chart of optimization based on (2.82).

2.3.5 Complexity Comparison

Suppose

$$M_{\min} = \begin{cases} 1, & K = 1, \\ 2, & K > 1. \end{cases} \tag{2.84}$$

First, consider the selection based on exhaustive search in Section 2.3.3. For each K, it needs to consider M that satisfies $M_{\min} \leq M \leq K$. Therefore, the computational complexity is given by

$$\sum_{k=K_{\min}}^{K_{\max}} (k - M_{\min} + 1) = \begin{cases} (K_{\max} - K_{\min} + 1)\left(\frac{K_{\max}+K_{\min}}{2} - 1\right), & K_{\min} > 1, \\ (K_{\max} - K_{\min} + 1)\left(\frac{K_{\max}+K_{\min}}{2} - 1\right) + 1, & K_{\min} = 1. \end{cases} \tag{2.85}$$

Second, consider the reduced complexity selection in Section 2.3.4. For $K = M$, it needs to consider only $K = K^*_{\text{conv}}$. For $M < K \leq 2M$, it needs to consider $M = K - 1$ and $M = K/2$ in $\lfloor M_2 \rfloor \leq M \leq \lceil M_1 \rceil$ and $\lfloor M_4 \rfloor \leq M \leq \lceil M_3 \rceil$, respectively. To consider $M = K - 1$, $\min\{\lceil M_1 \rceil, K_{\max}\} - \max\{\lfloor M_2 \rfloor, K_{\min}\} + 1$ computations are required. Since $M = K/2$ is meaningful if only if K is the even number, $\left\lfloor \frac{\min\{\lceil M_3 \rceil, K_{\max}\}}{2} \right\rfloor - \left\lfloor \frac{\max\{\lfloor M_4 \rfloor, K_{\min}\}-1}{2} \right\rfloor$ computations are required. For $K > 2M$, it needs to consider $M = K/l$ for $l \geq 3$. Therefore, $\sum_{k=2}^{\lfloor K_{\max}/3 \rfloor} \left\{ \left(\left\lfloor \frac{K_{\max}}{k} \right\rfloor - 2 \right)^+ - \left(\left\lfloor \frac{K_{\min}-1}{k} \right\rfloor - 2 \right)^+ \right\}$ computations are required. Overall, the computational complexity is given by

$$\begin{aligned} & 2 + \min\{\lceil M_1 \rceil, K_{\max}\} - \max\{\lfloor M_2 \rfloor, K_{\min}\} \\ & \quad + \left\lfloor \frac{\min\{\lceil M_3 \rceil, K_{\max}\}}{2} \right\rfloor - \left\lfloor \frac{\max\{\lfloor M_4 \rfloor, K_{\min}\} - 1}{2} \right\rfloor \\ & \quad + \sum_{k=2}^{\lfloor K_{\max}/3 \rfloor} \left\{ \left(\left\lfloor \frac{K_{\max}}{k} \right\rfloor - 2 \right)^+ - \left(\left\lfloor \frac{K_{\min} - 1}{k} \right\rfloor - 2 \right)^+ \right\}. \end{aligned} \tag{2.86}$$

Table 2.1 shows the example of computational complexity when the signal-to-noise ratio (SNR) P_{tot}/N_0 is 20dB. It is shown that the reduced complexity selection in Section 2.3.4 reduces the complexity significantly compared to the exhaustive search in Section 2.3.3.

2.3.6 Minimization of the total power

In Section through Section , we dealt with the optimization problem that minimizes the outage probability for given total available power. In this section, we deal with the optimization problem that minimizes the required total power for given target outage probability P_{target}. This problem is formulated as

(2.87)

$$\text{subject to}: \quad P_{out}(R) \leq P_{target} \tag{2.88}$$
$$(2.24), (2.25), \text{ and } (2.26).$$

The power allocation discussed in Section 2.3.2 and the reduced complexity selection of M and K discussed in Section 2.3.4 are still valid in this problem. Therefore, we consider P_0 obtained by (2.33) and Ω_2 in (2.83). The outage probability in (2.21) is represented using only P_0. Then, P_0 is a solution of $P_{out}(R) = P_{target}$. When $K = M$, it is given by

$$P_0 = -\frac{K\left(2^{KR}-1\right)}{\lambda_{0,1}\ln\left(1-P_{target}\right)}. \tag{2.89}$$

In other cases, it is obtained using a numerical method [77] as it is intractable to solve algebraically.

Table 2.1. Example of computational complexity

	Optimization using (2.37)	Optimization using (2.82)
$\alpha = 4, K_{\max} = 5$	11	5
$\alpha = 4, K_{\max} = 10$	46	9
$\alpha = 4, K_{\max} = 20$	191	23
$\alpha = 6, K_{\max} = 5$	11	3
$\alpha = 6, K_{\max} = 10$	46	10
$\alpha = 6, K_{\max} = 20$	191	24

We apply the Newton′s method [77]. Let q_i be P_0 in the i-th iteration of the Newton′s method. The relation between q_i and q_{i+1} is given by

$$q_{i+1} = q_i - \left[\frac{P_{out}(R)}{dP_{out}(R)/dP_0} \right]_{P_0=q_i}. \tag{2.90}$$

Note that the outage probability is bounded as

$$1 - \exp\left(-K \frac{2^{\tilde{M}R} - 1}{P_{K-1}\lambda_{0,1}} \right) \leq P_{out}(R) \leq 1 - \exp\left(-K \frac{2^{\tilde{M}R} - 1}{P_0 \lambda_{0,1}} \right). \tag{2.91}$$

Then, for given M and K, P_0 is bounded as

$$P_{lower} \triangleq -\frac{K\left(2^{\tilde{M}R} - 1\right)}{\lambda_{0,1} \ln(1 - P_{target})} \leq P_0 \leq f_K^{-1}\left(-\frac{K\left(2^{\tilde{M}R} - 1\right)}{\lambda_{0,1} \ln(1 - P_{target})} \right) \triangleq P_{upper}. \tag{2.92}$$

Therefore, q_i is also bounded as

$$P_{lower} \leq q_i \leq P_{upper} \tag{2.93}$$

If q_i obtained from (2.90) is larger than P_{upper} or smaller than P_{lower}, it is replaced to P_{upper} and P_{upper}, respectively. In the Newton′s method, it is important to determine the initial value. The initial value of P_0, q_0, is selected randomly in the range (2.93). The iteration is terminated when $0 < P_{target} - P_{out} < \delta$ for the pre-defined allowable error δ.

The flow chart of the optimization algorithm that minimizes the total power for given target outage probability is shown in Figure 2.7.

2.4 Numerical Results

Suppose that the maximum number of hops $K_{\max}$ is 20 and the minimum number of hops $K_{\min}$ is 1.

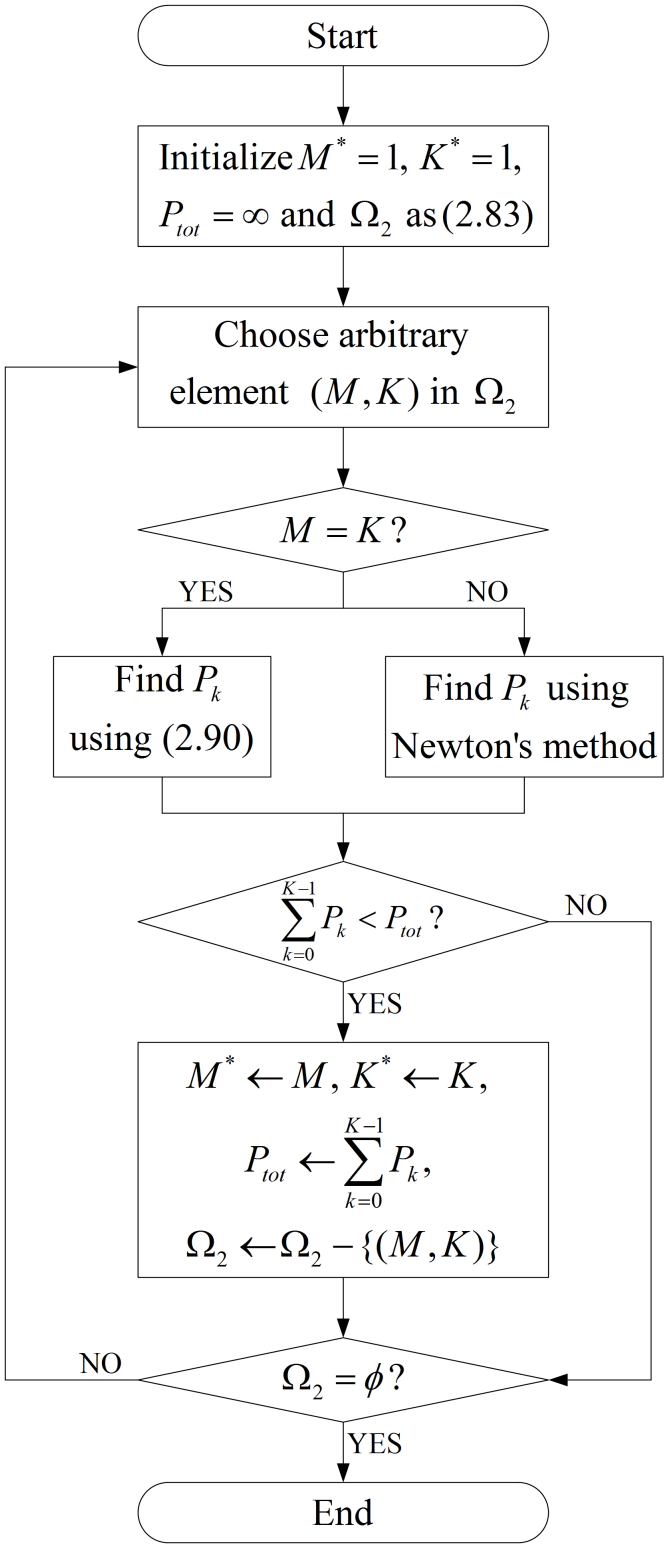

(a) Optimization algorithm

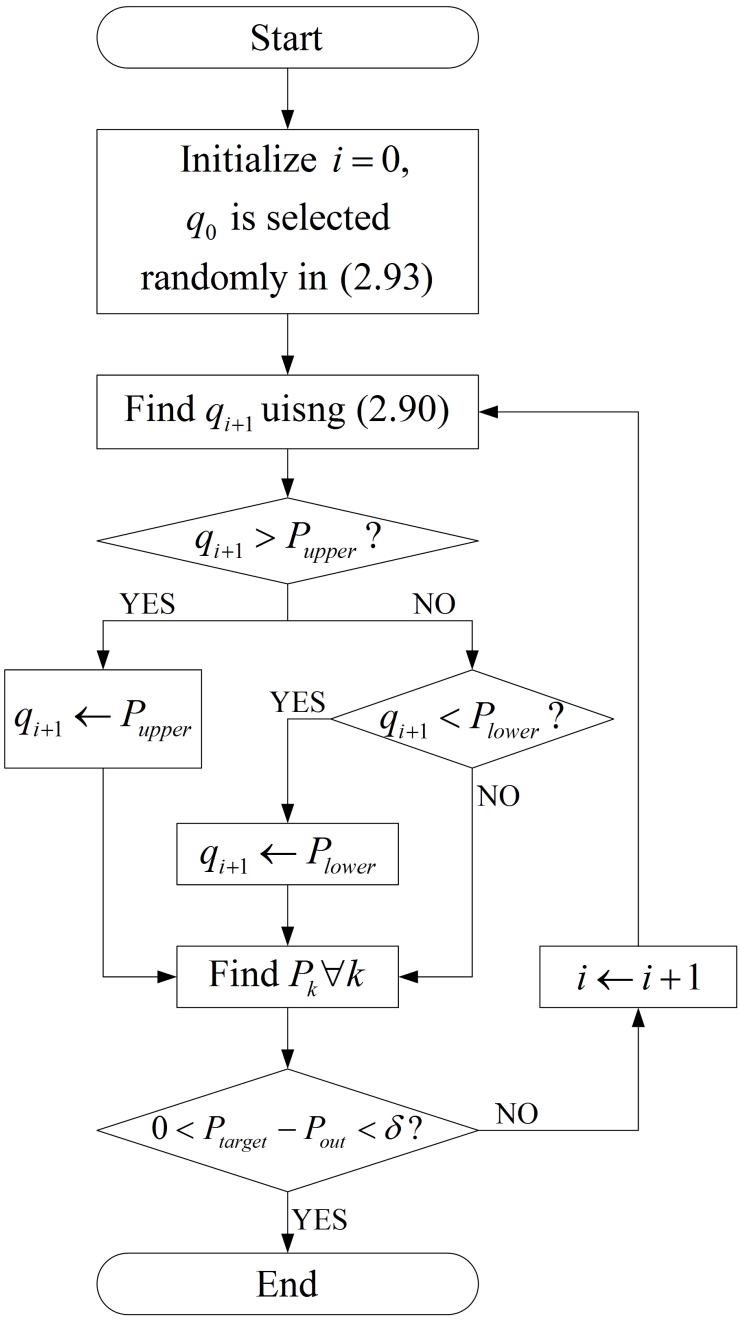

(b) Newton′s method

Figure 2.7. Flow chart of the optimization algorithm that minimizes the total power for given target outage probability.

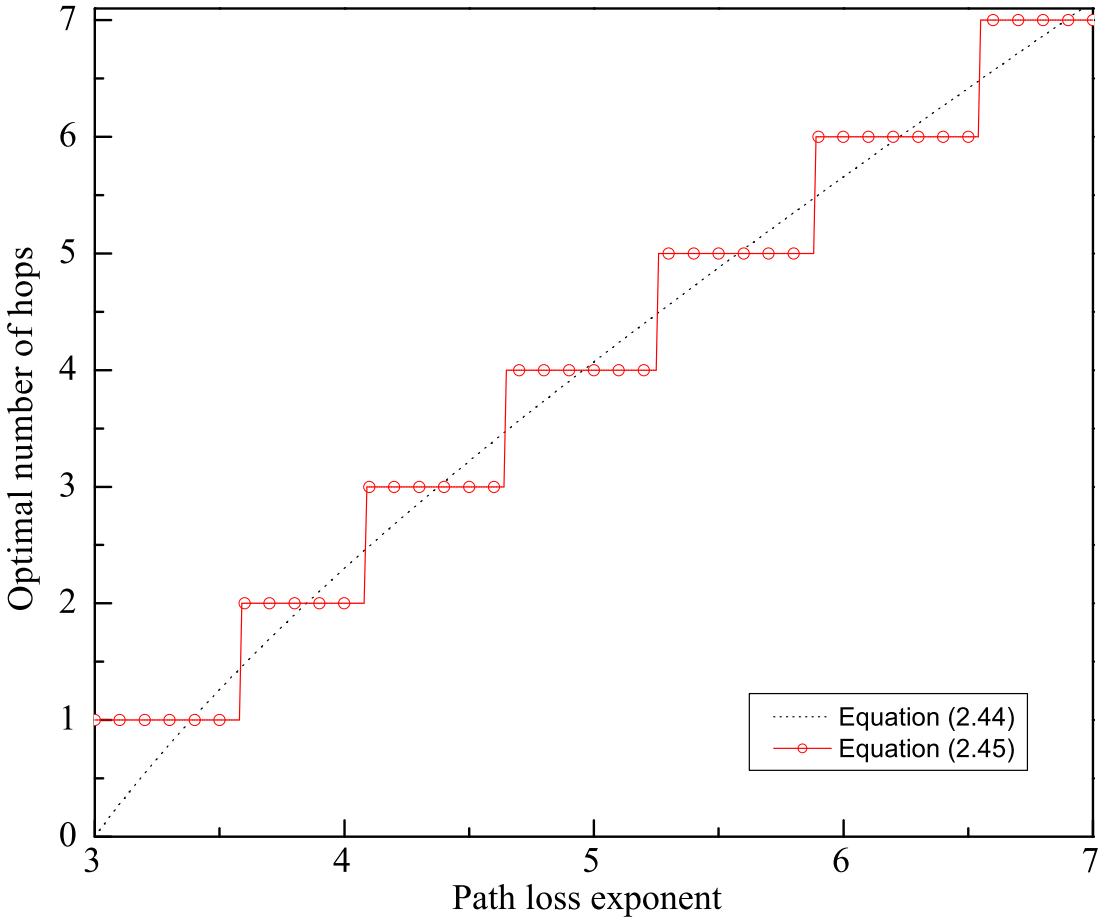

Figure 2.8. Optimal number of hops for the conventional multi-hop network according to the path-loss exponent for the target rate R=1b/s/Hz.

As discussed in Section 2.3.4, the optimal number of hops is related to only the path-loss exponent and the target rate for the conventional multi-hop network. Figure 2.8 shows the optimal number of hops for the conventional multi-hop network according to the path-loss exponent. The dotted line represents (2.44) which is the optimal number of hops obtained in the real number that minimizes the outage probability. However, the number of hops should be the positive integer. The dashed line with circle represents (2.45) which is the optimal number of hops obtained in the positive integer that minimizes the outage probability. It is shown that the optimal number of hops is larger as the path-loss exponent is higher.

Figure 2.9 shows the optimal number of hops based on (2.45) for the conventional multi-hop network according to the path-loss exponent for the target rate R=0.5, 1, and 2 b/s/Hz. It is shown that the optimal number of hops is larger as the path-loss exponent is higher. It is also shown that the optimal number of hops is larger as the target rate is higher. In addition, the optimal number of hops is more sensitive in terms of the path-loss exponent and becomes larger more rapidly as the target rate becomes lower. For the target rate R=0.5, 1, and 2 b/s/Hz, the single-hop protocol is more efficient than the multi-hop protocol when the path-loss exponent is lower than about 3.3, 3.6, and 4.3, respectively. Since our concern is the optimization of the multi-hop protocol, we do not consider the path-loss exponent in the range that the multi-hop protocol is worse than the single-hop protocol in the rest of this Chapter.

Figure 2.10 shows the outage probability of the multi-hop network applying the power allocation for various values of M and K with the target rate R=1, the path-loss exponent $\alpha = 6$, and the distance between the source and the destination $d_{0,K}$=1. The label of horizontal axis, SNR, represents P_t/N_0. The outage probability of the single-hop protocol and conventional multi-hop protocol is also shown for comparison. From

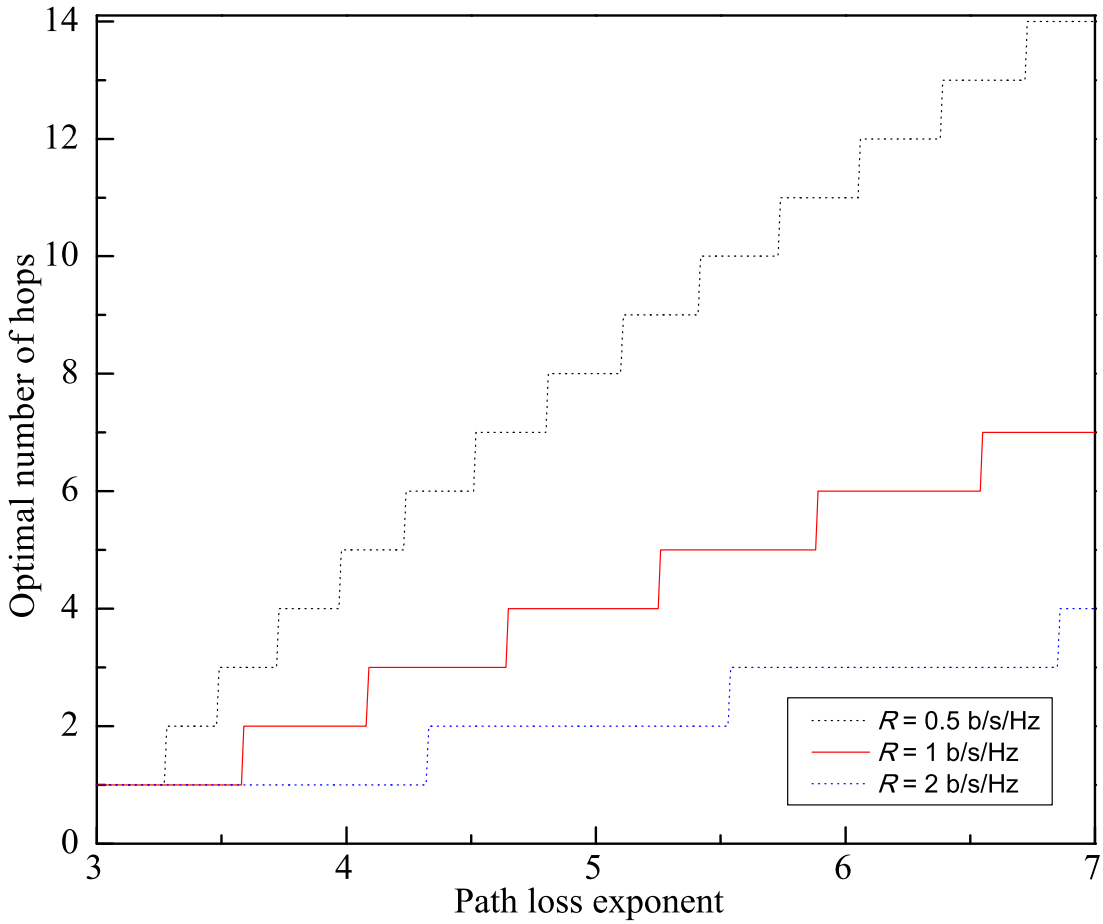

Figure 2.9. Optimal number of hops for the conventional multi-hop network according to the path-loss exponent for the target rate R=0.5, 1, and 2 b/s/Hz.

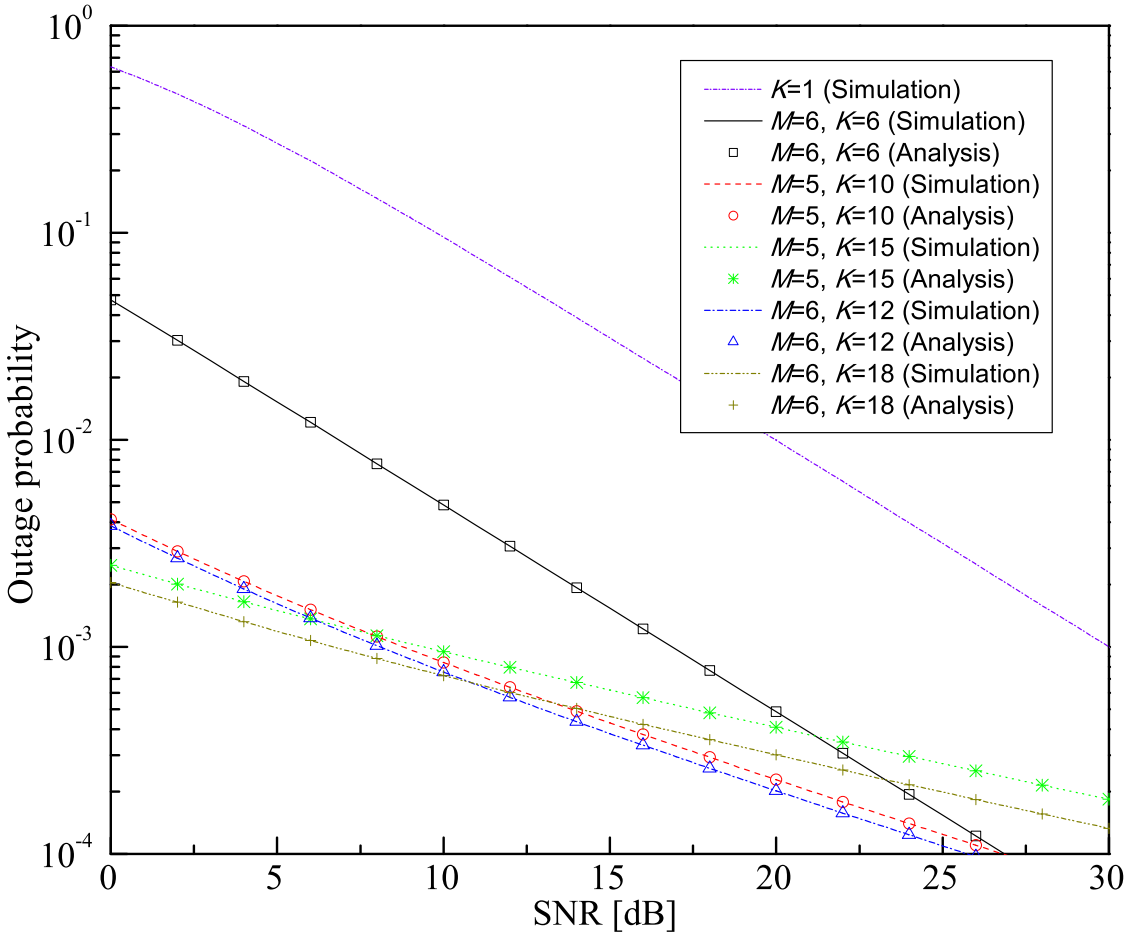

Figure 2.10. Outage probability of the multi-hop network applying the power allocation for various values of M and K with the target rate R=1, the path-loss exponent $\alpha = 6$, and the distance between the source and the destination $d_{0,K}$=1.

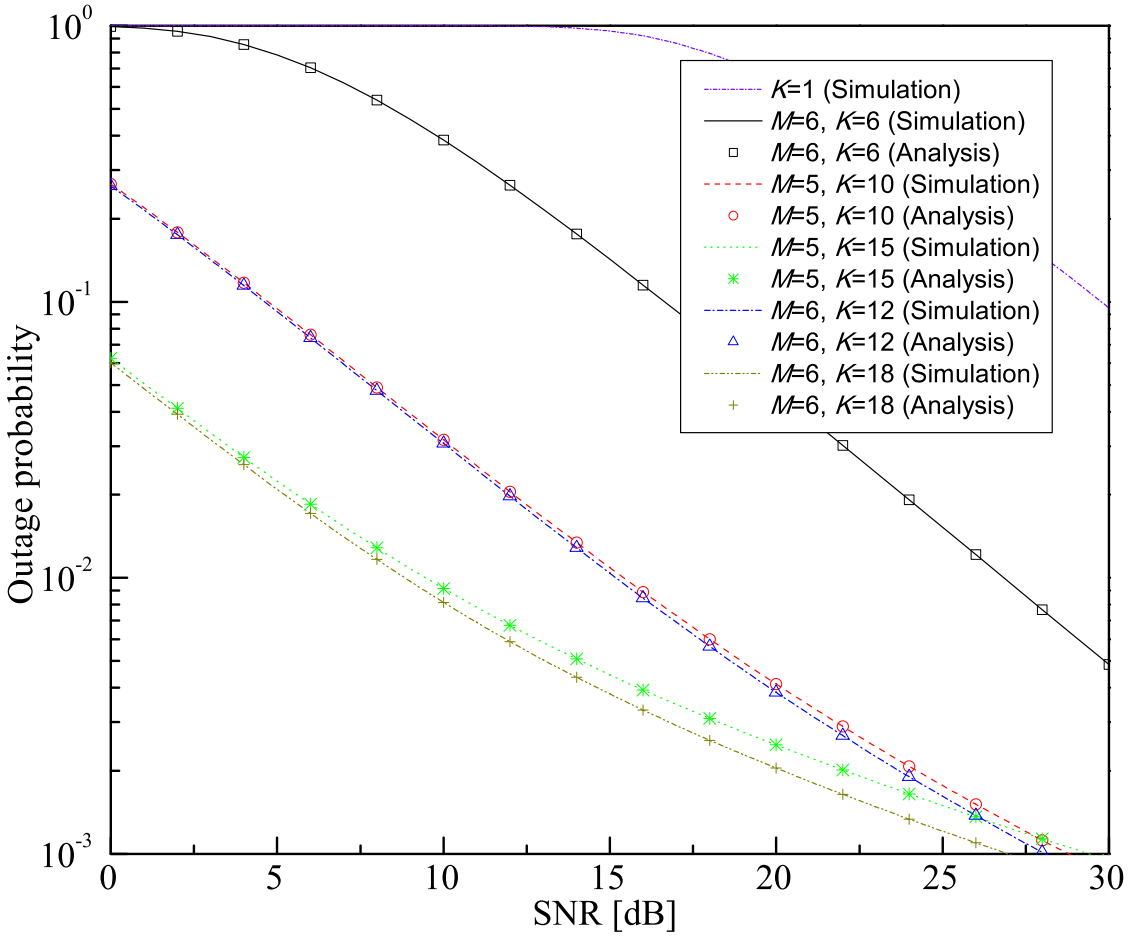

Figure 2.11. Outage probability of the multi-hop network applying the power allocation for various values of M and K with the target rate R=1, the path-loss exponent $\alpha = 6$, and the distance between the source and the destination $d_{0,K}$=10.

Figure 2.9, the optimal solution of the conventional multi-hop network is $K = M = 6$. It is shown that the conventional multi-hop network reduces the outage probability significantly compare to the single-hop protocol $K = 1$. Moreover, it is shown that the proper selection of M and K improves the outage probability compared to the conventional multi-hop network. The values of M and K are selected from the set Ω_2 in (2.83). The analytical results perfectly match the simulation results.

Since the channel variance is given by (2.3), the signal is not attenuated but amplified for $d < 1$. If the distance between the source and the destination $d_{0,K}$ is small, the effect of path-loss exponent is not evaluated properly. This is the reason that the system achieves the outage probability of 0.05 for conventional multi-hop network and the outage probability lower than 0.01 for proposed multi-hop network even though the SNR is 0dB in Figure 2.10. In Figure 2.11, we consider $d_{0,K}$=10. To compensate the distance, the horizontal axis, SNR, is normalized with the channel variance between the source and destination for the path-loss exponent $\alpha = 4$. Similar to Figure 2.10, the proposed multi-hop network provides lower outage probability than the single-hop protocol as well as conventional multi-hop protocol with proper selection of M and K outperforms the conventional multi-hop network. Also, it is shown that the analytical results and the simulation results are in perfect agreement.

Figure 2.12 shows the outage probability for various target rates R and path-loss exponents α with the distance between the source and the destination $d_{0,K}$=10. It is shown that the proposed multi-hop protocol provides lower outage probability than the conventional multi-hop protocol in low SNR region. However, the outage probability of the proposed multi-hop protocol converges to and eventually becomes same to the outage probability of the conventional multi-hop protocol as SNR increases. The reason is as follows. As the SNR increases, the effect of the noise becomes ignorable

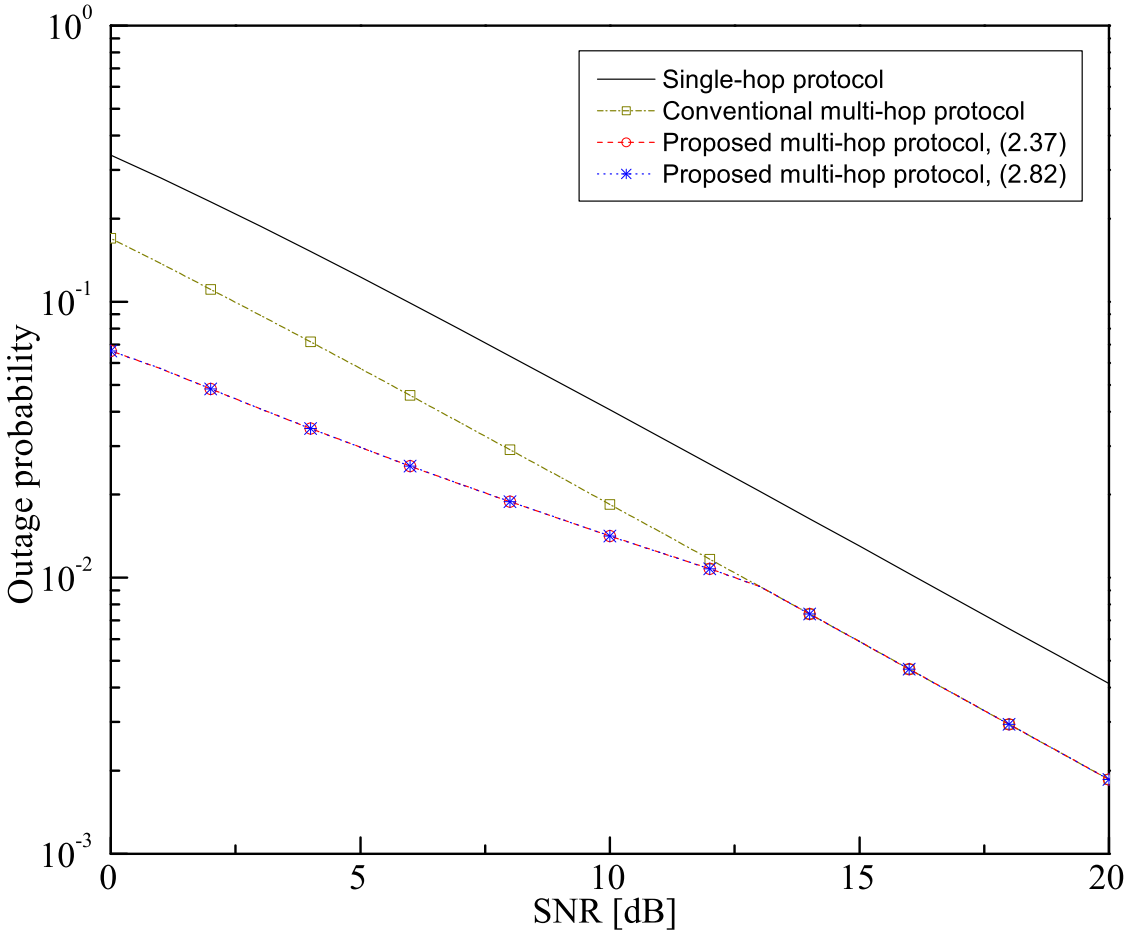

(a) $R = 0.5$ b/s/Hz, $\alpha = 4$

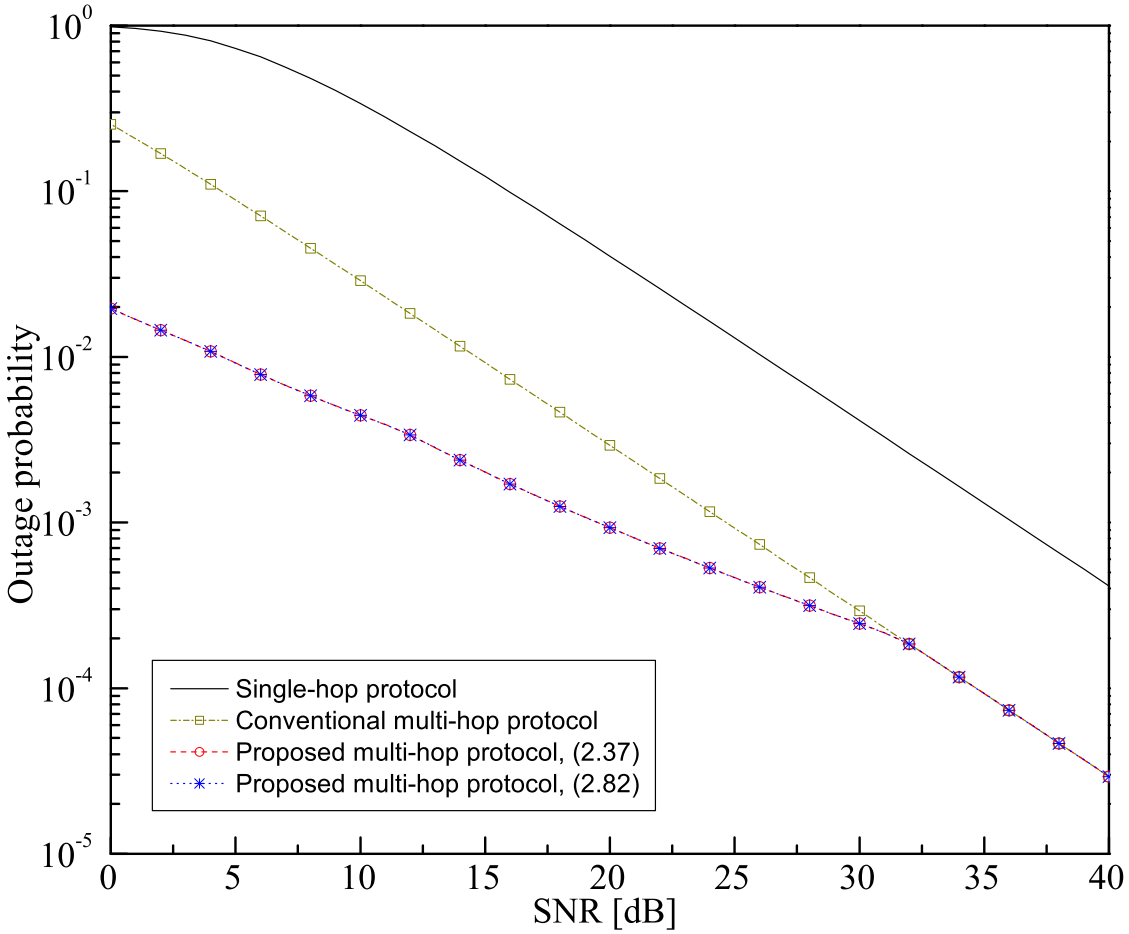

(b) $R = 0.5$ b/s/Hz, $\alpha = 5$

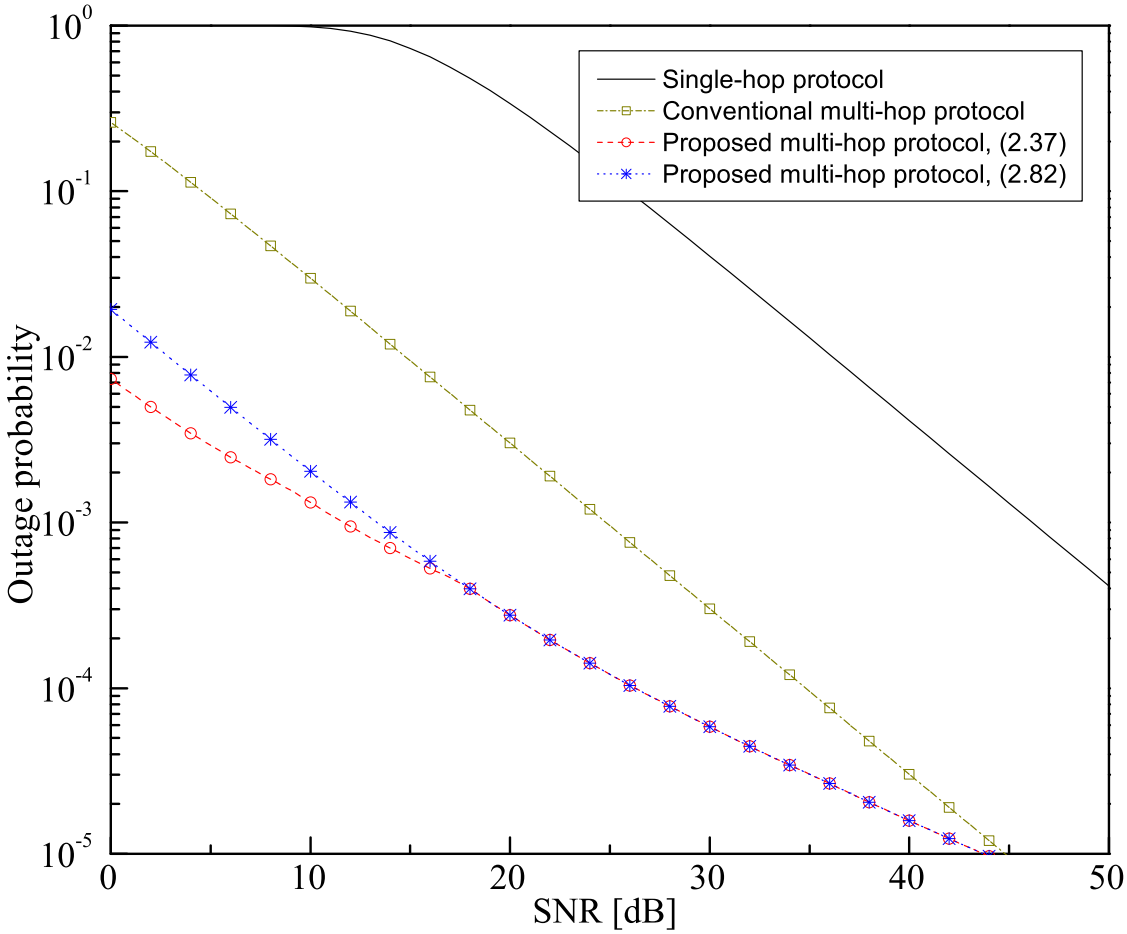

(c) $R = 0.5$ b/s/Hz, $\alpha = 6$

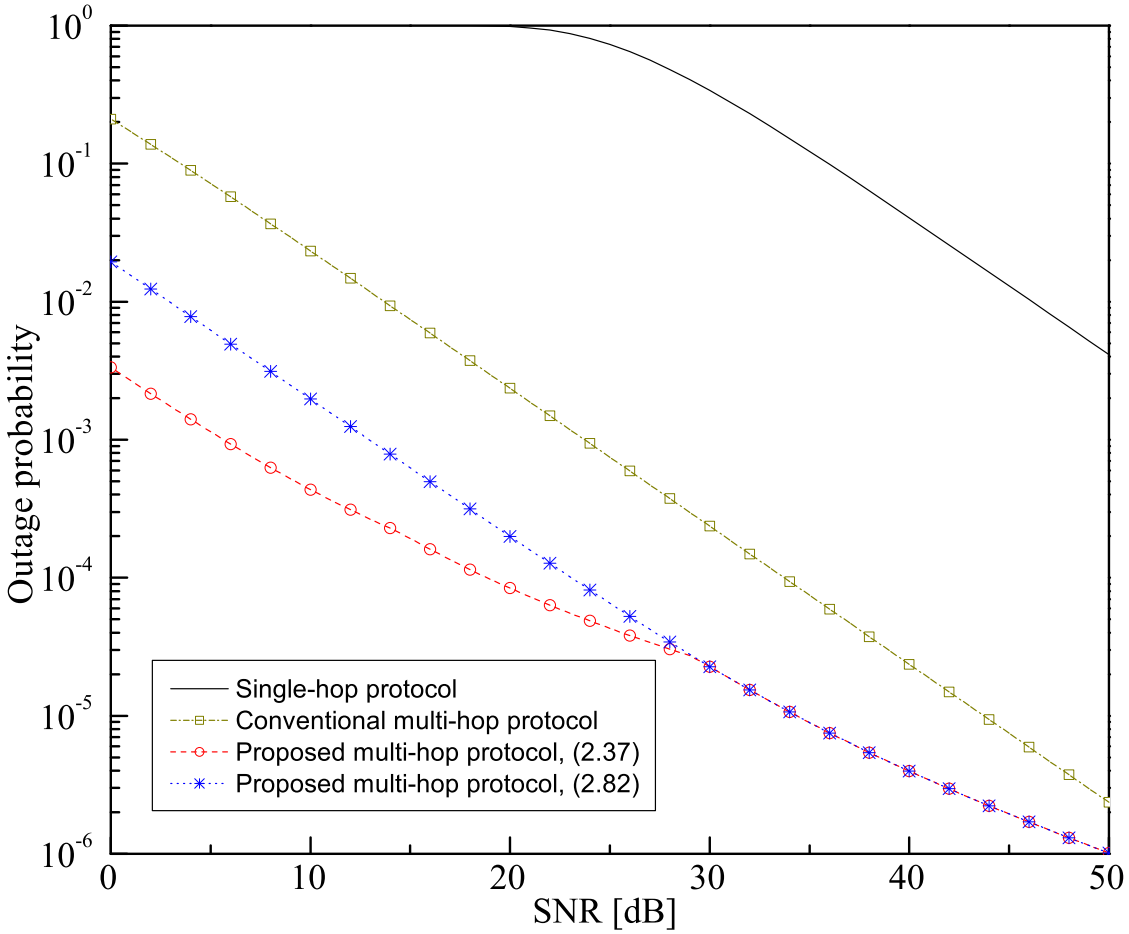

(d) $R = 0.5$ b/s/Hz, $\alpha = 7$

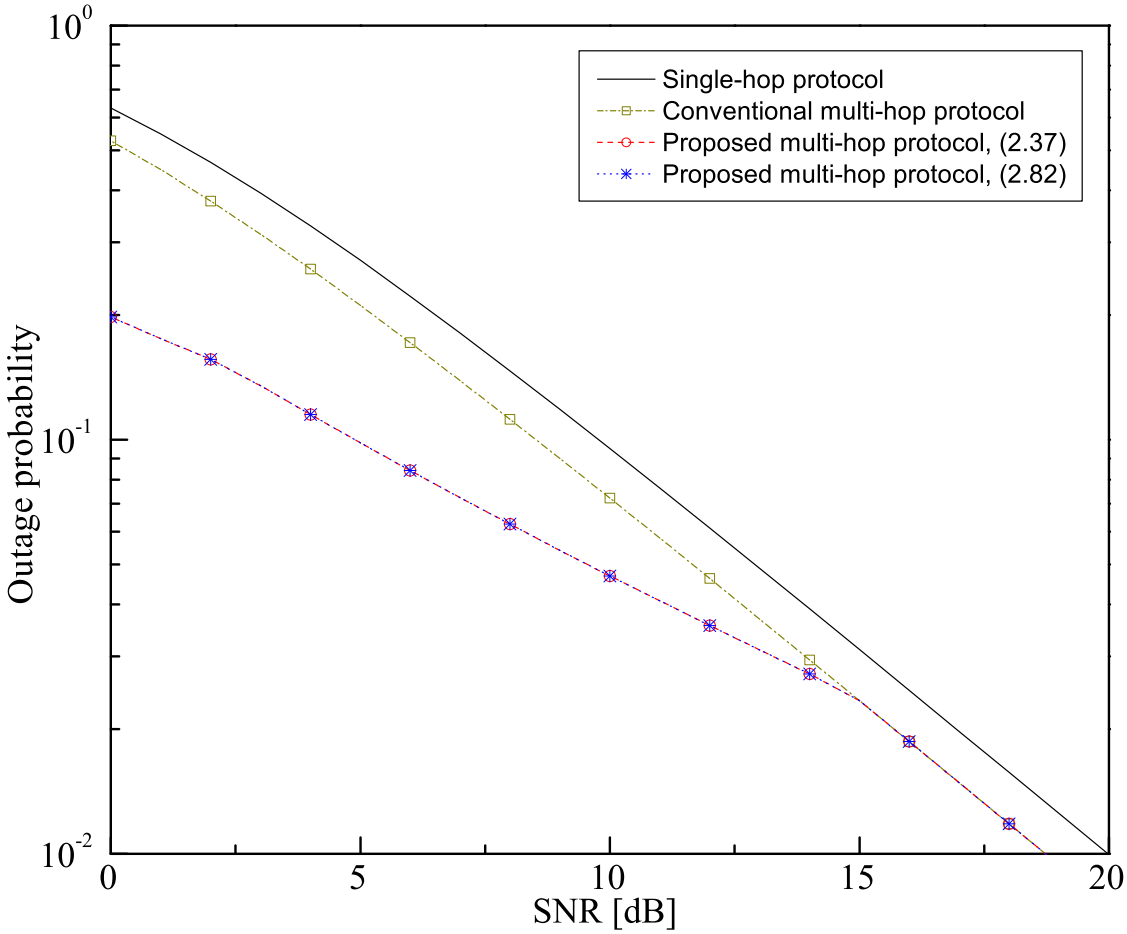

(e) $R = 1$ b/s/Hz, $\alpha = 4$

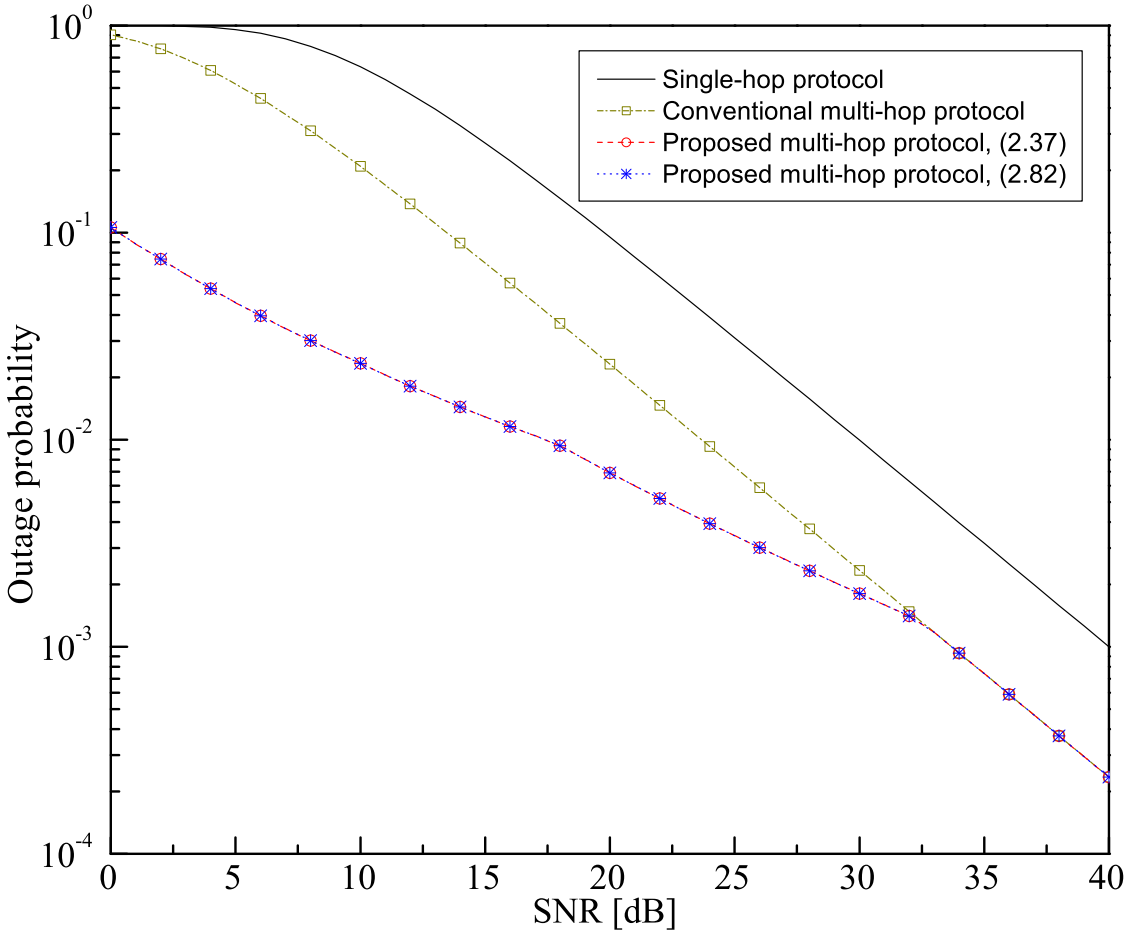

(f) $R = 1$ b/s/Hz, $\alpha = 5$

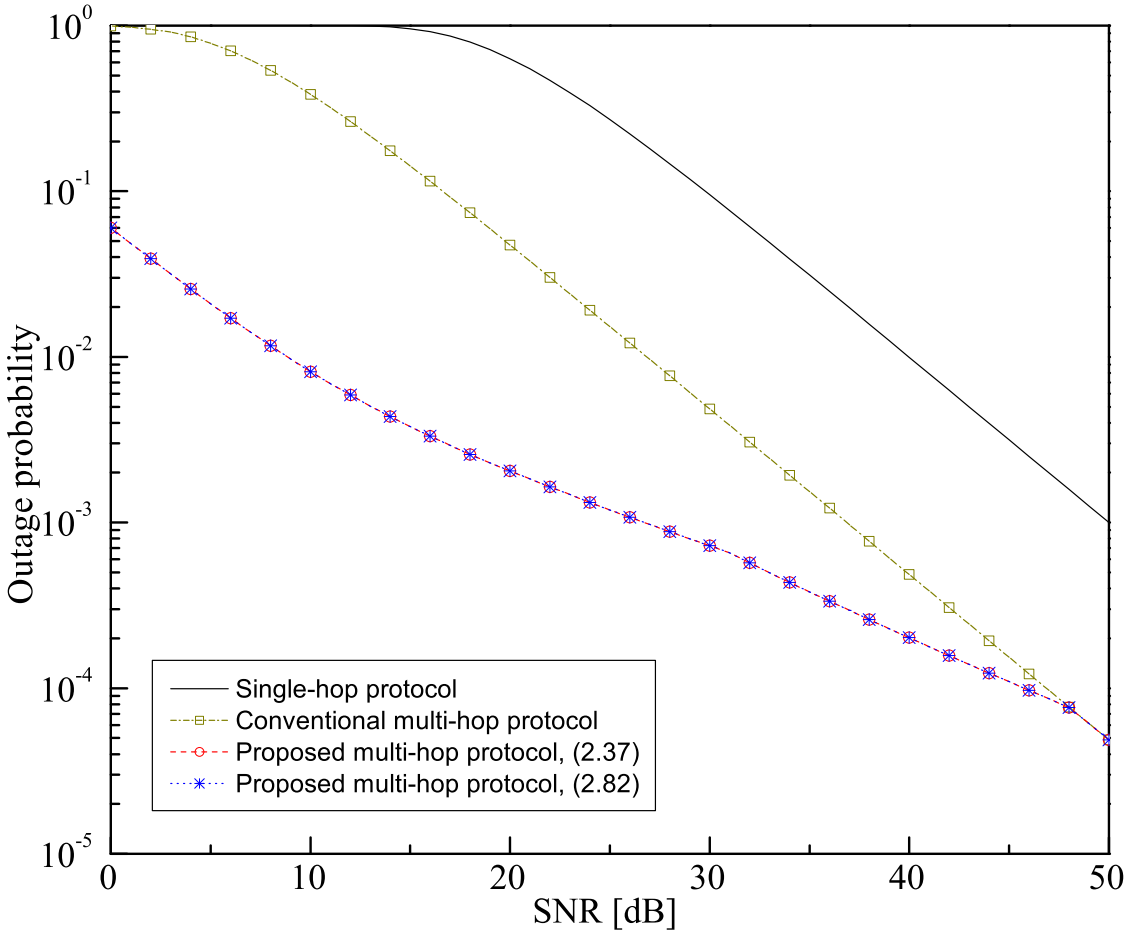

(g) $R = 1$ b/s/Hz, $\alpha = 6$

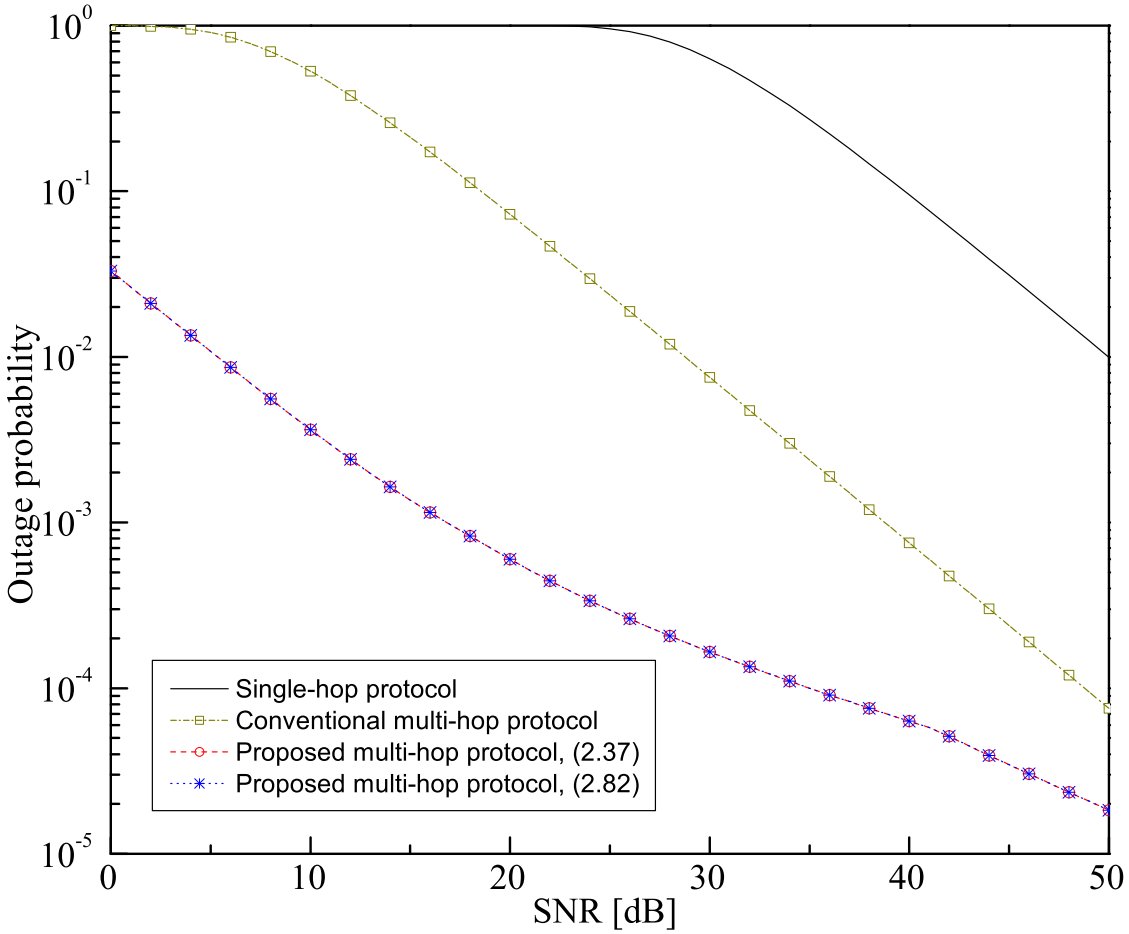

(h) $R = 1$ b/s/Hz, $\alpha = 7$

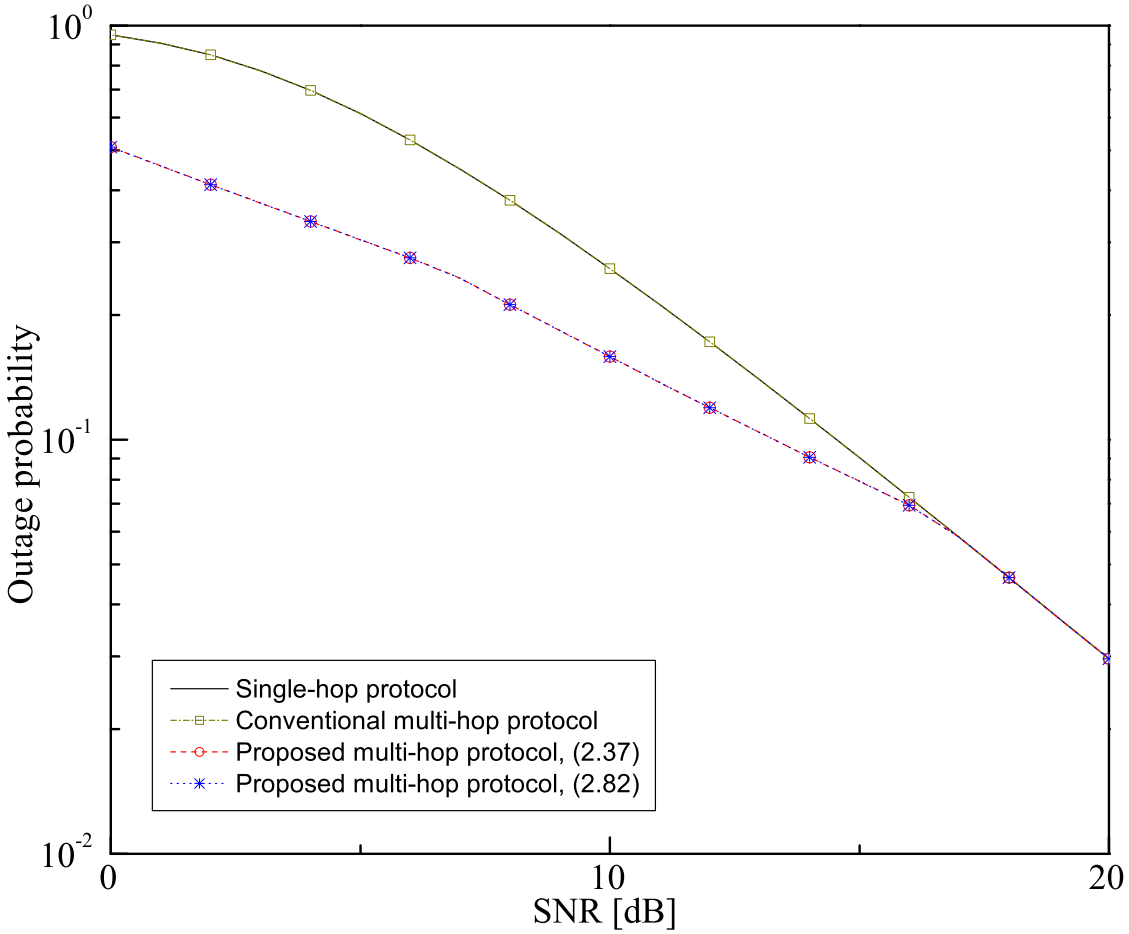

(i) $R = 2$ b/s/Hz, $\alpha = 4$

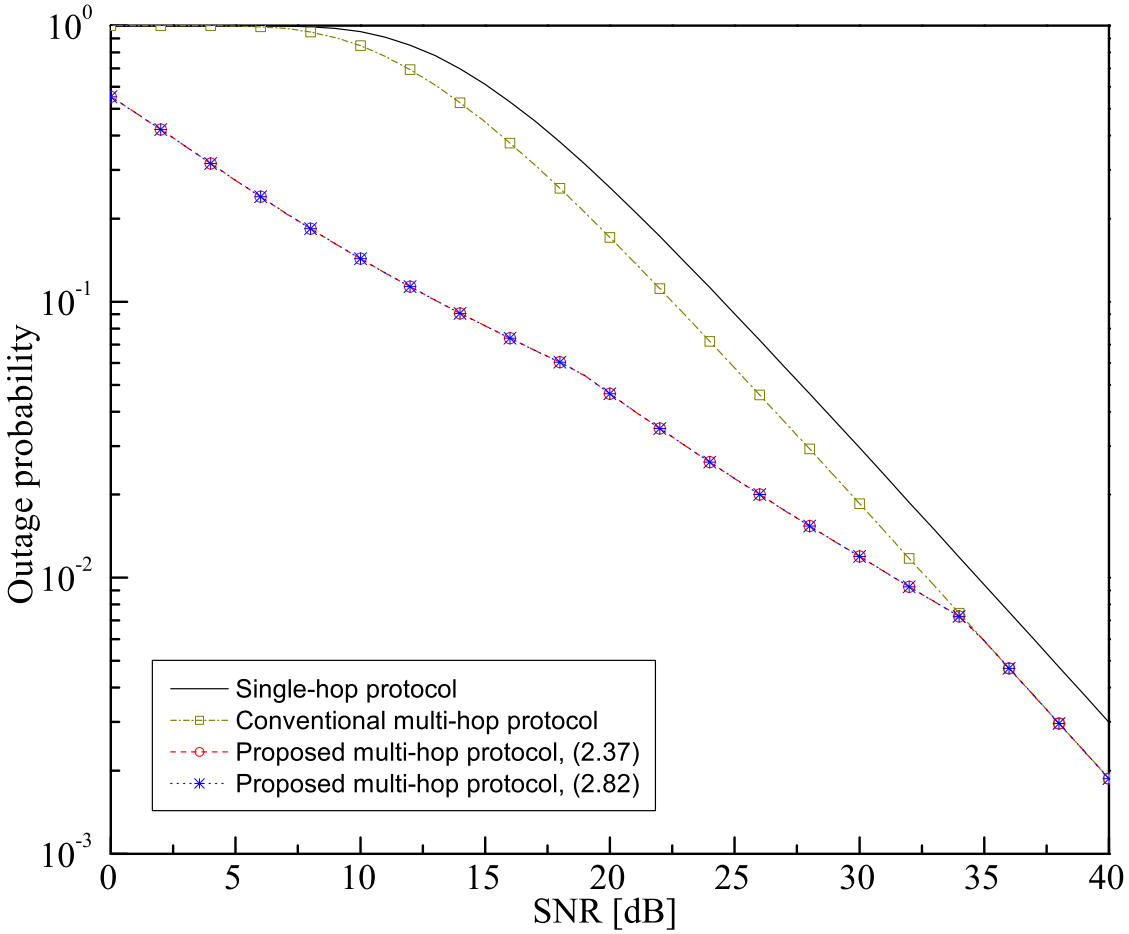

(j) $R = 2$ b/s/Hz, $\alpha = 5$

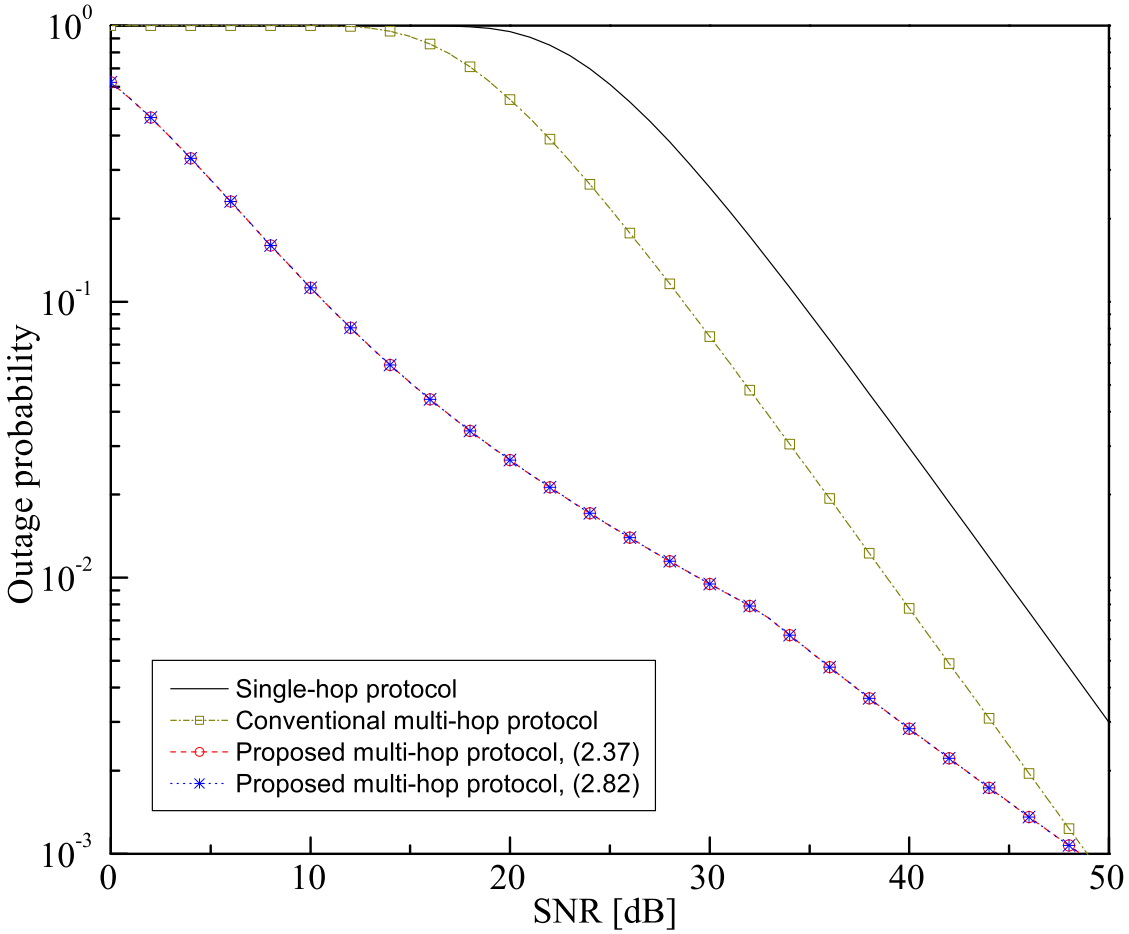

(k) $R = 2$ b/s/Hz, $\alpha = 6$

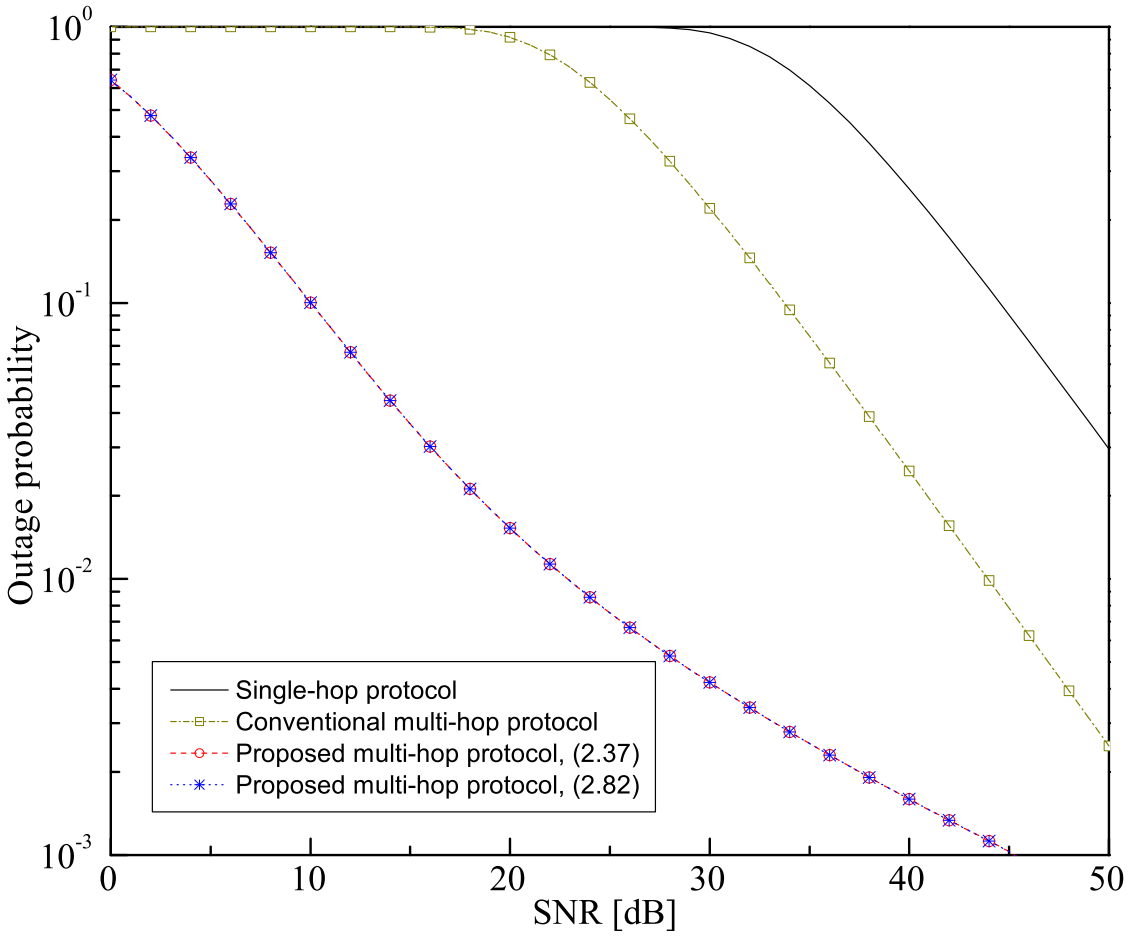

(l) $R = 2$ b/s/Hz, $\alpha = 7$

Figure 2.12. Outage probability for various target rates R and path-loss exponents α with the distance between the source and the destination $d_{0,K}$=10.

and the inter-relay interference becomes the main factor on the outage probability. To reduce the inter-relay interference, the solutions in (2.37) and (2.82) become same to the solution in (2.45). It is also shown that the selection of M and K based on (2.82) mostly provides the same outage probability to the selection of M and K based on (2.37) except for the low SNR region in Figure 2.12 (c) and Figure 2.12 (d). The reason is that there is no (M, K) pair that satisfies both $\lfloor M_4 \rfloor < M < \lceil M_3 \rceil$ and $K \geq 3M$.

Figure 2.13 shows the outage probability according to the path-loss exponent for the multi-hop network with the target rate $R = 1$ b/s/Hz and the distance between the source and the destination $d_{0,K}$=10. It is shown that the gap between the conventional and proposed multi-hop protocols is larger as the path-loss exponent is higher. In Figure 2.12, the SNR of intersection of the outage probability curves of conventional and proposed multi-hop protocols is higher as the path-loss exponent is higher. From these results, it is reasonable to say that the proposed multi-hop protocol is more efficient for high path-loss exponent. The reason is as follows. As the path-loss exponent is higher, the effect of inter-relay interference is more ignorable, thereby, the system has more chances of simultaneous transmission. The high path-loss exponent is appeared in some applications. It is up to 6 for obstructed in-building environment [78] and is up to 7 for a human-body sensor network [79], [80].

Figure 2.14 shows the required transmission SNR versus the target outage probability for the multi-hop network with the target rate $R = 1$ b/s/Hz and the distance between the source and the destination $d_{0,K}$=10. It is shown that the proposed and conventional multi-hop protocol requires lower transmission power than the single-hop protocol. It is also shown that the proposed multi-hop protocol requires lower transmission power than the conventional multi-hop protocol in low SNR region. However,

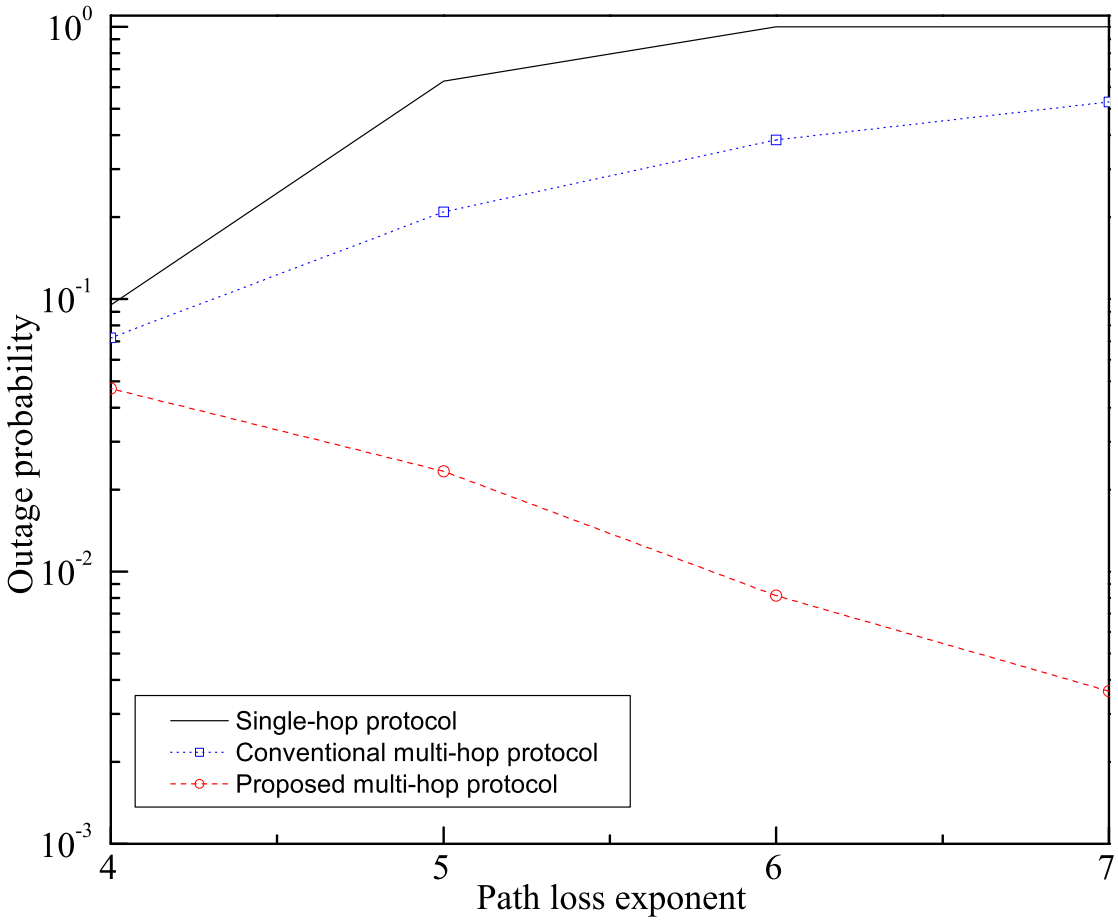
Outage probability
Path loss exponent
Single-hop protocol
Conventional multi-hop protocol
Proposed multi-hop protocol

(a) SNR=10dB

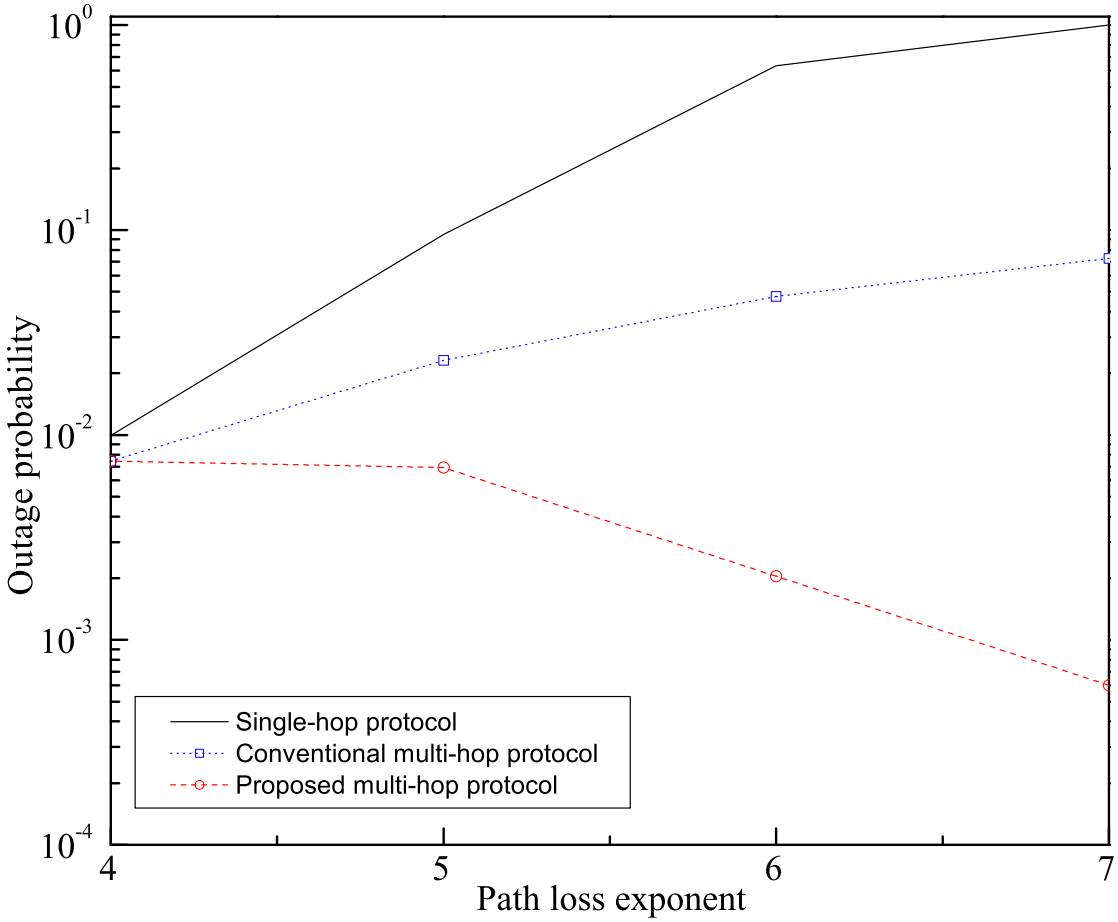
Outage probability
Path loss exponent
Single-hop protocol
Conventional multi-hop protocol
Proposed multi-hop protocol

(b) SNR=20dB

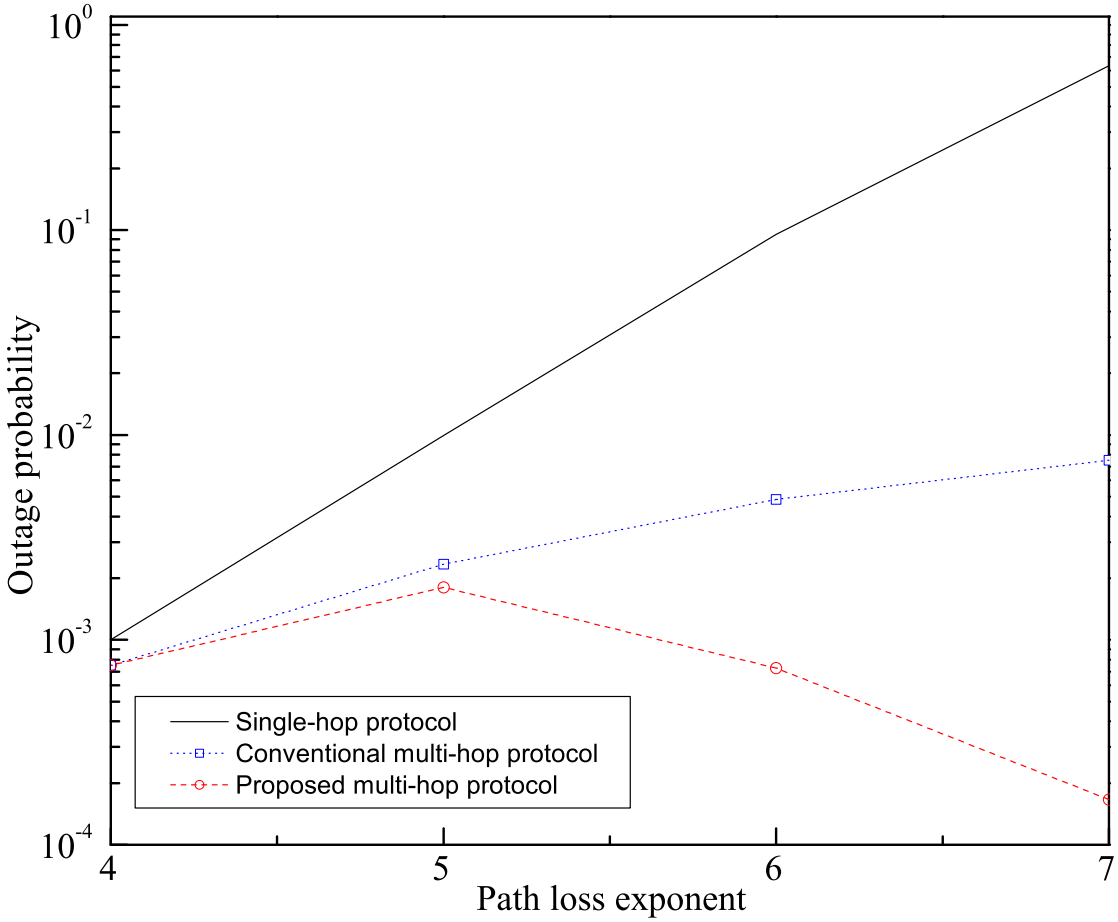

(c) SNR=30dB

Figure 2.13. Outage probability according to the path-loss exponent for the multi-hop network with the target rate $R = 1$ b/s/Hz and the distance between the source and the destination $d_{0,K}$=10.

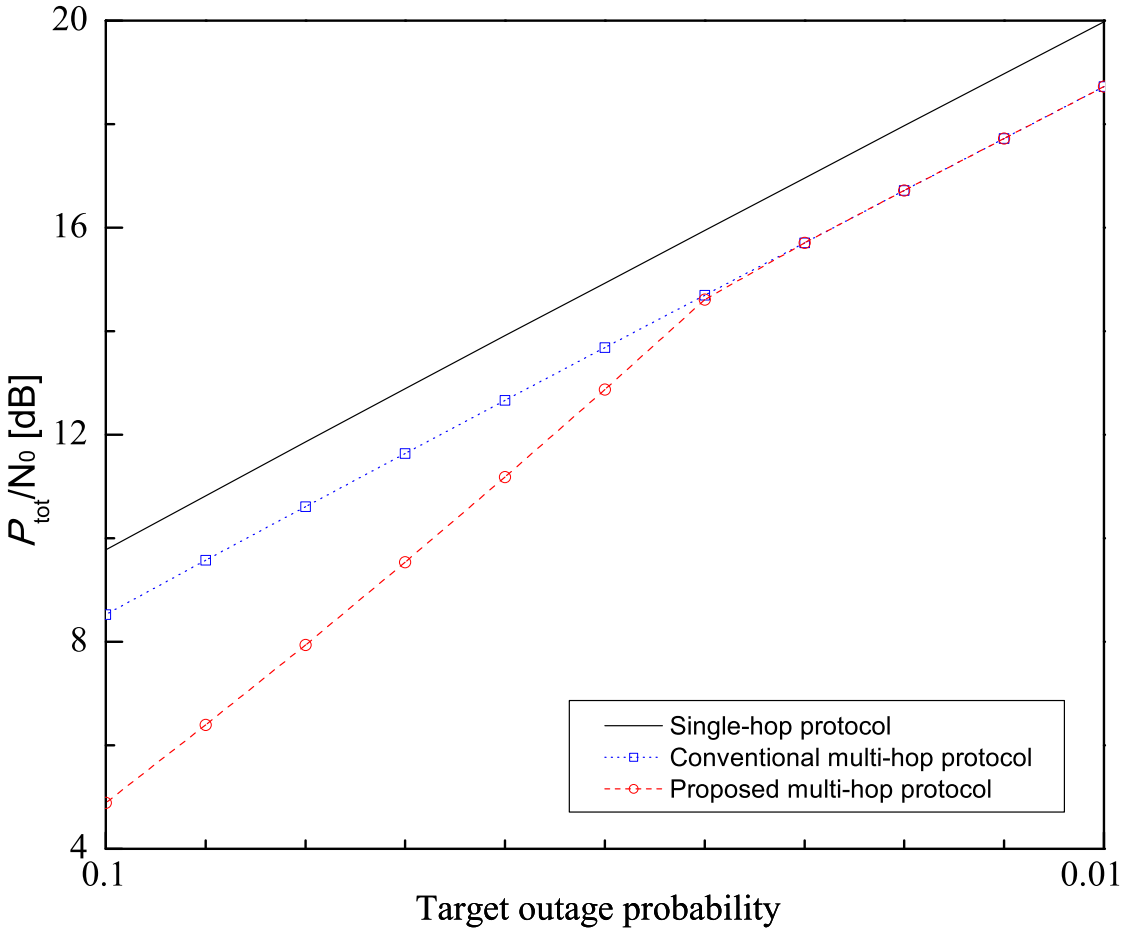
20
16
12
8
4
0.1
0.01
P_{tot}/N_0 [dB]
Target outage probability
Single-hop protocol
Conventional multi-hop protocol
Proposed multi-hop protocol

(a) α=4

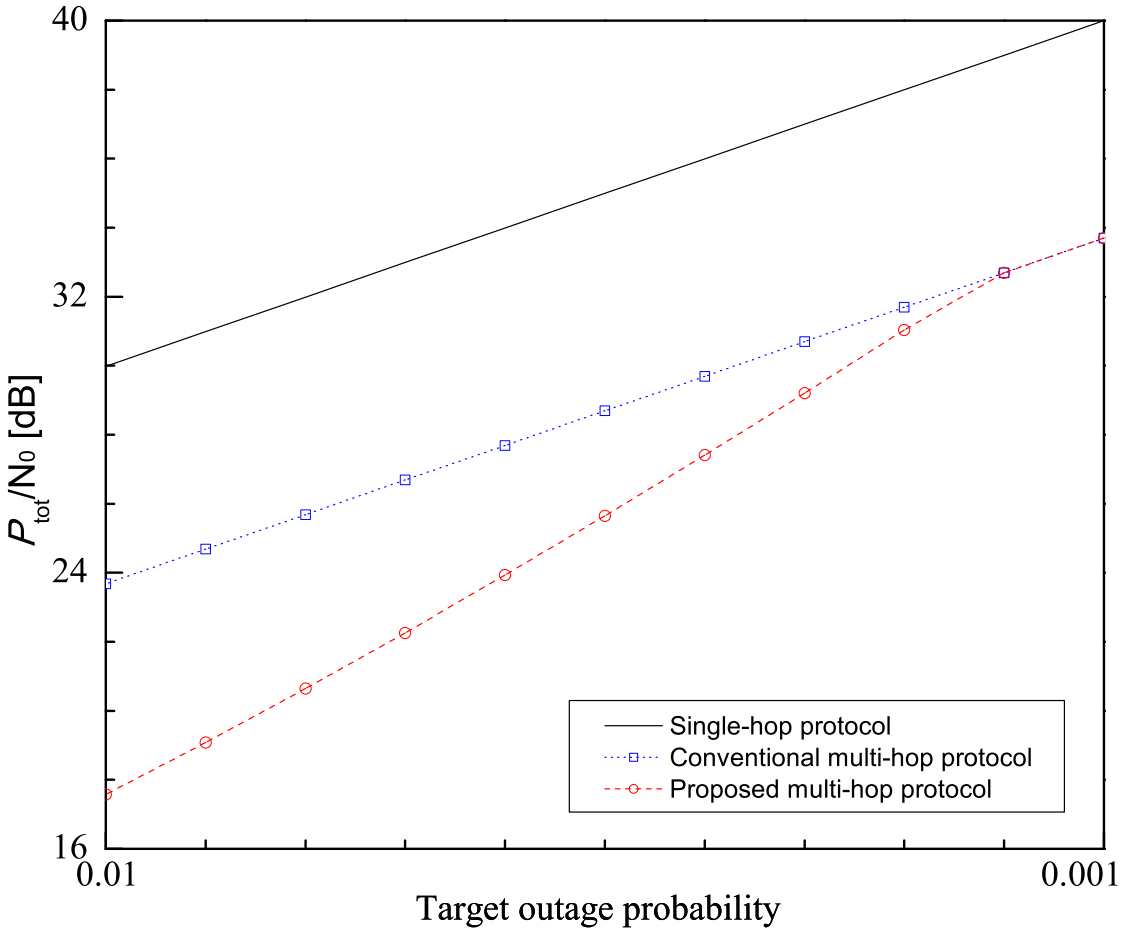
40
32
24
16
P_{tot}/N_0 [dB]
0.01
0.001
Target outage probability
Single-hop protocol
Conventional multi-hop protocol
Proposed multi-hop protocol

(b) α=5

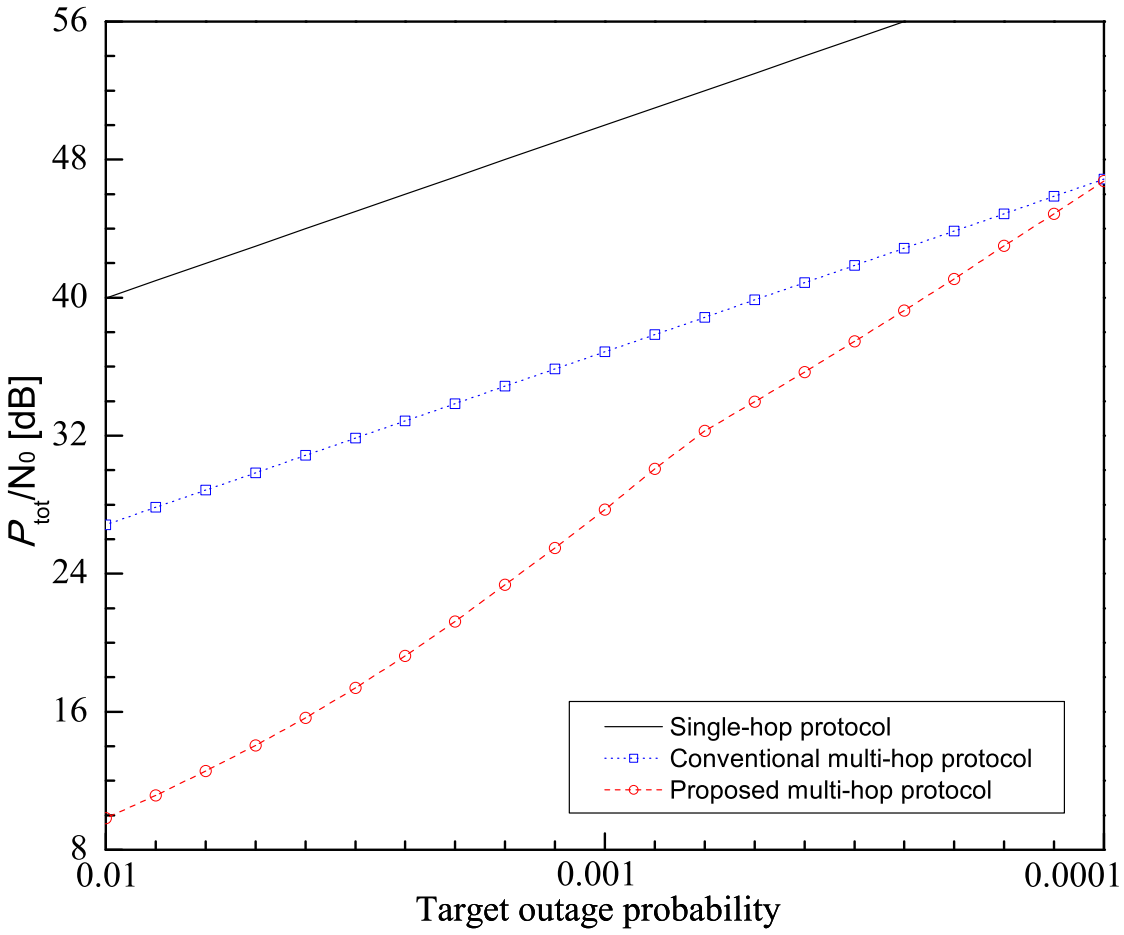

(c) α=6

Figure 2.14. Required transmission SNR versus the target outage probability for the multi-hop network with the target rate $R = 1$ b/s/Hz and the distance between the source and the destination $d_{0,K}$=10.

it converges to and eventually becomes same to that of the conventional multi-hop protocol as SNR increases.

2.5 Extension to an AF protocol

The concept of the proposed novel DF protocol is extended the AF protocol. That is, the relays in Figure 2.1 are assumed to be the AF relays. In the m-th phase of n-th frame, the received signal is given by

$$y_k = G_{k-1} h_{k-1,k} y_{k-1} + \sum_{i=0}^{\frac{k-m-M}{M}} G_{k_i} h_{k_i,k} y_{k_i} + \omega_k \tag{2.94}$$

rather than (2.5) where G_i is the amplification factor at T_i. The amplification factor is given by

$$G_k = \begin{cases} \sqrt{P_0}, & k = 0, \\ \sqrt{\dfrac{P_k}{|h_{k-1,k}|^2 P_{k-1} + \sum\limits_{i=0}^{\frac{k-m-M}{M}} |h_{k_i,k}|^2 P_{k_i} + 1}}, & \text{otherwise.} \end{cases} \tag{2.95}$$

The received SINR at T_K is given by

$$\gamma_{K-1,K}^{AF} = \frac{\prod\limits_{k=1}^{K} G_{k-1}^2 |h_{k-1,k}|^2}{\sum\limits_{k=1}^{K} \left\{ \left(\sum\limits_{i=0}^{\frac{k-m-M}{M}} G_{k_i}^2 |h_{k_i,k}|^2 + 1 \right) \prod\limits_{j=k}^{K-1} G_j^2 |h_{j,j+1}|^2 \right\} + 1}. \tag{2.96}$$

At the high SNR region and by assuming $G_k^2 = 1/|h_{k-1,k}|^2$ which is a benchmark for an AF protocol [81], it is approximated as

$$\gamma_{K-1,K}^{AF} \approx \left(\sum_{k=1}^{K} \frac{\sum\limits_{i=0}^{\left\lfloor \frac{k-M-1}{M} \right\rfloor} P_{k_i} |h_{k_i,k}|^2 + 1}{P_{k-1} |h_{k-1,k}|^2} \right)^{-1} = \left(\sum_{k=1}^{K} \frac{1}{\gamma_{k-1,k}} \right)^{-1}. \tag{2.97}$$

This is maximized when $\gamma_{0,1} = \gamma_{1,2} = \cdots = \gamma_{k-1,k}$. Then, the power allocation becomes identical to Section 2.3.2. Also, the values of M and K are obtained similarly to Section 2.3.3.

Figure 2.15 shows the outage probability for various path-loss exponents α with the target rate R=1 and the distance between the source and the destination $d_{0,K}$=10. It is shown that the outage probability of the AF multi-hop protocol is lower than that of the conventional AF multi-hop protocol in low SNR region and converges to that of the conventional AF multi-hop protocol as SNR increases similar to the DF multi-hop protocol. It is also shown that the AF multi-hop protocol achieves higher outage probability than the DF multi-hop protocol due to the interference and noise amplification.

2.6 Summary

In this chapter, we propose a novel DF protocol for a multi-hop network. In the proposed protocol, multiple terminals transmit simultaneously to minimize the outage probability. We analyze the outage probability of the proposed protocol. Also, we propose an optimization algorithm that minimize the outage probability. The optimization algorithm includes the power allocation and the selection of the number of hops and phases. Also, we propose the reduced complexity selection of the number of hops and phases by using some approximations and mathematical manipulations. Some examples show that the reduced complexity selection reduces the computational complexity significantly. Numerical results verify the validity of theoretical analysis by comparison with Monte Carlo simulation results. It is shown that the proposed multi-hop protocol provides lower outage probability than the conventional multi-hop

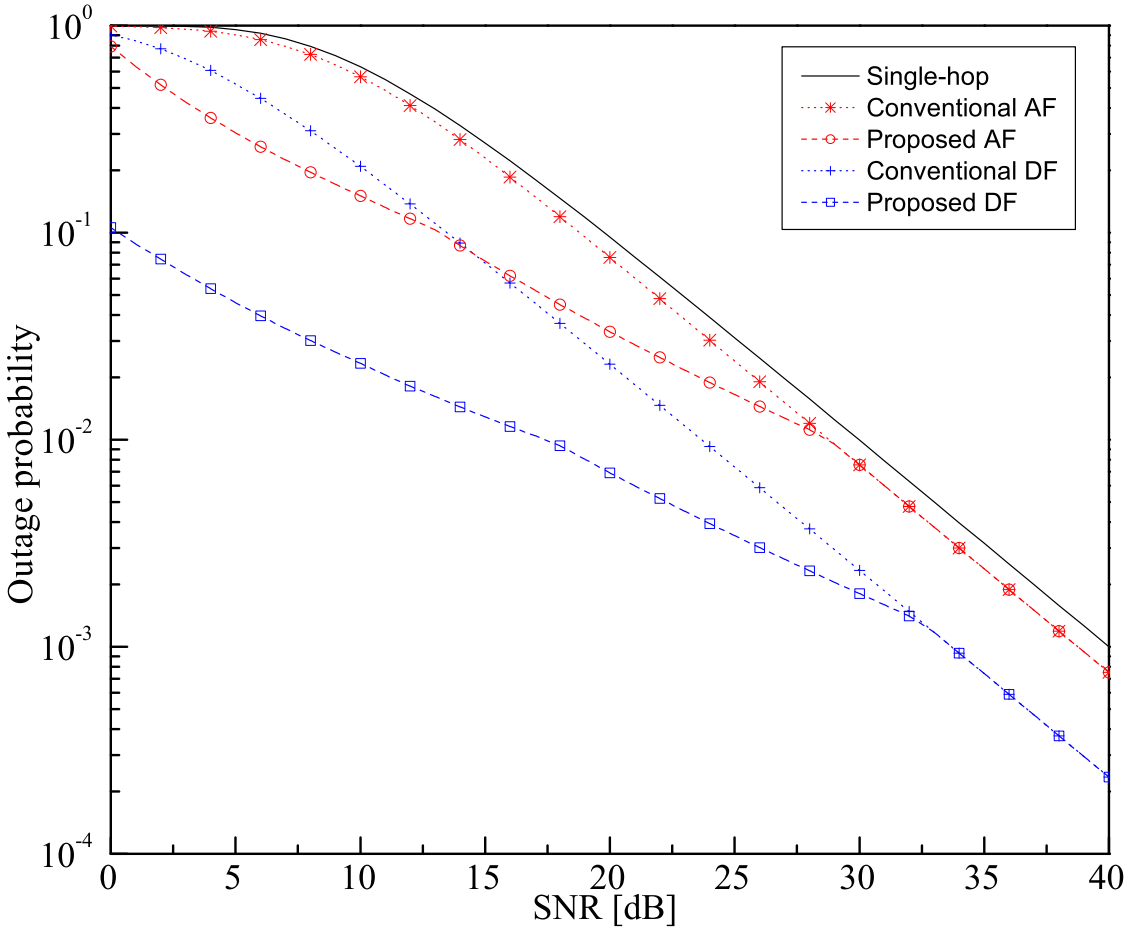
Single-hop
Conventional AF
Proposed AF
Conventional DF
Proposed DF
Outage probability
SNR [dB]
10^0
10^-1
10^-2
10^-3
10^-4
0
5
10
15
20
25
30
35
40

(a) $\alpha = 5$

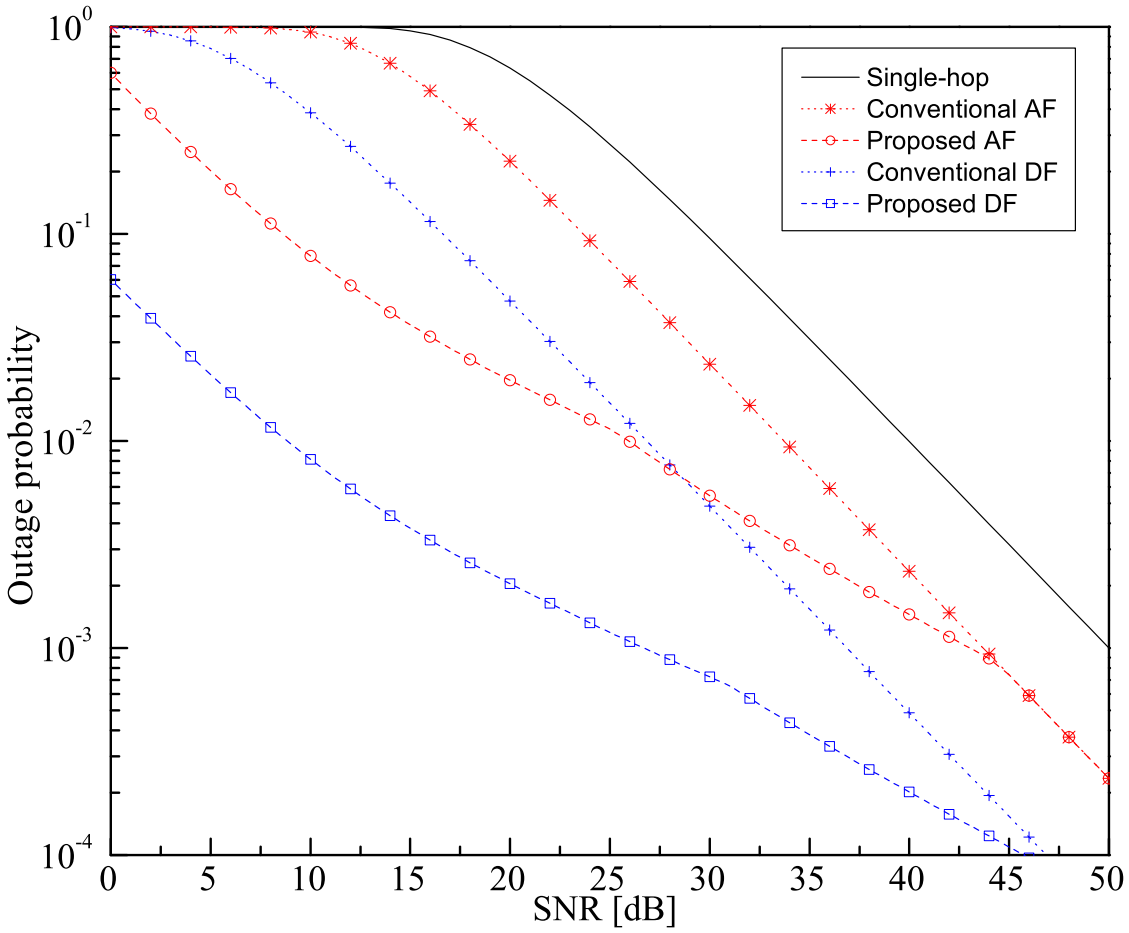

(b) $\alpha = 6$

Figure 2.15. Outage probability for various path-loss exponents α with the target rate R=1 and the distance between the source and the destination $d_{0,K}$=10.

protocol as well as single-hop protocol. Especially, the proposed multi-hop protocol is more attractive in the case of low signal-to-noise ratio (SNR) and that of high path-loss exponent. It is also shown that the reduced complexity selection provides almost same outage probability to the exhaustive search in most regions. In addition, we extend the concept of the proposed DF protocol to the AF protocol.

Chapter 3

Spectrum Sharing Cognitive Radio Network

As the demands for wireless services are growing rapidly, the demands for spectrum resources are also growing rapidly. In conventional policies, most of spectrum bands are exclusively allocated and only the PUs, the users in the primary network (licensed network), are allowed to utilize the spectrum bands. According to some surveys of spectrum utilization, it is found that the spectrum occupancy is very low and it needs to improve the spectrum utilization efficiency [45]-[47]. For example, the spectrum occupancy is 13.1% in New York City and 35% in Washington, D.C., at the spectrum bands below 3GHz [48]. Also, the spectrum occupancy varies significantly in time, spectrum bands, and locations.

As the residual spectrum resources are deficient and the additional demands for spectrum resources are growing, a new approach called a CR network is introduced [49], [50]. In the CR network, the SUs, the users in the secondary network (unlicensed network), are allowed to utilize the unlicensed spectrum according to its

surrounding environment [51]. Generally, the performance of the secondary network is worse than the primary network due to its essential utilization property. As an attractive approach to improve the performance of the secondary network, the relay communication is drawing a lot of interest.

There are mainly two approaches in the CR network: spectrum sensing and spectrum sharing. In the spectrum sensing CR network, the SUs are allowed to utilize the unlicensed spectrum if and only if the PUs do not utilize the spectrum bands [52]. The relay communication is applied in the spectrum sensing CR network in two different ways. First way is so-called cooperative spectrum sensing. For the utilization of the unlicensed network, the SUs should observe the signal from the PUs carefully. In the cooperative spectrum sensing, multiple SUs act as the relays by forwarding the observed signal to the fusion center [48]. The performance of cooperative spectrum sensing is investigated in terms of the missed-detection probability and the false alarm probability [53]-[57]. Second way is the dual-hop communication between the source and destination in the secondary network. The performance of the dual-hop communication in the secondary network is investigated in terms of the outage probability [58]-[60].

In the spectrum sharing CR network, the SUs are allowed to utilize the unlicensed spectrum if the QoS of PUs is guaranteed though the PUs utilize the spectrum bands [61]. The SUs in the spectrum sharing CR network is more probable to utilize the unlicensed spectrum compared to the spectrum sensing CR network. However, the signal from PUs becomes the interference in the SUs and vice versa as both PUs and SUs utilize the same spectrum simultaneously. The relay communication in the spectrum sharing CR network has been studied as follows. In [62], Y. Zou *et al.* analyze the outage probability of the best relay selection for the secondary network interfered

by the signal from PUs. However, they did not consider the interference at the PUs by the SUs. In [63] and [64], J. Lee and D. Li *et al.* analyze the outage probability of the best relay selection for the secondary network where the transmission power is limited by the interference to the PUs. However, they did not consider the interference from the PUs. In [65], W. Xu *et al.* analyze the outage probability of the secondary network considering both interference. However, they consider one relay. Also, most of works on the spectrum sharing CR network assumed the perfect synchronization and perfect CSI between the primary network and the secondary network. However, since the primary network the secondary network can not controlled by one central unit simultaneously, this is impractical.

This chapter investigates the spectrum sharing CR network. We suppose multiple relays and the both interference interacted between the primary network and the secondary network. We consider three network scenarios according to the relation of the primary network and secondary network: one that the primary network and secondary network are synchronized, one that the primary network and secondary network are not synchronized with same frame length, and one that the frame lengths of the primary network and secondary network are different. For each scenario, we propose an power allocation and relay selection. Also, we analyze the outage probability.

The remainder of this chapter is organized as follows. Section 3.1 describes the system model and three scenarios. In Section 3.2, we propose the power allocation and relay selection for each scenario. In Section 3.3, we derive the outage probability for each scenario. In Section 3.4, numerical results verify the validity of the performance analysis by comparison with Monte Carlo simulation results. Also, we compare the performance of the proposed relay selection with the random relay selection. Finally, this Chapter is summarized in Section 3.6.

3.1 System Model and Network Scenarios

Consider a spectrum sharing CR network where the primary network and the secondary network co-exist as shown in Figure 3.1. The primary network consists of M source and destination pairs, PS_m and $PD_m, m = 1, \cdots, M$. The secondary network consists of a source S, a destination D, and K relays $R_k, k = 1, \cdots, K$. The transmission of the primary network is the interference in the secondary network and vice versa. The solid lines and dashed lines in Figure 3.1 represent the desired transmission and the interfered transmission, respectively.

Assume that the channel between the terminal i and the terminal j has the channel coefficient $h_{i,j}$ which is a zero-mean circularly symmetric complex Gaussian random variable with the variance $\lambda_{i,j}$. The channel variance is given by (2.3). Assume that the terminals in the primary network are placed contiguously and so do the terminals in the secondary network. Especially, the relays are placed very contiguously. Then, we have

$$d_{S,R_k} = d_{S,R} \quad \forall k, \tag{3.1}$$

$$d_{R_k,D} = d_{R,D} \quad \forall k, \tag{3.2}$$

$$d_{PS_m,R_k} = d_{PS,R} \quad \forall k, m, \tag{3.3}$$

$$d_{PS_m,D} = d_{PS,D} \quad \forall m, \tag{3.4}$$

$$d_{S,PD_m} = d_{S,PD} \quad \forall m, \tag{3.5}$$

$$d_{R_k,PD_m} = d_{R,PD} \quad \forall k, m \tag{3.6}$$

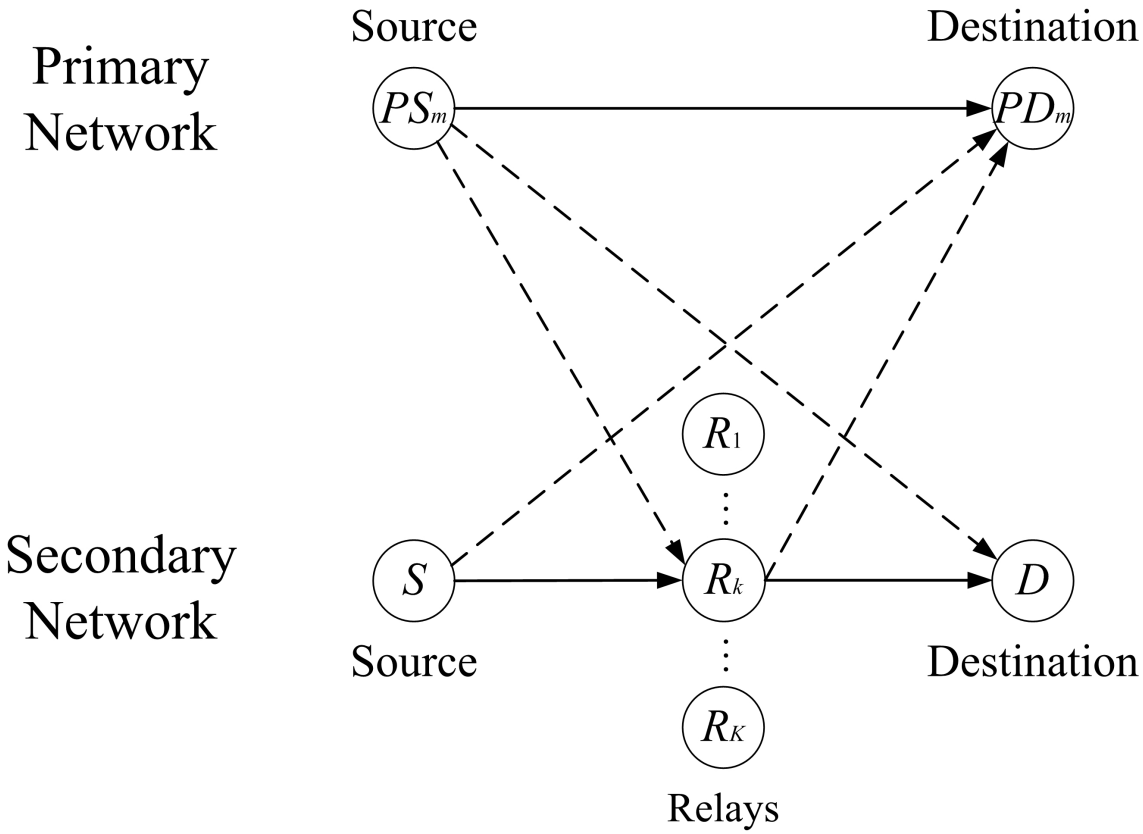

Figure 3.1. System model of the cognitive radio network where the primary network and the secondary network co-exist. Solid lines and dashed lines represent the desired transmission and the interfered transmission, respectively.

which imply

$$\lambda_{S,R_k} = \lambda_{S,R} \quad \forall k, \tag{3.7}$$

$$\lambda_{R_k,D} = \lambda_{R,D} \quad \forall k, \tag{3.8}$$

$$\lambda_{PS_m,R_k} = \lambda_{PS,R} \quad \forall k, m, \tag{3.9}$$

$$\lambda_{PS_m,D} = \lambda_{PS,D} \quad \forall m, \tag{3.10}$$

$$\lambda_{S,PD_m} = \lambda_{S,PD} \quad \forall m, \tag{3.11}$$

$$\lambda_{R_k,PD_m} = \lambda_{R,PD} \quad \forall k, m. \tag{3.12}$$

Assume that the direct path between S and D is not available and S transmits its data signal to D over two phases. In the first phase, S transmits its data signal s_S with power P_S to all relays.

Suppose that the relay decodes the signal from the source s_S successfully if the SINR is larger than or equal to the threshold SINR γ_{th}. The threshold SINR is given by

$$\gamma_{th} = 2^{2R} - 1 \tag{3.13}$$

for the target rate R. This equation is derived from

$$R = \frac{1}{2} \log \left(1 + \gamma_{th}\right) \tag{3.14}$$

where the pre-log factor $1/2$ comes from the fact that the source transmits its data to the destination over two phases. If there is one relay, i.e., $K = 1$, the relay decodes and forward the signal from the source without the relay selection. If there is multiple relay, i.e., $K \neq 1$, the relay is selected based on the decoding set. The decoding set $\mathcal{D}$ is given by

$$\mathcal{D} = \left\{R_k : \gamma_{S,R_k} \geq \gamma_{th}\right\}. \tag{3.15}$$

where $\gamma_{i,j}$ is the received SINR of the channel from the terminal i to the terminal j. Then, the relay is selected such that

$$R^* = \arg \max_{R_k \in \mathcal{D}} \mathbb{E}\left[\gamma_{R_k,D}\right]. \tag{3.16}$$

The selected relay R^* transmits s_S to D with power P_R in the second phase.

In the primary network, one source PS_m is active on the certain moment. PS_m transmits its data signal s_{PS_m} with power P_{PS}. We consider three network scenarios according to the relation of the primary and secondary networks as shown in Figure 3.2.

In the scenario 1, the frame length of two networks are same and the frames are synchronized perfectly as the terminals in the secondary network fully know the information of the primary network. Also, the terminals in the secondary network know the instantaneous CSI from and to the terminals in the primary network as well as the terminals in the secondary network.

In the scenario 2, the frame length of two networks are same but the frames are not synchronized. Each terminal in the secondary network knows only the statistical CSI from and to the terminals in the primary network while it knows the instantaneous CSI from and to the terminals in the secondary network.

In the scenario 3, both the frame length and timing of two networks are not matched as the terminals in the secondary network have little information of the primary network. Similar to the scenario 2, each terminal in the secondary network know only the statistical CSI from and to the terminals in the primary network and the instantaneous CSI from and to the terminals in the secondary network. For convenience, assume that the frame length of the primary network T_P is longer than the frame length of the secondary network T_S.

Figure 3.3 shows the transmission protocol of the CR network for one frame of

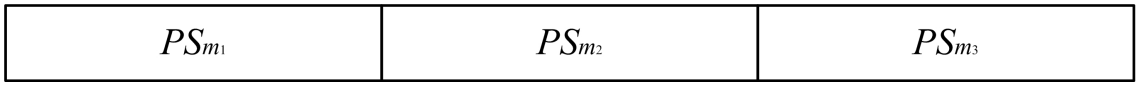

(a) Primary network

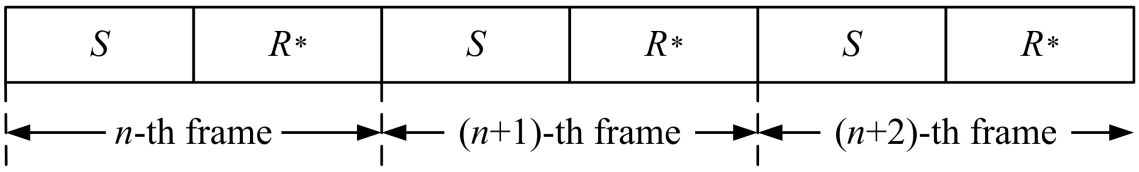

(b) Secondary network of scenario 1

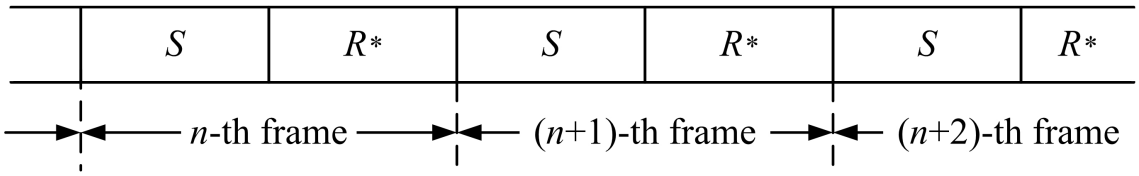

(c) Secondary network of scenario 2

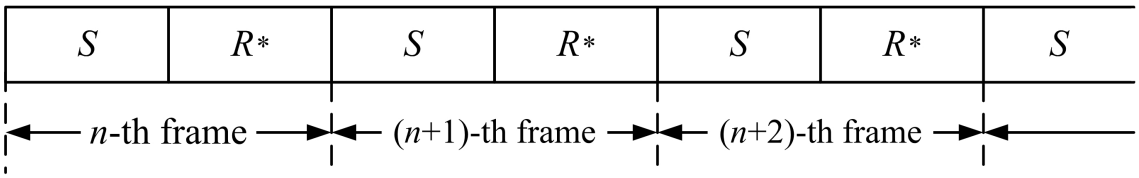

(d) Secondary network of scenario 3

Figure 3.2. Transmission protocol of the cognitive radio network for three network scenarios according to the relation of the primary and secondary networks.

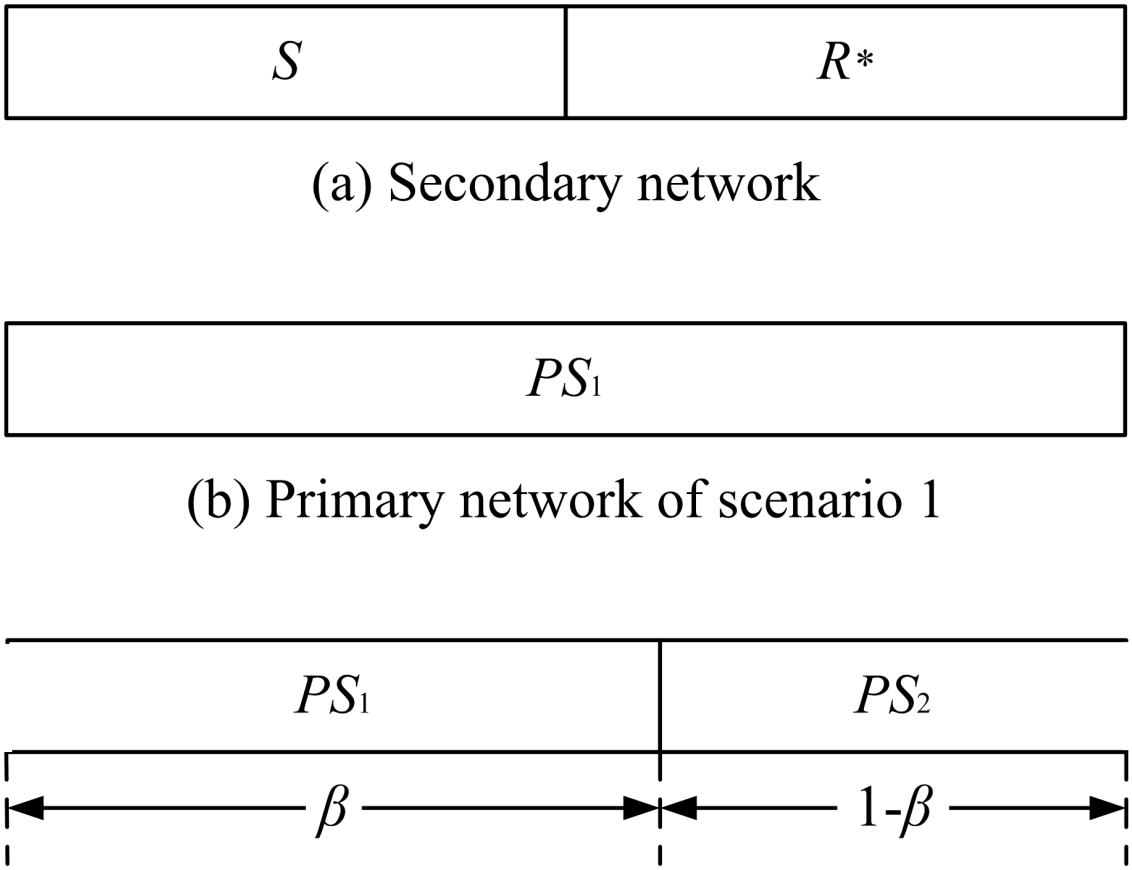

Figure 3.3. Transmission protocol of the cognitive radio network for one frame of secondary network.

secondary network. Without loss of generality, it is possible to use only PS_1 and PS_2 to indicate the sources in the primary network. In Figure 3.3. (c), β is the time fractions of PS_1 and it is in the range $(0, 1]$. In the scenario 2, β is a fixed value. However, in the scenario 3, β is a variable value. Note that β is the mixed discrete-continuous random variable [82]. Its CDF is given by

$$F_\beta(b) = \begin{cases} bT_S/T_P, & 0 < b < 1, \\ 1, & b = 1. \end{cases} \tag{3.17}$$

3.2 Power Allocation and Relay Selection

3.2.1 Scenario 1

There are two constraints on the transmission power of the secondary network: the maximum power constraint and the interference constraint [63]. The former is given by

$$P_i \leq P_i^{\max} \tag{3.18}$$

where $P_i^{\max}$ is the maximum transmission power of the terminal i.

The latter is required to guarantee the quality of service (QoS). This constraint is given by

$$P_i \leq \frac{\bar{I}}{|h_{i,PD_m}|^2} \tag{3.19}$$

where $\bar{I}$ is the pre-determined interference threshold.

It is well known that each terminal should use the maximum transmit power to maximizes the performance, e.g., to minimize the outage performance or to maximize the SINR when each terminal has its own power limit [39]. Hence, the transmission power is given by

$$P_i = \min\left\{\frac{\bar{I}}{|h_{i,PD_m}|^2}, P_i^{\max}\right\}. \tag{3.20}$$

On the other hand, the received SINR at R_k is given by

$$\gamma_{S,R_k} = \frac{|h_{S,R_k}|^2 P_S}{|h_{PS_1,R_k}|^2 P_{PS_1} + 1}. \tag{3.21}$$

If the relay R_k is selected, the received SINR at D is given by

$$\gamma_{R_k,D} = \frac{|h_{R_k,D}|^2 P_{R_k}}{|h_{PS_1,D}|^2 P_{PS_1} + 1}. \tag{3.22}$$

Since the terminals in the secondary network know all CSI in (3.21) and (3.22), the relay selection (3.16) becomes

$$R^* = \arg \max_{R_k \in \mathcal{D}} \gamma_{R_k,D}. \tag{3.23}$$

This is identical to [30]

$$R^* = \max_k \min\{\gamma_{S,R_k}, \gamma_{R_k,D}\}. \tag{3.24}$$

The relay is selected either in centralized manner or in distributed manner. In the centralized manner, the central unit selects R^* and let the relays know the selected relay. The distributed manner is applied similar to [29]. Each relay in $\mathcal{D}$ starts its own timer inversely proportional to $\gamma_{R_k,D}$. The relay broadcasts the flag packet to other relay as soon as the the timer reduced to zero. If the relay receives the flag packet from other relay, the relay stops all procedures. Then, the relay that satisfies (3.23) is selected.

3.2.2 Scenarios 2 and 3

The power allocation and relay selection for the scenarios 2 and 3 are identical. The maximum power constraint is given by (3.18). The interference constraint is different to (3.19) since the terminals in the secondary network know only the statistical CSI from and to the terminals in the primary network. It is given by [83], [84]

$$\Pr[P_i |h_{i,PD_m}|^2 \geq \bar{I}] \leq \epsilon \tag{3.25}$$

where ϵ is the pre-determined tolerable probability threshold. Let

$$X_{i,j} = P_i |h_{i,j}|^2 \tag{3.26}$$

similar to (2.7). The PDF and CDF of $X_{i,j}$ is given by [73]

$$f_{X_{i,j}}(x) = \frac{1}{P_i \lambda_{i,j}} \exp\left(-\frac{x}{P_i \lambda_{i,j}}\right), \tag{3.27}$$

$$F_{X_{i,j}}(x) = 1 - \exp\left(-\frac{x}{P_i \lambda_{i,j}}\right). \tag{3.28}$$

Using (3.28), the left-hand side of (3.25) becomes

$$\Pr[P_i |h_{i,PD_m}|^2 \geq \bar{I}] = \Pr\left[X_{i,PD_m} \geq \bar{I}\right] = \exp\left(-\frac{\bar{I}}{P_i \lambda_{i,PD}}\right). \tag{3.29}$$

Substituting (3.29) into (3.25), the interference constraint is given by

$$P_i \leq \frac{-\bar{I}}{\lambda_{i,PD} \ln \epsilon}. \tag{3.30}$$

From (3.18) and (3.30), the transmission power is given by

$$P_i = \min\left\{P_i^{\max}, \frac{-\bar{I}}{\lambda_{i,PD} \ln \epsilon}\right\}. \tag{3.31}$$

Suppose $\beta \leq 1/2$. The received SINR at R_k is given by

$$\gamma_{S,R_k} = \frac{|h_{S,R_k}|^2 P_S}{2\beta |h_{PS_1,R_k}|^2 P_{PS} + (1-2\beta)|h_{PS_2,R_k}|^2 P_{PS} + 1}. \tag{3.32}$$

If the relay R_k is selected, the received SINR at D is given by

$$\gamma_{R_k,D} = \frac{|h_{R_k,D}|^2 P_{R_k}}{|h_{PS_2,D}|^2 P_{PS} + 1}. \tag{3.33}$$

Next, suppose $\beta > 1/2$. The received SINR at R_k is given by

$$\gamma_{S,R_k} = \frac{|h_{S,R_k}|^2 P_S}{|h_{PS_1,R_k}|^2 P_{PS} + 1}. \tag{3.34}$$

If the relay R_k is selected, the received SINR at D is given by

$$\gamma_{R_k,D} = \frac{|h_{R_k,D}|^2 P_{R_k}}{(2\beta-1)|h_{PS_1,D}|^2 P_{PS} + 2(1-\beta)|h_{PS_2,D}|^2 P_{PS} + 1}. \tag{3.35}$$

After some manipulations, the relay selection (3.16) is simplified to

$$R^* = \arg\max_{R_k \in \mathcal{D}} |h_{R_k,D}|^2. \tag{3.36}$$

The distributed relay selection is similar to that in Section 3.2.1 with the timer inversely proportional to $|h_{R_k,D}|^2$.

3.3 Outage Probability

3.3.1 Scenario 1

Based on the relay selection in (3.24), the outage probability is given by

$$\begin{aligned} P_{out} &= \Pr[\max_k \min\{\gamma_{S,R_k}, \gamma_{R_k,D}\} < \gamma_{th}] \\ &= \prod_{k=1}^{K} \Pr[\min\{\gamma_{S,R_k}, \gamma_{R_k,D}\} < \gamma_{th}] \\ &= \prod_{k=1}^{K} \Pr[\gamma_{S,R_k} < \gamma_{th}] \times \Pr[\gamma_{R_k,D} < \gamma_{th}]. \end{aligned} \tag{3.37}$$

Theorem 2. *Let $Y_i, i = 1,2,3$, be the independent exponential random variables with mean λ_i. The CDF of a random variable $Z_1 = \frac{Y_1 \min\left\{\frac{c_1}{Y_2}, c_2\right\}}{c_3 Y_3 + 1}$ for the constants*

$c_i, i = 1, 2, 3,$ *is given by*

$$\begin{aligned} F_{Z_1}(z) &= g(\lambda_1, \lambda_2, \lambda_3, c_1, c_2, c_3, z) \\ &\triangleq 1 - \frac{c_2\lambda_1}{c_2\lambda_1 + c_3\lambda_3 z} \exp\left(-\frac{z}{c_2\lambda_1}\right) \left\{1 - \exp\left(-\frac{c_1}{c_2\lambda_2}\right)\right\} \\ &\quad - \frac{c_1\lambda_1}{c_3\lambda_2\lambda_3 z} \exp\left\{\frac{1}{c_3\lambda_3}\left(\frac{c_1\lambda_1}{\lambda_2 z} + 1\right)\right\} E_1\left[\frac{1}{c_3\lambda_3}\left(\frac{c_1\lambda_1}{\lambda_2 z} + 1\right) + \frac{1}{c_2}\left(\frac{c_1}{\lambda_2} + \frac{z}{\lambda_1}\right)\right]. \end{aligned} \tag{3.38}$$

Proof. See Appendix A. □

Substituting (3.20) into (3.21) and (3.22), γ_{S,R_k} and $\gamma_{R_k,D}$ are the random variables considered in *Theorem* 2. Applying *Theorem* 2 to (3.37), the outage probability is given by

$$\begin{aligned} P_{out} = \big[1 - \big\{1 - g\left(\lambda_{S,R}, \lambda_{S,PD}, \lambda_{PS,R}, \bar{I}, P_S^{\max}, P_{PS}, \gamma_{th}\right)\big\} \\ \times \big\{1 - g\left(\lambda_{R,D}, \lambda_{R,PD}, \lambda_{PS,D}, \bar{I}, P_R^{\max}, P_{PS}, \gamma_{th}\right)\big\}\big]^K. \end{aligned} \tag{3.39}$$

3.3.2 Scenario 2

The outage probability is given by

$$P_{out} = \Pr\left[\gamma_{R^*,D} < \gamma_{th}\right]. \tag{3.40}$$

We derive the outage probability according to the range of β.

Theorem 3. *For $0 < \beta < 1/4$ or $1/4 < \beta < 1/2$, the outage probability is given by*

$$\begin{aligned} P_{out,0<\beta<\frac{1}{4}} &= P_{out,\frac{1}{4}<\beta<\frac{1}{2}} \\ &= \left\{1 - \eta_1 \exp\left(-\frac{\gamma_{th}}{P_R\lambda_{R,D}}\right)\right\}^K \\ &\quad + K! \exp\left(\frac{1}{P_{PS}\lambda_{PS,D}}\right) \sum_{d=1}^{K} \frac{\eta_1^d (1-\eta_1)^{K-d}}{(K-d)!(d-1)!} \\ &\quad \times B_{\exp\left(-\frac{\gamma_{th}}{P_R\lambda_{R,D}}\right)}\left(1 + \frac{P_R\lambda_{R,D}}{P_{PS}\lambda_{PS,D}\gamma_{th}}, d\right) \end{aligned} \tag{3.41}$$

where

$$\begin{aligned} \eta_1 = &\frac{1}{(4\beta-1)P_{PS}\lambda_{PS,R}} \exp\left(-\frac{\gamma_{th}}{P_S\lambda_{S,R}}\right) \\ &\times \left\{\left(\frac{\gamma_{th}}{P_S\lambda_{S,R}} + \frac{1}{2\beta P_{PS}\lambda_{PS,R}}\right)^{-1}\right. \\ &\quad \left. - \left(\frac{\gamma_{th}}{P_S\lambda_{S,R}} + \frac{1}{(1-2\beta)P_{PS}\lambda_{PS,R}}\right)^{-1}\right\}. \end{aligned} \tag{3.42}$$

Proof. See Appendix B. □

Theorem 4. *For $\beta = 1/4$, the outage probability is given by*

$$\begin{aligned} P_{out,\beta=\frac{1}{4}} &= \left\{1 - \eta_2 \exp\left(-\frac{\gamma_{th}}{P_R\lambda_{R,D}}\right)\right\}^K \\ &\quad + K! \exp\left(\frac{1}{P_{PS}\lambda_{PS,D}}\right) \sum_{d=1}^{K} \frac{\eta_2^d (1-\eta_2)^{K-d}}{(K-d)!(d-1)!} \\ &\quad \times B_{\exp\left(-\frac{\gamma_{th}}{P_R\lambda_{R,D}}\right)}\left(1 + \frac{P_R\lambda_{R,D}}{P_{PS}\lambda_{PS,D}\gamma_{th}}, d\right) \end{aligned} \tag{3.43}$$

where

$$\eta_2 = \frac{4}{\left(P_{PS}\lambda_{PS,R}\right)^2} \exp\left(-\frac{\gamma_{th}}{P_S\lambda_{S,R}}\right) \left(\frac{\gamma_{th}}{P_S\lambda_{S,R}} + \frac{2}{P_{PS}\lambda_{PS,R}}\right)^{-2}. \tag{3.44}$$

Proof. See Appendix C. □

Theorem 5. *For $1/2 < \beta < 3/4$ or $3/4 < \beta < 1$, the outage probability is given by*

$$\begin{aligned}
P_{out,\frac{1}{2}<\beta<\frac{3}{4}} &= P_{out,\frac{3}{4}<\beta<1} \\
&= \left\{1 - \eta_3 \exp\left(-\frac{\gamma_{th}}{P_R\lambda_{R,D}}\right)\right\}^K \\
&\quad + K!\frac{2\beta-1}{4\beta-3}\exp\left(\frac{1}{(2\beta-1)P_{PS}\lambda_{PS,D}}\right) \\
&\quad \times \sum_{d=1}^{K} \frac{\eta_3^d(1-\eta_3)^{K-d}}{(K-d)!(d-1)!} B_{\exp\left(-\frac{\gamma_{th}}{P_R\lambda_{R,D}}\right)}\left(1 + \frac{P_R\lambda_{R,D}}{(2\beta-1)P_{PS}\lambda_{PS,D}\gamma_{th}}, d\right) \\
&\quad - K!\frac{2(1-\beta)}{4\beta-3}\exp\left(\frac{1}{2(1-\beta)P_{PS}\lambda_{PS,D}}\right) \\
&\quad \times \sum_{d=1}^{K} \frac{\eta_3^d(1-\eta_3)^{K-d}}{(K-d)!(d-1)!} B_{\exp\left(-\frac{\gamma_{th}}{P_R\lambda_{R,D}}\right)}\left(1 + \frac{P_R\lambda_{R,D}}{2(1-\beta)P_{PS}\lambda_{PS,D}\gamma_{th}}, d\right)
\end{aligned} \tag{3.45}$$

where

$$\eta_3 = \exp\left(-\frac{\gamma_{th}}{P_S\lambda_{S,R}}\right)\left(1 + \frac{P_{PS}\lambda_{S,R}}{P_S\lambda_{S,R}}\gamma_{th}\right)^{-1}. \tag{3.46}$$

Proof. See Appendix D. □

Theorem 6. *For $\beta = 3/4$, the outage probability is given by*

$$\begin{aligned}
P_{out,\beta=\frac{3}{4}} &= \left\{1 - \eta_3 \exp\left(-\frac{\gamma_{th}}{P_R\lambda_{R,D}}\right)\right\}^K \\
&\quad + K!\exp\left(\frac{2}{P_{PS}\lambda_{PS,D}}\right) \\
&\quad \times \sum_{d=1}^{K} \frac{\eta_3^d(1-\eta_3)^{K-d}}{(K-d)!(d-1)!} B_{\exp\left(-\frac{\gamma_{th}}{P_R\lambda_{R,D}}\right)}\left(1 + \frac{2P_R\lambda_{R,D}}{P_{PS}\lambda_{PS,D}\gamma_{th}}, d\right) \\
&\quad + K!\frac{2\gamma_{th}}{P_{PS}\lambda_{PS,D}P_R\lambda_{R,D}}\exp\left(-\frac{\gamma_{th}}{P_R\lambda_{R,D}}\right)\left(\frac{2}{P_{PS}\lambda_{PS,D}} + \frac{\gamma_{th}}{P_R\lambda_{R,D}}\right)^{-2} \\
&\quad \times \sum_{d=1}^{K} \frac{\eta_3^d(1-\eta_3)^{K-d}}{(K-d)!(d-1)!} {}_3F_2\left[\frac{2P_R\lambda_{R,D}}{P_{PS}\lambda_{PS,D}\gamma_{th}} + 1, \frac{2P_R\lambda_{R,D}}{P_{PS}\lambda_{PS,D}\gamma_{th}} + 1, 1-d;\right. \\
&\qquad \left. \frac{2P_R\lambda_{R,D}}{P_{PS}\lambda_{PS,D}\gamma_{th}} + 2, \frac{2P_R\lambda_{R,D}}{P_{PS}\lambda_{PS,D}\gamma_{th}} + 2; \exp\left(-\frac{\gamma_{th}}{P_R\lambda_{R,D}}\right)\right].
\end{aligned} \tag{3.47}$$

Proof. See Appendix E. □

Theorem 7. *For $\beta = 1/2$ or $\beta = 1$, the outage probability is given by*

$$\begin{aligned} P_{out,\beta=\frac{1}{2}} &= P_{out,\beta=1} \\ &= \left\{1 - \eta_3 \exp\left(-\frac{\gamma_{th}}{P_R\lambda_{R,D}}\right)\right\}^K \\ &\quad + K! \exp\left(\frac{1}{P_{PS}\lambda_{PS,D}}\right) \sum_{d=1}^{K} \frac{\eta_3^d (1-\eta_3)^{K-d}}{(K-d)!(d-1)!} \\ &\quad \times B_{\exp\left(-\frac{\gamma_{th}}{P_R\lambda_{R,D}}\right)}\left(1 + \frac{P_R\lambda_{R,D}}{P_{PS}\lambda_{PS,D}\gamma_{th}}, d\right). \end{aligned} \tag{3.48}$$

Proof. The probability of decoding set is given by (D.2). The probability that the outage event occurs for the decoding set $\mathcal{D}$ is given by (B.5). Substituting (B.5) and (D.2) into (B.8), we obtain (3.48). □

Corollary 3. *If there is only one relay, i.e., $K = 1$, the outage probability is given by*

$$P_{out,0<\beta<\frac{1}{4}} = P_{out,\frac{1}{4}<\beta<\frac{1}{2}} = 1 - \eta_1 \exp\left(-\frac{\gamma_{th}}{P_R\lambda_{R,D}}\right)\left(\frac{P_{PS}\lambda_{PS,D}}{P_R\lambda_{R,D}}\gamma_{th} + 1\right)^{-1}, \tag{3.49}$$

$$P_{out,\beta=\frac{1}{4}} = 1 - \eta_2 \exp\left(-\frac{\gamma_{th}}{P_R\lambda_{R,D}}\right)\left(\frac{P_{PS}\lambda_{PS,D}}{P_R\lambda_{R,D}}\gamma_{th} + 1\right)^{-1}, \tag{3.50}$$

$$\begin{aligned} P_{out,\frac{1}{2}<\beta<\frac{3}{4}} = P_{out,\frac{3}{4}<\beta<1} &= 1 - \frac{\eta_3}{(4\beta-3)} \exp\left(-\frac{\gamma_{th}}{P_R\lambda_{R,D}}\right) \\ &\quad \times \left\{\left(\frac{P_{PS}\lambda_{PS,D}}{P_R\lambda_{R,D}}\gamma_{th} + \frac{1}{2\beta-1}\right)^{-1}\right. \\ &\quad \left. - \left(\frac{P_{PS}\lambda_{PS,D}}{P_R\lambda_{R,D}}\gamma_{th} + \frac{1}{2(1-\beta)}\right)^{-1}\right\}, \end{aligned} \tag{3.51}$$

$$\begin{aligned} P_{out,\beta=\frac{3}{4}} &= 1 - \frac{4\eta_3}{\left(P_{PS}\lambda_{PS,D}\right)^2} \exp\left(-\frac{\gamma_{th}}{P_R\lambda_{R,D}}\right) \\ &\quad \times \left(\frac{\gamma_{th}}{P_R\lambda_{R,D}} + \frac{2}{P_{PS}\lambda_{PS,D}}\right)^{-2}, \end{aligned} \tag{3.52}$$

$$P_{out,\beta=\frac{1}{2}} = P_{out,\beta=1} = 1 - \eta_3 \exp\left(-\frac{\gamma_{th}}{P_R\lambda_{R,D}}\right)\left(\frac{P_{PS}\lambda_{PS,D}}{P_R\lambda_{R,D}}\gamma_{th} + 1\right)^{-1}. \tag{3.53}$$

Proof. See Appendix F. □

3.3.3 Scenario 3

The outage probability is given by

$$P_{out} = \int_0^1 \Pr\left[\gamma_{R*,D} < \gamma_{th} | \beta = b\right] f_\beta(b) db. \tag{3.54}$$

Using (3.17), it becomes

$$P_{out} = \frac{T_s}{T_P}\left(\int_0^{1/4} P_{out,0<\beta<\frac{1}{4}} d\beta + \int_{1/4}^{1/2} P_{out,\frac{1}{4}<\beta<\frac{1}{2}} d\beta + \int_{1/2}^{3/4} P_{out,\frac{1}{2}<\beta<\frac{3}{4}} d\beta + \int_{3/4}^{1} P_{out,\frac{3}{4}<\beta<1} d\beta\right) + \left(1 - \frac{T_s}{T_P}\right) P_{out,\beta=1}. \tag{3.55}$$

Since $P_{out,0<\beta<\frac{1}{4}} = P_{out,\frac{1}{4}<\beta<\frac{1}{2}}$ and $P_{out,\frac{1}{2}<\beta<\frac{3}{4}} = P_{out,\frac{3}{4}<\beta<1}$, is becomes

$$P_{out} = \frac{T_s}{T_P}\left(\int_0^{1/2} P_{out,0<\beta<\frac{1}{4}} d\beta + \int_{1/2}^{1} P_{out,\frac{3}{4}<\beta<1} d\beta\right) + \left(1 - \frac{T_s}{T_P}\right) P_{out,\beta=1}. \tag{3.56}$$

3.4 Numerical Results

Suppose that the target rate R is 1 b/s/Hz, the path-loss exponent α is 4, the distance between the source and relays in the secondary network $d_{S,R}$ is 1, the distance between the relays and destination in the secondary network $d_{R,D}$ is 1, the maximum transmission power of the source and relays is same, i.e., $P_S^{\max} = P_R^{\max}$, and the frame lengths of the primary network and secondary network, T_P and T_S are 1 and 0.9, respectively for the scenario 3. Also, suppose the distances between the terminals in the primary network and the terminals in the secondary network are almost same, i.e., $d_{PS,R} = d_{PS,D} = d_{S,PD} = d_{R,PD} = d$ where d is the distance between the primary network and secondary network.

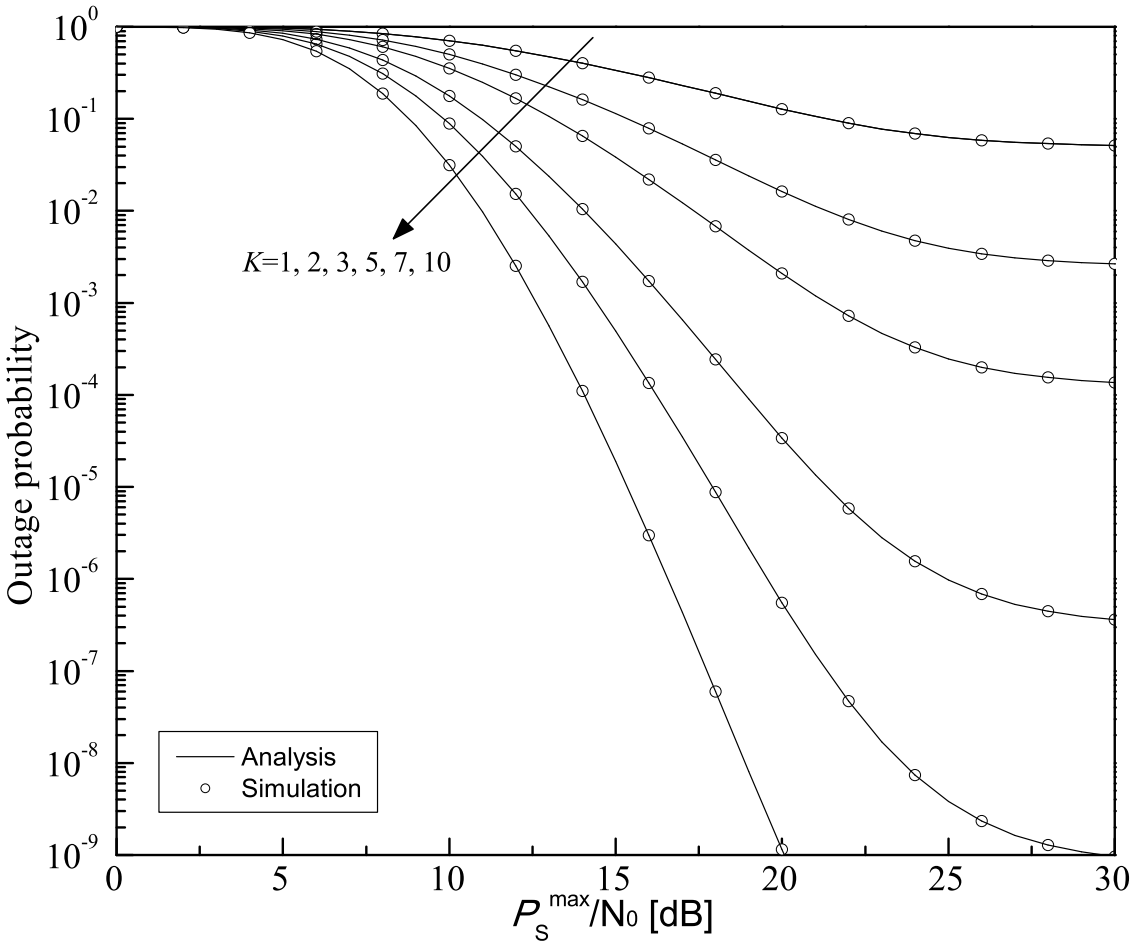
Outage probability
10^{0}
10^{-1}
10^{-2}
10^{-3}
10^{-4}
10^{-5}
10^{-6}
10^{-7}
10^{-8}
10^{-9}
0
5
10
15
20
25
30
P_S^{max}/N_0 [dB]
K=1, 2, 3, 5, 7, 10
Analysis
Simulation

(a) Scenario 1

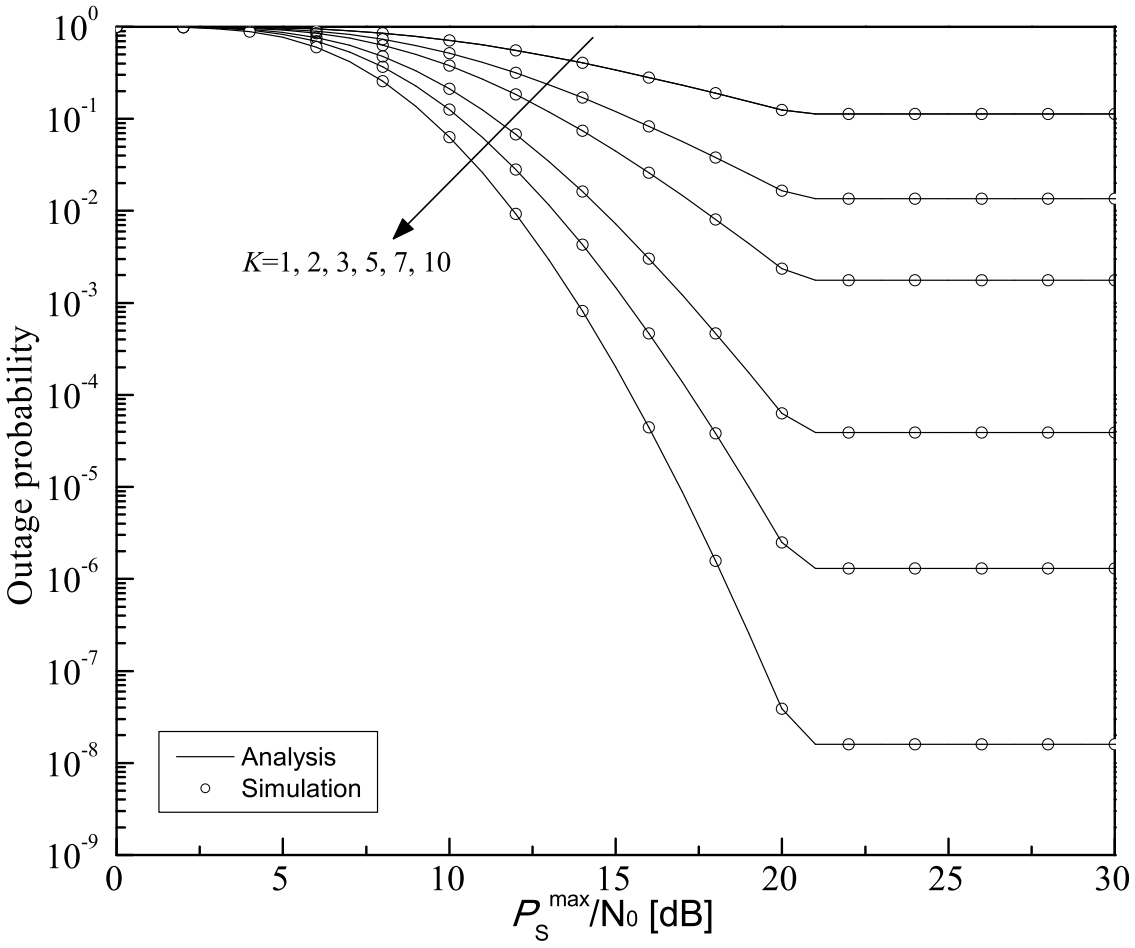

(b) Scenario 2, $\beta = 0.25$

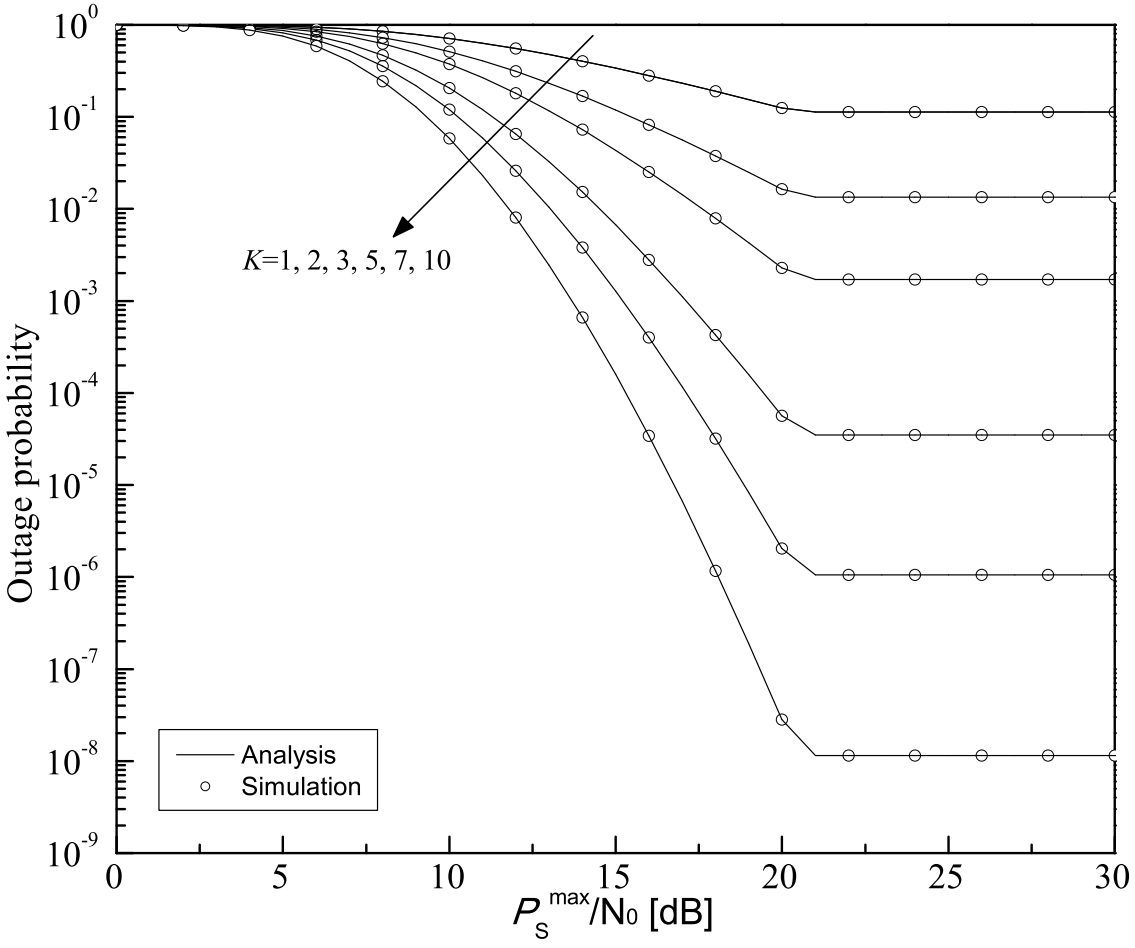

(c) Scenario 3

Figure 3.4. Outage probability of the secondary network with the interference threshold $\bar{I}/N_0 = 5$dB, the transmit SNR of the PUs P_{PS}/N_0=20dB, the distance between the primary network and secondary network $d = 3$, the tolerable probability threshold $\epsilon = 0.1$, and various numbers of relays.

Figure 3.4 shows the outage probability of the secondary network with the interference threshold $\bar{I}/N_0 = 5$dB, the transmit SNR of the PUs P_{PS}/N_0=20dB, the distance between the primary network and secondary network $d = 3$, the tolerable probability threshold $\epsilon = 0.1$, and various numbers of relays. The floor in the outage probability curve is shown. The reason is that although $P_S^{\max}$ and $P_R^{\max}$ grow, P_S and P_R are limited as shown in (3.20) and (3.31) due to the interference constraint. Moreover, it is shown that the outage probability is converged smoothly in the scenario 1 and the cusps are shown in the scenarios 2 and 3. The reason is that while the transmission power for the scenario 1 is determined adaptively, that for the scenarios 2 and 3 is fixed. Also, it is shown that as the number of relay increases, the slope of the outage probability curve increases and the floor level decreases.

Figure 3.5 shows the outage probability of the secondary network with the number of relays $K = 5$, the transmit SNR of the PUs P_{PS}/N_0=20dB, the distance between the primary network and secondary network $d = 3$, the tolerable probability threshold $\epsilon = 0.1$, and various interference thresholds. In this Figure, $\bar{I}/N_0 = \infty$dB represents that there is only interference from the primary network without interference to the primary network. It is shown that as the interference threshold increases, the floor level decreases. Moreover, there is no floor of outage probability curve for $\bar{I}/N_0 = \infty$dB since P_S and P_R are not limited. It is also shown that the interference threshold rarely affects the slope of the outage probability curve. The reason is that the transmission power is determined mainly by $P_S^{\max}$ and not by $\bar{I}$ in this region.

Figure 3.6 shows the outage probability of the secondary network with the number of relays $K = 5$, the interference threshold $\bar{I}/N_0 = 5$dB, the distance between the primary network and secondary network $d = 3$, the tolerable probability threshold $\epsilon = 0.1$, and various transmit SNRs of the PUs. In this Figure, $\bar{I}/N_0 = -\infty$dB

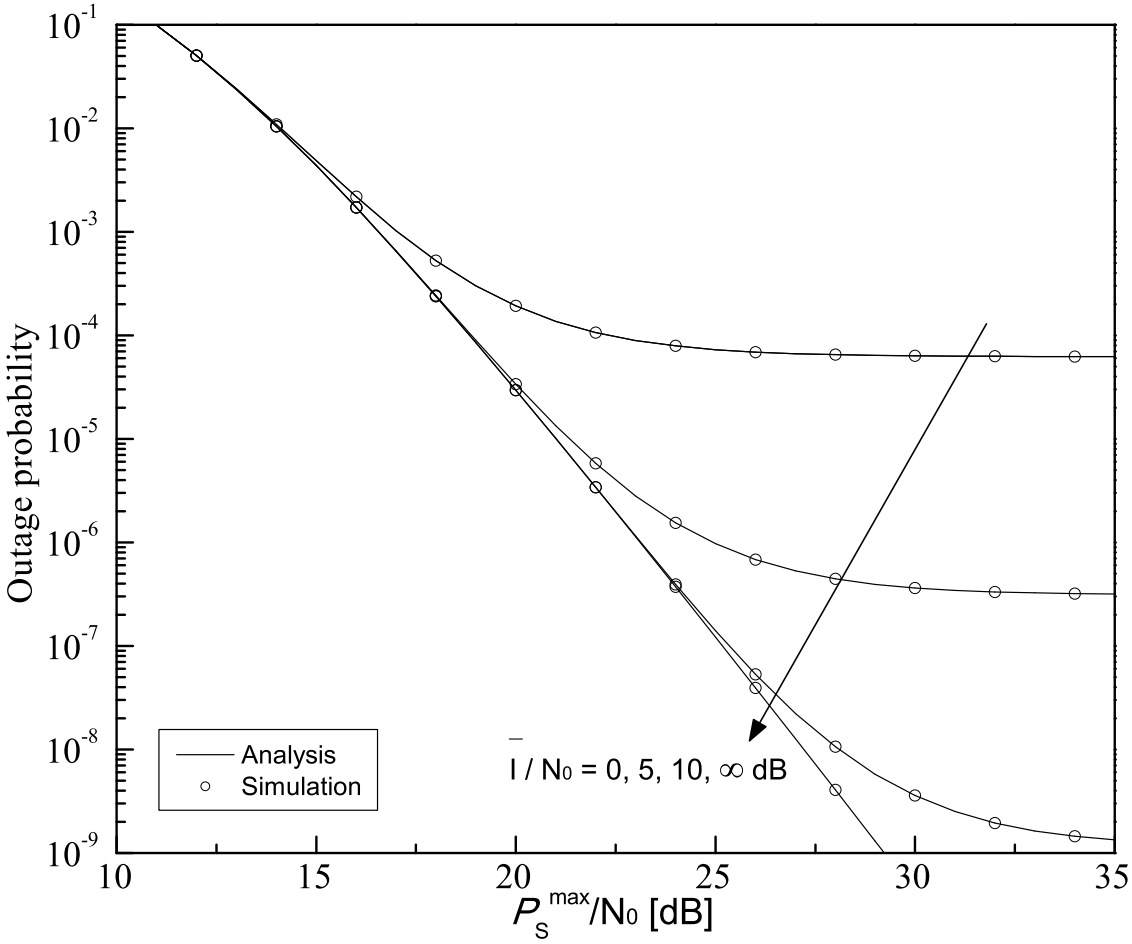
Outage probability
10^{-1}
10^{-2}
10^{-3}
10^{-4}
10^{-5}
10^{-6}
10^{-7}
10^{-8}
10^{-9}
10
15
20
25
30
35
P_S^{max}/N_0 [dB]
Analysis
Simulation
$\bar{I} / N_0$ = 0, 5, 10, ∞ dB

(a) Scenario 1

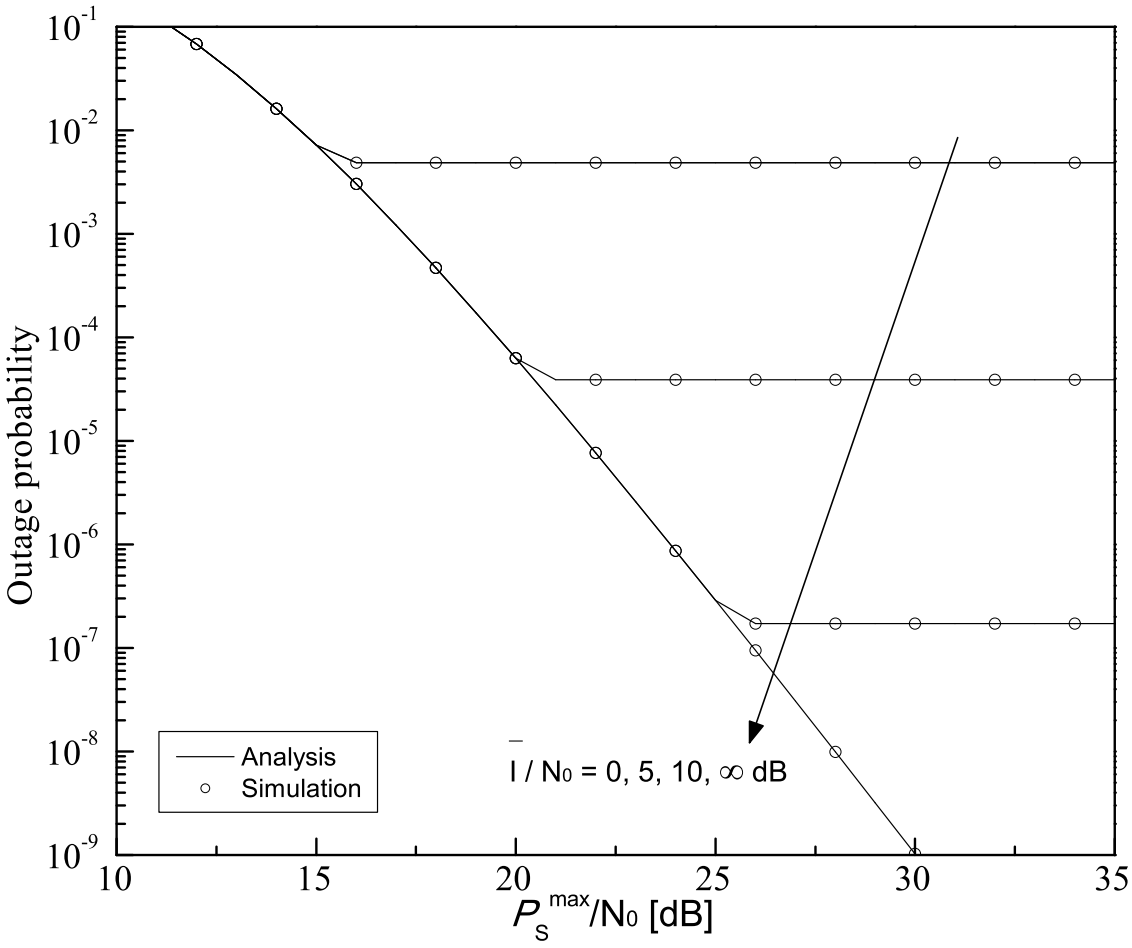

(b) Scenario 2, $\beta = 0.25$

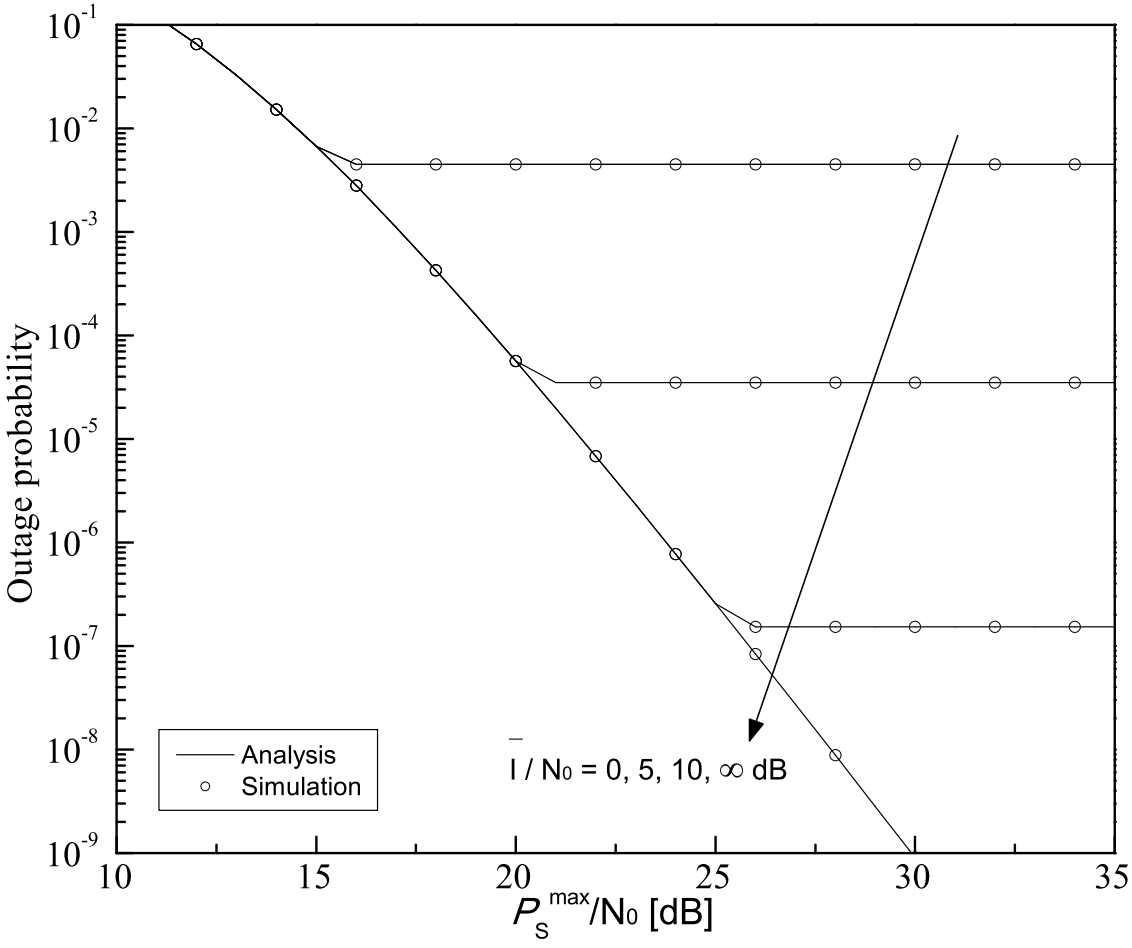

(c) Scenario 3

Figure 3.5. Outage probability of the secondary network with the number of relays $K = 5$, the transmit SNR of the PUs P_{PS}/N_0=20dB, the distance between the primary network and secondary network $d = 3$, the tolerable probability threshold $\epsilon = 0.1$, and various interference thresholds.

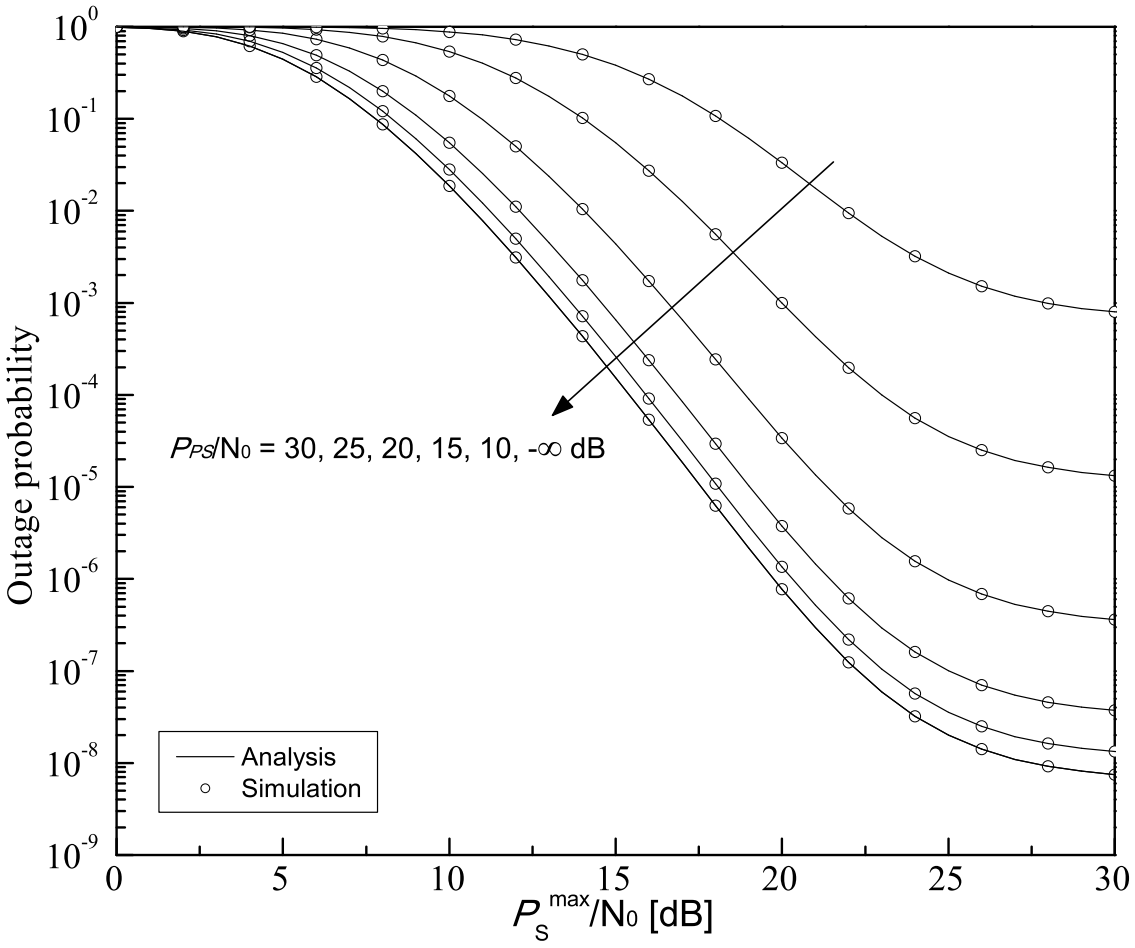
Outage probability
10^{0}
10^{-1}
10^{-2}
10^{-3}
10^{-4}
10^{-5}
10^{-6}
10^{-7}
10^{-8}
10^{-9}
P_{PS}/N_0 = 30, 25, 20, 15, 10, -∞ dB
Analysis
Simulation
0
5
10
15
20
25
30
P_S^{max}/N_0 [dB]

(a) Scenario 1

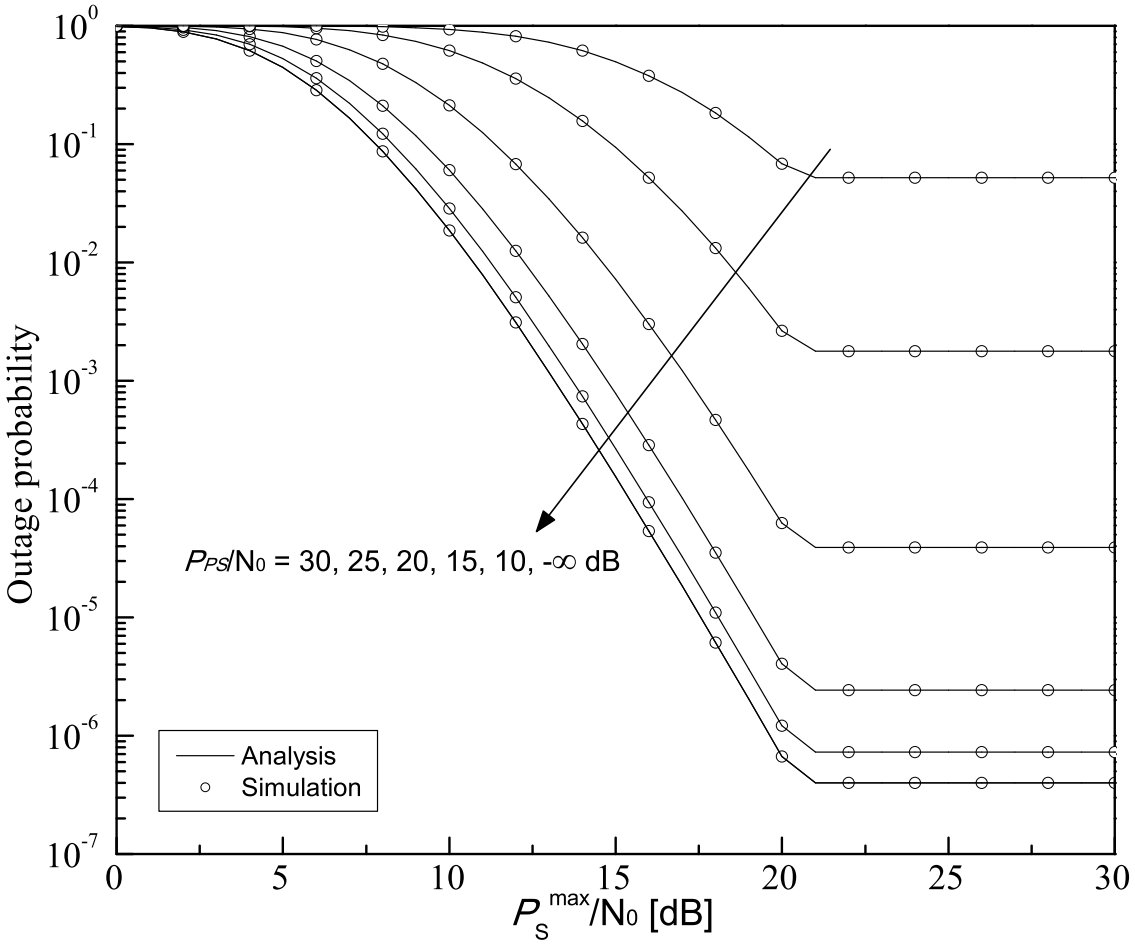

(b) Scenario 2, $\beta = 0.25$

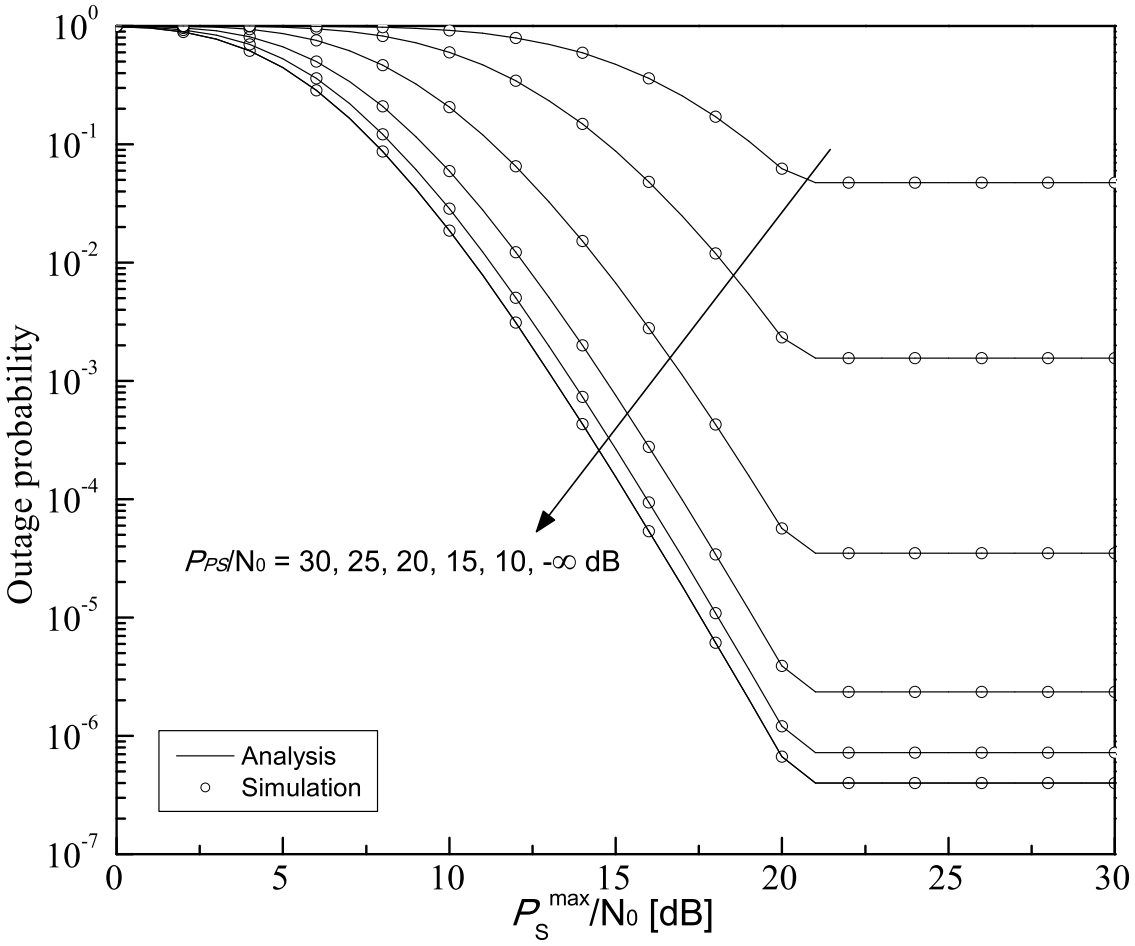

(c) Scenario 3

Figure 3.6. Outage probability of the secondary network with the number of relays $K = 5$, the interference threshold $\bar{I}/N_0 = 5$dB, the distance between the primary network and secondary network $d = 3$, the tolerable probability threshold $\epsilon = 0.1$, and various transmit SNRs of the PUs.

represents that there is only interference to the primary network without interference from the primary network. It is shown that as the transmit SNR of the PUs decreases, the slope of the outage probability curve increases and floor level decreases. It is shown that there is the floor although there is no interference from the primary network.

Figure 3.7 shows the outage probability of the secondary network with the number of relays $K = 5$, the interference threshold $\bar{I}/N_0 = 5$dB, the transmit SNR of the PUs P_{PS}/N_0=20dB, the tolerable probability threshold $\epsilon = 0.1$, and various distances between the primary network and secondary network. In this Figure, $d = \infty$ represents that there is no interference, i.e., the non-cognitive radio network that monopolize the spectrum bands. It is shown that as the distance between the primary network and secondary network increases, the slope of the outage probability curve increases, the floor level decreases, and the outage probability approaches the non-cognitive radio network that monopolize the spectrum bands.

Figure 3.8 shows the outage probability of the secondary network with the number of relays $K = 5$, the interference threshold $\bar{I}/N_0 = 5$dB, the transmit SNR of the PUs P_{PS}/N_0=20dB, the distance between the primary network and secondary network $d = 3$, and various tolerable probability thresholds. In this Figure, $\epsilon = 1$ represents that there is only interference from the primary network without interference to the primary network. It is shown that as the tolerable probability threshold increases, the floor level decreases. Moreover, there is no floor for $\epsilon = 1$. It is also shown that the tolerable probability threshold rarely affects the slope of the outage probability curve.

Figure 3.9 shows the outage probability of the secondary network according to β with the interference threshold $\bar{I}/N_0 = 5$dB, the transmit SNR of the PSs P_{PS}/N_0=20dB, the maximum transmit SNR of the SU $P_S^{\max}/N_0 = 10$dB the tolerable probability

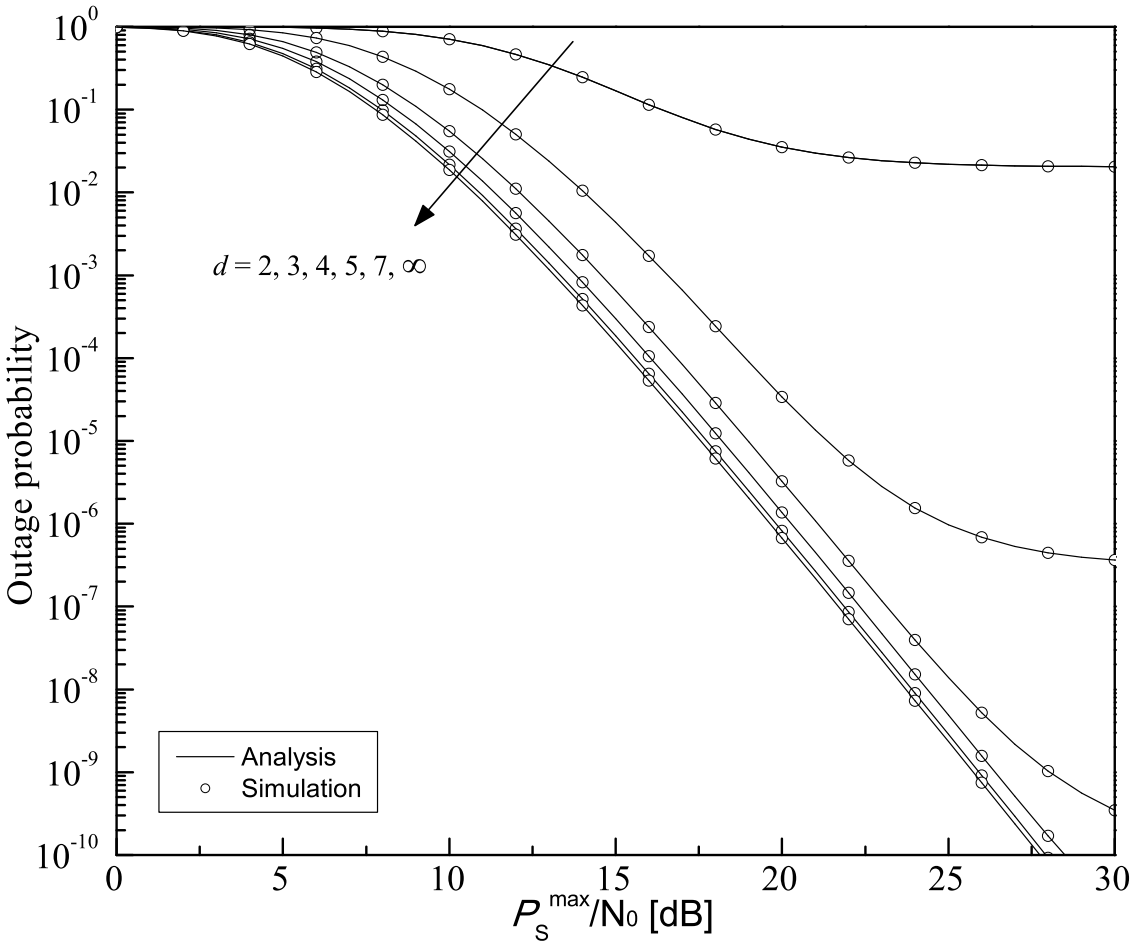
Outage probability
10^{0}
10^{-1}
10^{-2}
10^{-3}
10^{-4}
10^{-5}
10^{-6}
10^{-7}
10^{-8}
10^{-9}
10^{-10}
d = 2, 3, 4, 5, 7, ∞
Analysis
Simulation
0
5
10
15
20
25
30
P_S^{max}/N_0 [dB]

(a) Scenario 1

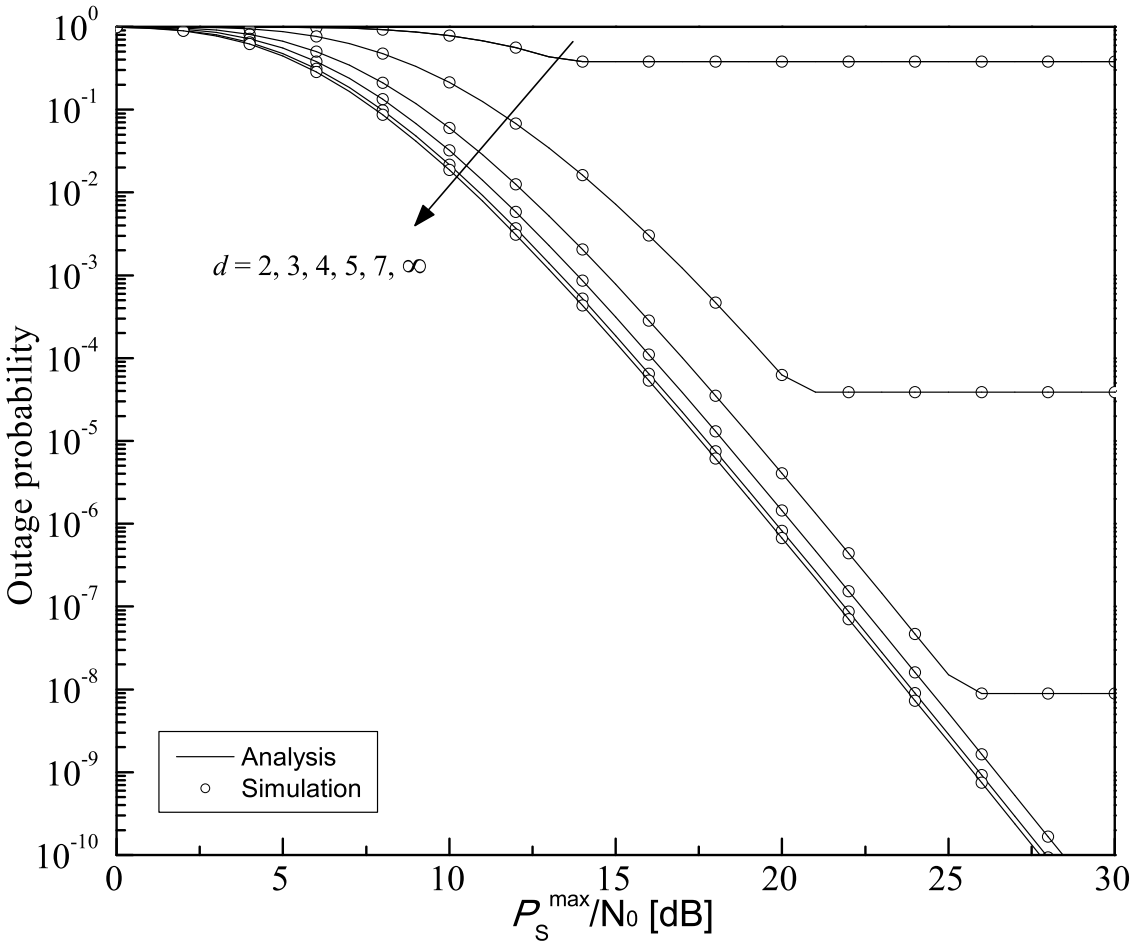

(b) Scenario 2, $\beta = 0.25$

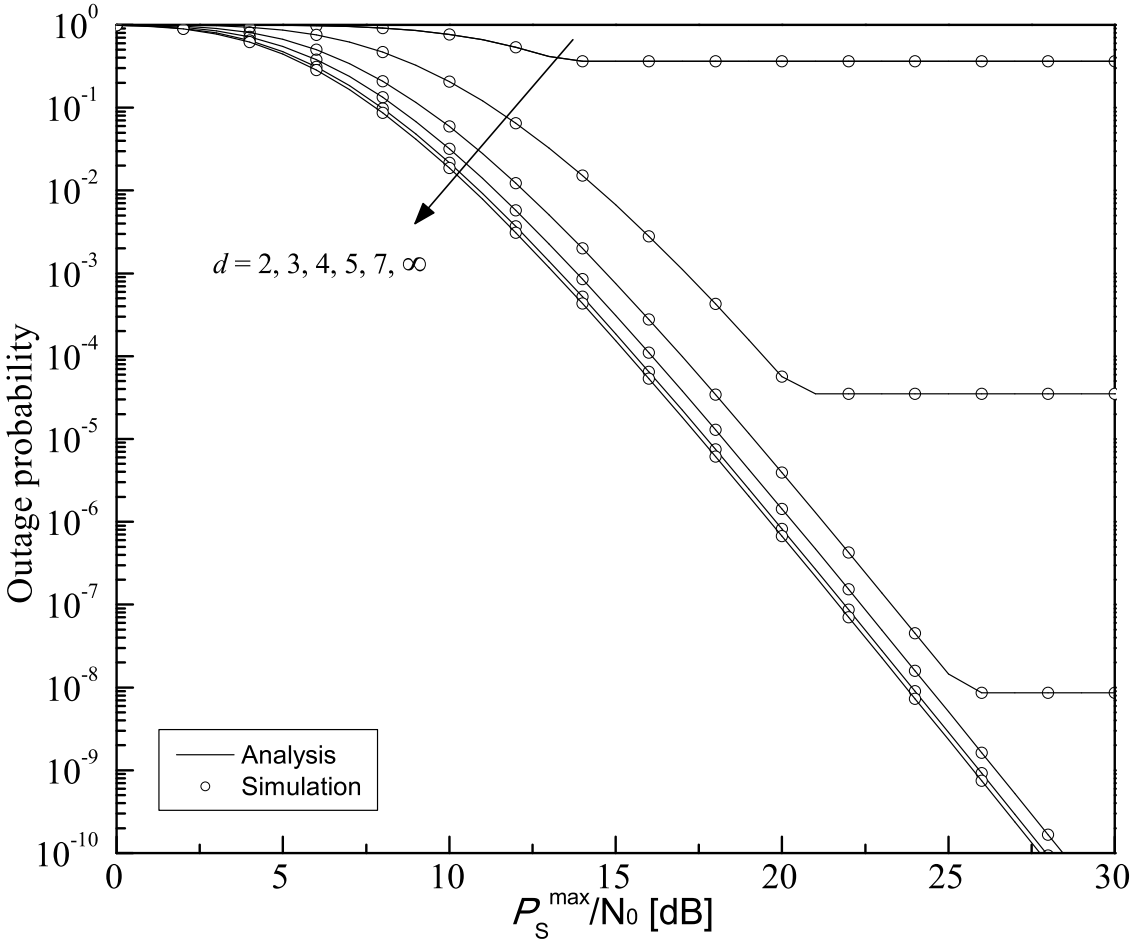

(c) Scenario 3

Figure 3.7. Outage probability of the secondary network with the number of relays $K = 5$, the interference threshold $\bar{I}/N_0 = 5$dB, the transmit SNR of the PUs P_{PS}/N_0=20dB, the tolerable probability threshold $\epsilon = 0.1$, and various distances between the primary network and secondary network.

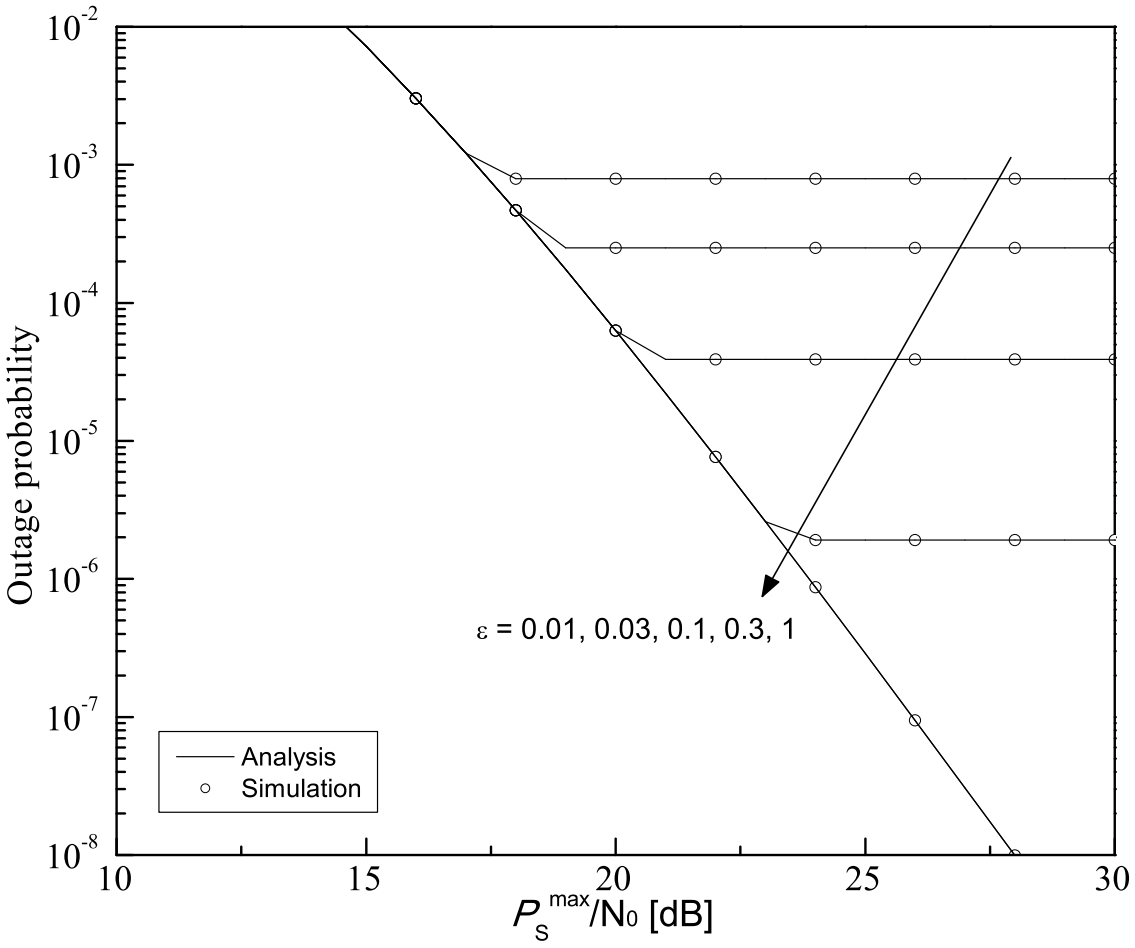

(a) Scenario 2, $\beta = 0.25$

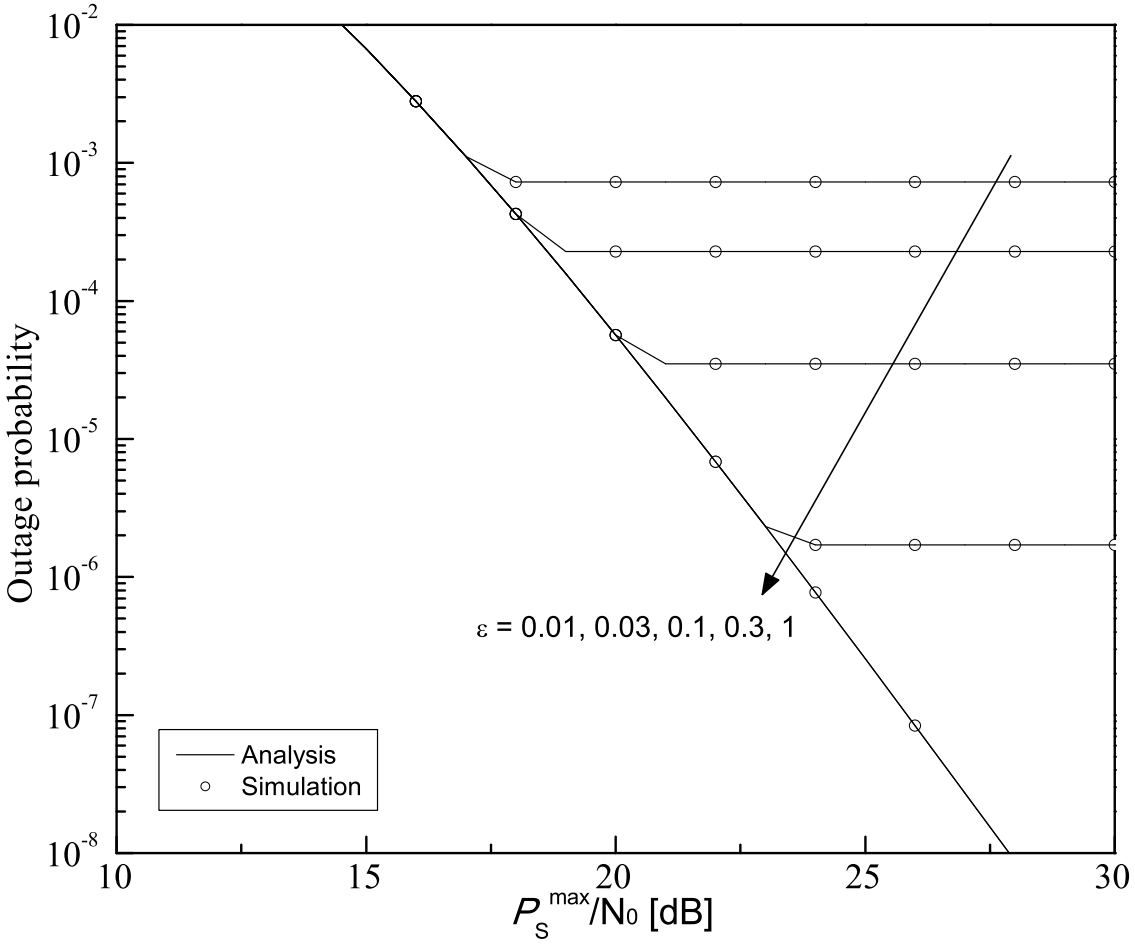

(b) Scenario 3

Figure 3.8. Outage probability of the secondary network with the number of relays $K = 5$, the interference threshold $\bar{I}/N_0 = 5$dB, the transmit SNR of the PUs P_{PS}/N_0=20dB, the distance between the primary network and secondary network $d = 3$, and various tolerable probability thresholds.

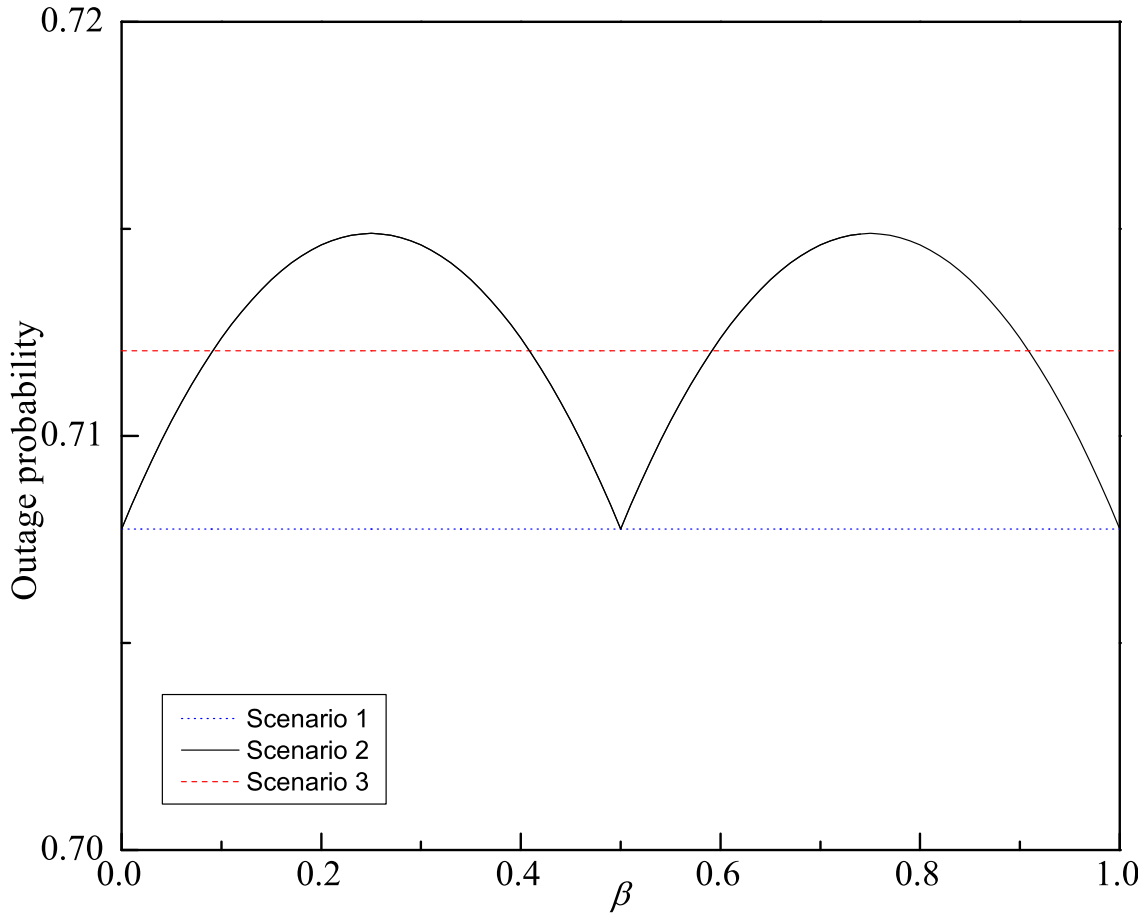
0.72
0.71
0.70
Outage probability
0.0
0.2
0.4
0.6
0.8
1.0
β
Scenario 1
Scenario 2
Scenario 3

(a) K=1

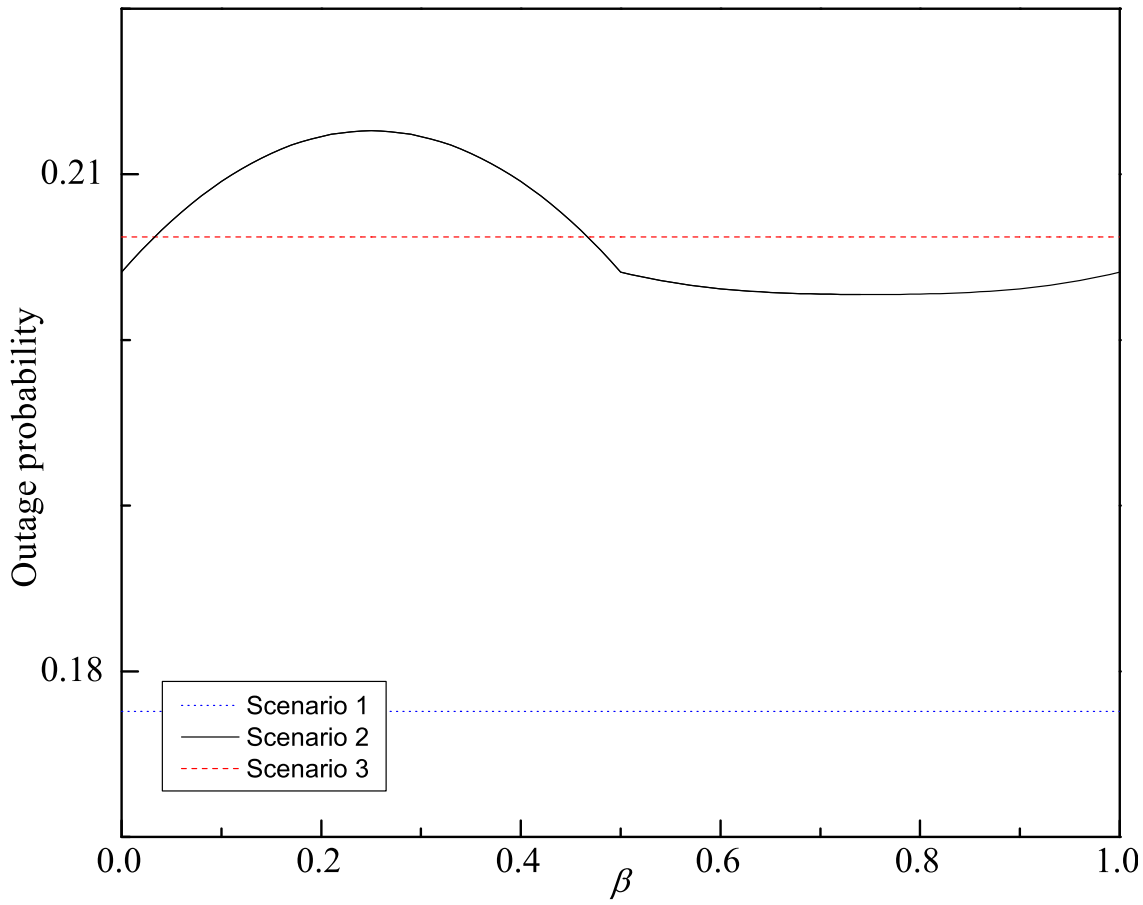

(b) K=5

Figure 3.9. Outage probability of the secondary network according to β with the interference threshold $\bar{I}/N_0$ = 5dB, the transmit SNR of the PSs P_{PS}/N_0=20dB, the maximum transmit SNR of the SU $P_S^{\max}/N_0$ = 10dB the tolerable probability threshold ϵ = 0.1, and the distance between the primary network and secondary network $d = 3$.

threshold $\epsilon = 0.1$, and the distance between the primary network and secondary network $d = 3$. In Figure 3.9 (a), it is shown that the outage probability is maximized at $\beta = 0.25$ or $\beta = 0.75$ and minimized at $\beta = 0.5$ or $\beta = 1$. In Figure 3.9 (b), somewhat different result is shown. The outage probability is maximized at $\beta = 0.25$ and minimized at $\beta = 0.75$. From these results, we can conclude that the outage probability of one path becomes worse but the better relay is selected as the secondary network becomes asynchronous with the primary network. Also, it is shown that the ratio of the minimum to maximum outage probabilities for the scenario 2 is about 0.99 in Figure 3.9 (a) and about 0.95 in Figure 3.9 (b). That is, the effect of β is not critical to the outage probability.

Figure 3.10 shows the outage probability of the secondary network with the number of relays $K = 5$, the interference threshold $\bar{I}/N_0 = 5$dB, the transmit SNR of the PUs P_{PS}/N_0=20dB, the tolerable probability threshold $\epsilon = 0.1$, and the distance between the primary network and secondary network $d = 3$. It is shown that the outage probability of scenarios 2 and 3 is close to that of scenario 1 for the SNR lower than the SNR that the floor is appeared. It is also shown that the floor level of scenario 1 is much lower than that of scenarios 2 and 3.

3.5 Single-hop Spectrum Sharing Cognitive Radio Network

To take a close look at the effect of various network scenarios, we investigate the outage probability of single-hop spectrum sharing cognitive radio network. In this model, there is no relay in the secondary network. Different to Figures 3.2 and 3.3, one frame is not divided into two phase and only S transmits its data signal to D.

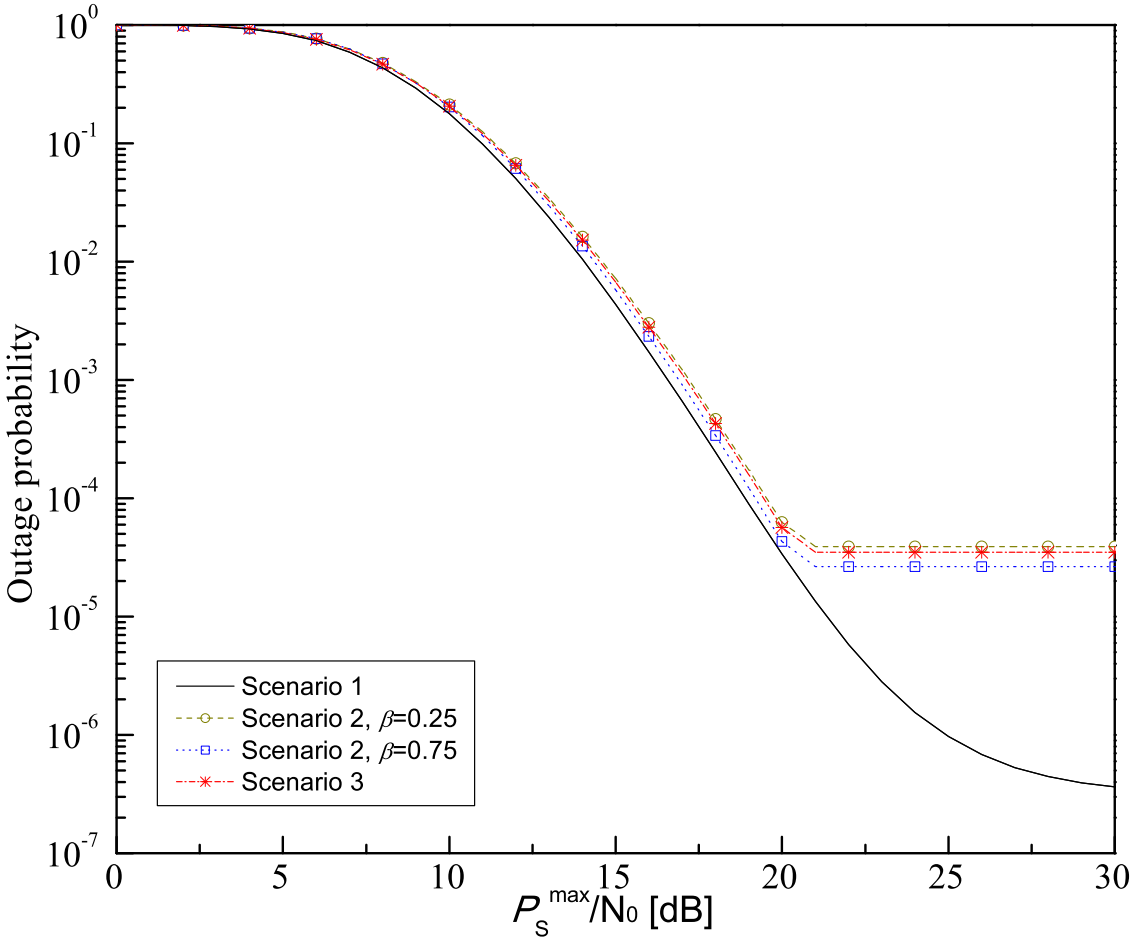

Figure 3.10. Outage probability of the secondary network with the number of relays $K = 5$, the interference threshold $\bar{I}/N_0 = 5$dB, the transmit SNR of the PUs P_{PS}/N_0=20dB, the tolerable probability threshold $\epsilon = 0.1$, and the distance between the primary network and secondary network $d = 3$.

Then, the threshold SINR is given by $\gamma_{th} = 2^R - 1$ rather than (3.13). The power allocation of S in Section 3.2 is valid but the power allocation of R_k and the relay selection are not required.

In the scenario 1, the received SINR at D is given by

$$\gamma_{S,D} = \frac{|h_{S,D}|^2 P_S}{|h_{PS_1,D}|^2 P_{PS_1} + 1}. \tag{3.57}$$

Applying *Theorem* 2 to (3.57), the outage probability is given by

$$P_{out} = g\left(\lambda_{S,D}, \lambda_{S,PD}, \lambda_{PS,D}, \bar{I}, P_S^{\max}, P_{PS}, \gamma_{th}\right). \tag{3.58}$$

In the scenario 2, the received SINR D is given by

$$\gamma_{S,D} = \frac{|h_{S,D}|^2 P_S}{\beta|h_{PS_1,D}|^2 P_{PS} + (1-\beta)|h_{PS_2,D}|^2 P_{PS} + 1}. \tag{3.59}$$

Then, we have the following theorem.

Theorem 8. *The outage probability is given by*

$$\begin{aligned} P_{out,0<\beta<\frac{1}{2}} &= P_{out,\frac{1}{2}<\beta<1} \\ &= \frac{1}{(2\beta-1)P_{PS}\lambda_{PS,D}} \exp\left(-\frac{\gamma_{th}}{P_S\lambda_{S,D}}\right) \\ &\quad \times \left\{ \left(\frac{\gamma_{th}}{P_S\lambda_{S,D}} + \frac{1}{\beta P_{PS}\lambda_{PS,D}}\right)^{-1} \right. \\ &\quad \left. - \left(\frac{\gamma_{th}}{P_S\lambda_{S,D}} + \frac{1}{(1-\beta)P_{PS}\lambda_{PS,D}}\right)^{-1} \right\}, \end{aligned} \tag{3.60}$$

$$P_{out,\beta=\frac{1}{2}} = \frac{4}{\left(P_{PS}\lambda_{PS,D}\right)^2} \exp\left(-\frac{\gamma_{th}}{P_S\lambda_{S,D}}\right) \left(\frac{\gamma_{th}}{P_S\lambda_{S,D}} + \frac{2}{P_{PS}\lambda_{PS,D}}\right)^{-2}, \tag{3.61}$$

$$P_{out,\beta=1} = \exp\left(-\frac{\gamma_{th}}{P_S\lambda_{S,D}}\right) \left(\frac{P_{PS}\lambda_{PS,D}}{P_S\lambda_{S,D}}\gamma_{th} + 1\right)^{-1}. \tag{3.62}$$

Proof. See Appendix G. □

In the scenario 3, similar to Section 3.3.3, the outage probability is given by

$$P_{out} = \frac{T_s}{T_P}\int_0^1 P_{out,0<\beta<\frac{1}{2}} d\beta + \left(1 - \frac{T_s}{T_P}\right) P_{out,\beta=1}. \tag{3.63}$$

Suppose that the target rate R is 1 b/s/Hz, the path-loss exponent α is 4, the distance between the source and relays in the secondary network $d_{S,D}$ is 1, the distances between the terminals in the primary network and the terminals in the secondary network are almost same, i.e., $d_{PS,D} = d_{S,PD} = d$, the maximum transmission power of the source and relays is same, i.e., $P_S^{\max} = P_R^{\max}$, and the frame lengths of the primary network and secondary network, T_P and T_S are 1 and 0.9, respectively for the scenario 3.

Figure 3.11 shows the outage probability of the single-hop secondary network with the transmit SNR of the PUs P_{PS}/N_0=20dB, the distance between the primary network and secondary network $d = 3$, the tolerable probability threshold $\epsilon = 0.1$, and various interference thresholds. It is shown that as the interference threshold increases, the floor level decreases. Moreover, there is no floor of outage probability curve for $\bar{I}/N_0 = \infty$dB since P_S and P_R are not limited. It is also shown that the interference threshold rarely affects the slope of the outage probability curve.

Figure 3.12 shows the outage probability of the single-hop secondary network with the interference threshold $\bar{I}/N_0 = 5$dB, the distance between the primary network and secondary network $d = 3$, the tolerable probability threshold $\epsilon = 0.1$, and various transmit SNRs of the PUs. It is shown that as the transmit SNR of the PUs decreases, the slope of the outage probability curve increases and outage probability decreases. It is shown that there is the floor although there is no interference from the primary network.

Figure 3.13 shows the outage probability of the single-hop secondary network with the interference threshold $\bar{I}/N_0 = 5$dB, the transmit SNR of the PUs P_{PS}/N_0=20dB,

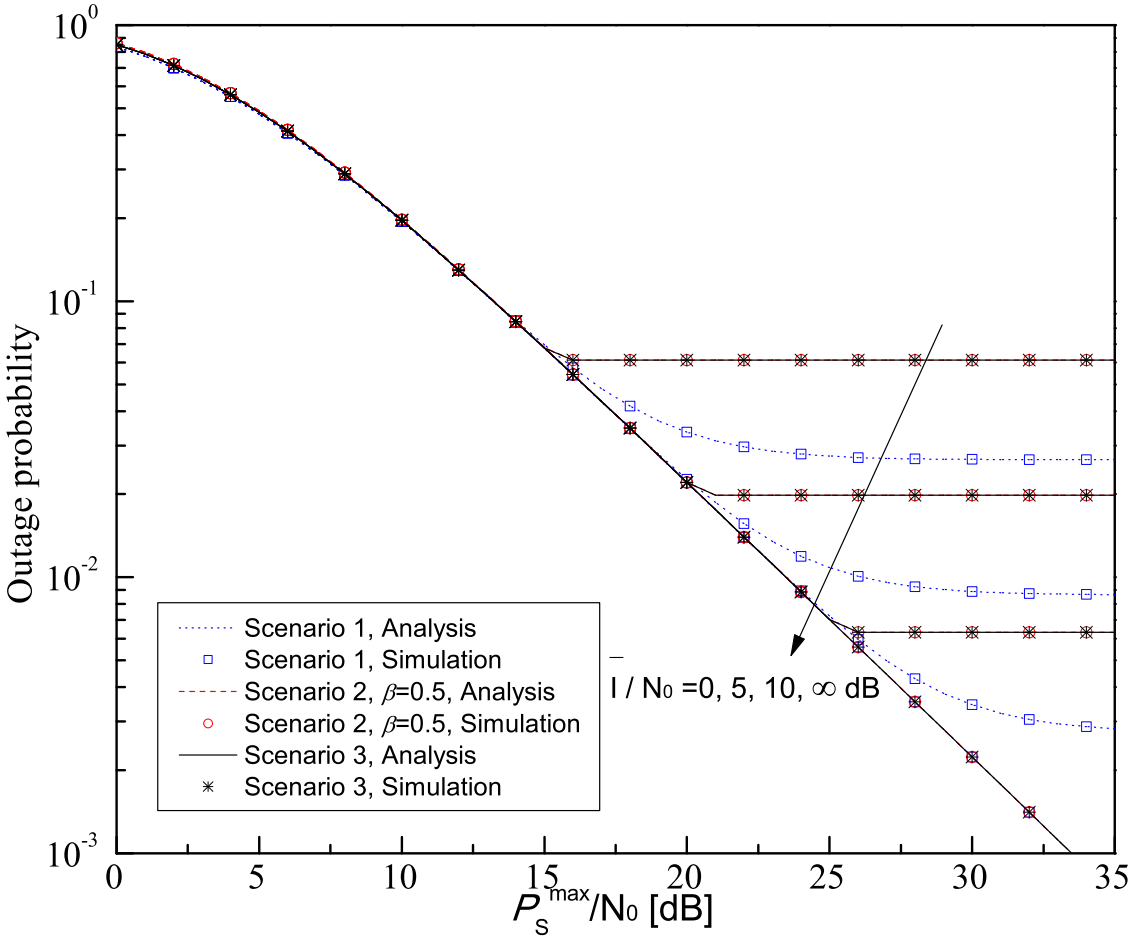

Figure 3.11. Outage probability of the single-hop secondary network with the transmit SNR of the PUs P_{PS}/N_0=20dB, the distance between the primary network and secondary network $d = 3$, the tolerable probability threshold $\epsilon = 0.1$, and various interference thresholds.

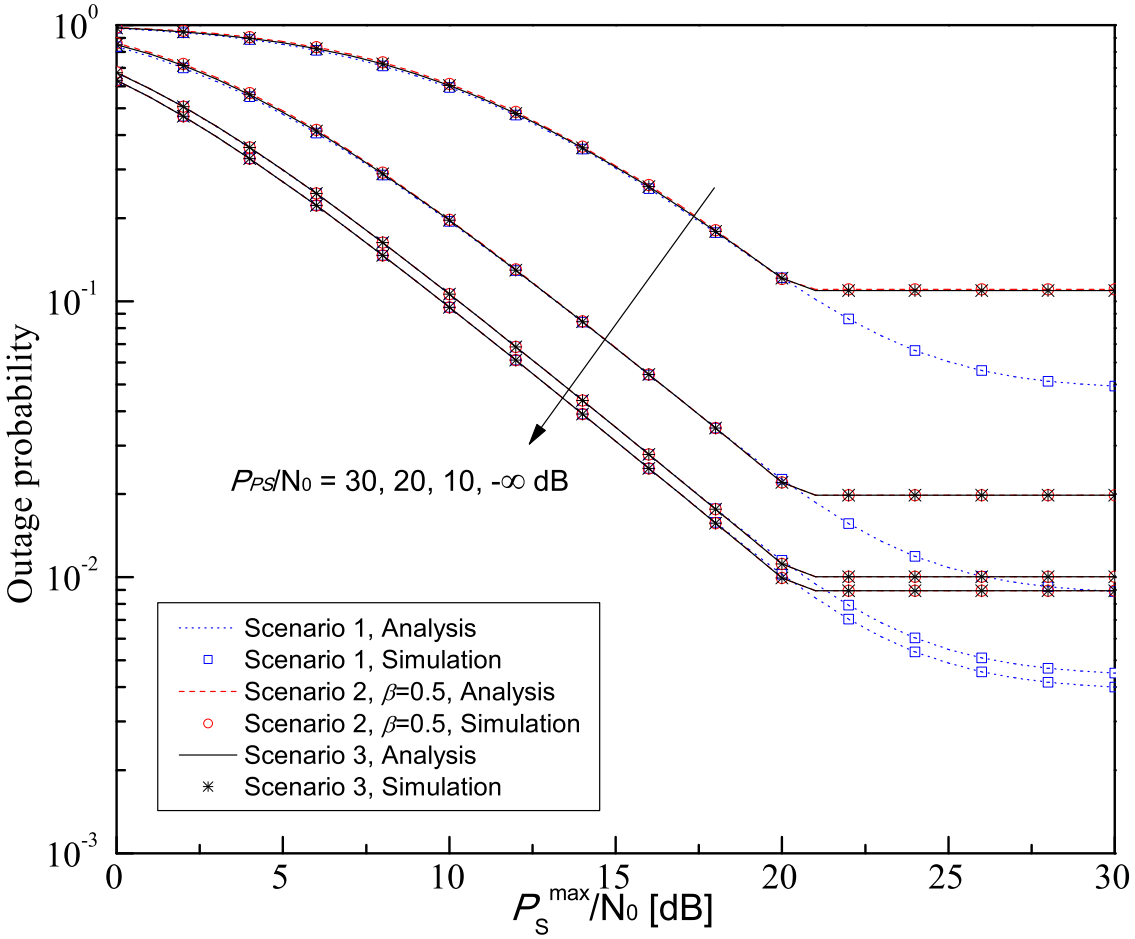

Figure 3.12. Outage probability of the single-hop secondary network with the interference threshold $\bar{I}/N_0 = 5$dB, the distance between the primary network and secondary network $d = 3$, the tolerable probability threshold $\epsilon = 0.1$, and various transmit SNRs of the PUs.

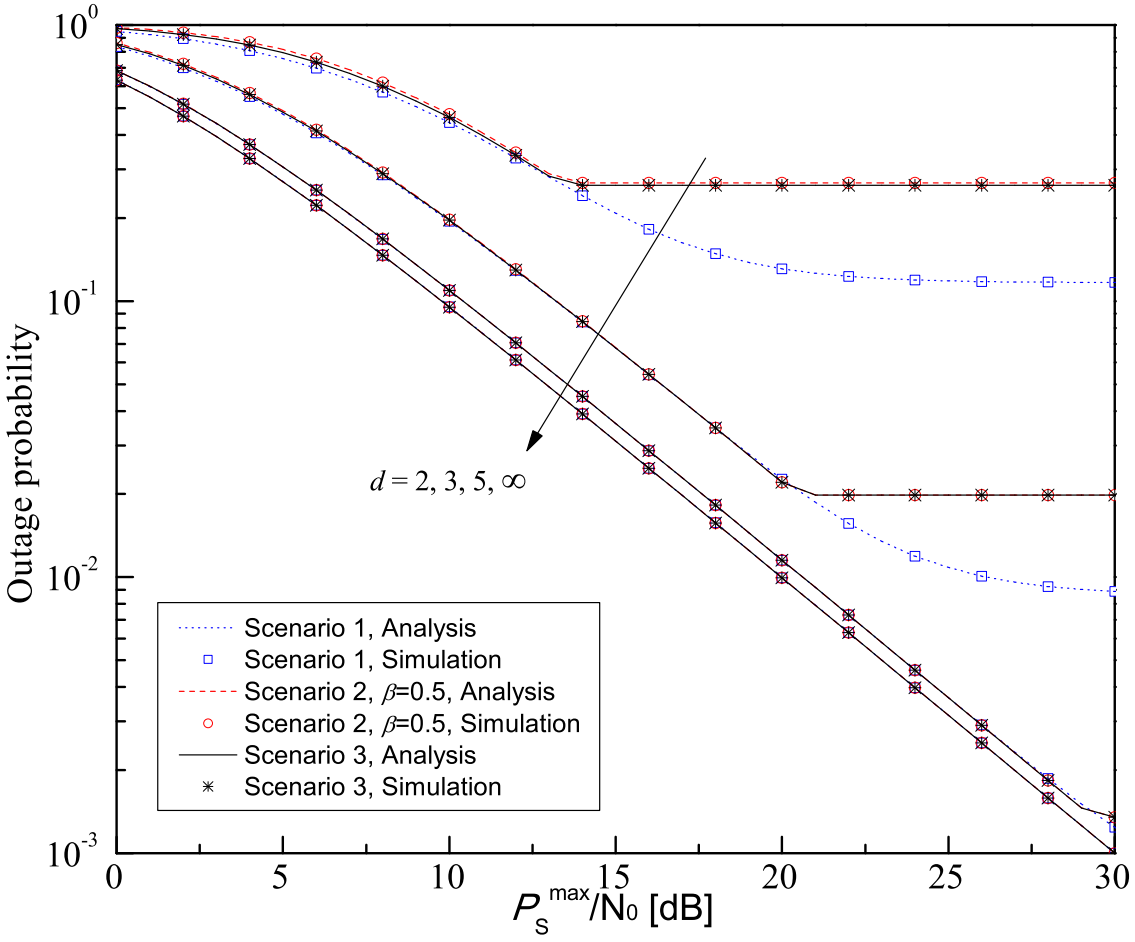

Figure 3.13. Outage probability of the single-hop secondary network with the interference threshold $\bar{I}/N_0 = 5$dB, the transmit SNR of the PUs P_{PS}/N_0=20dB, the tolerable probability threshold $\epsilon = 0.1$, and various distances between the primary network and secondary network.

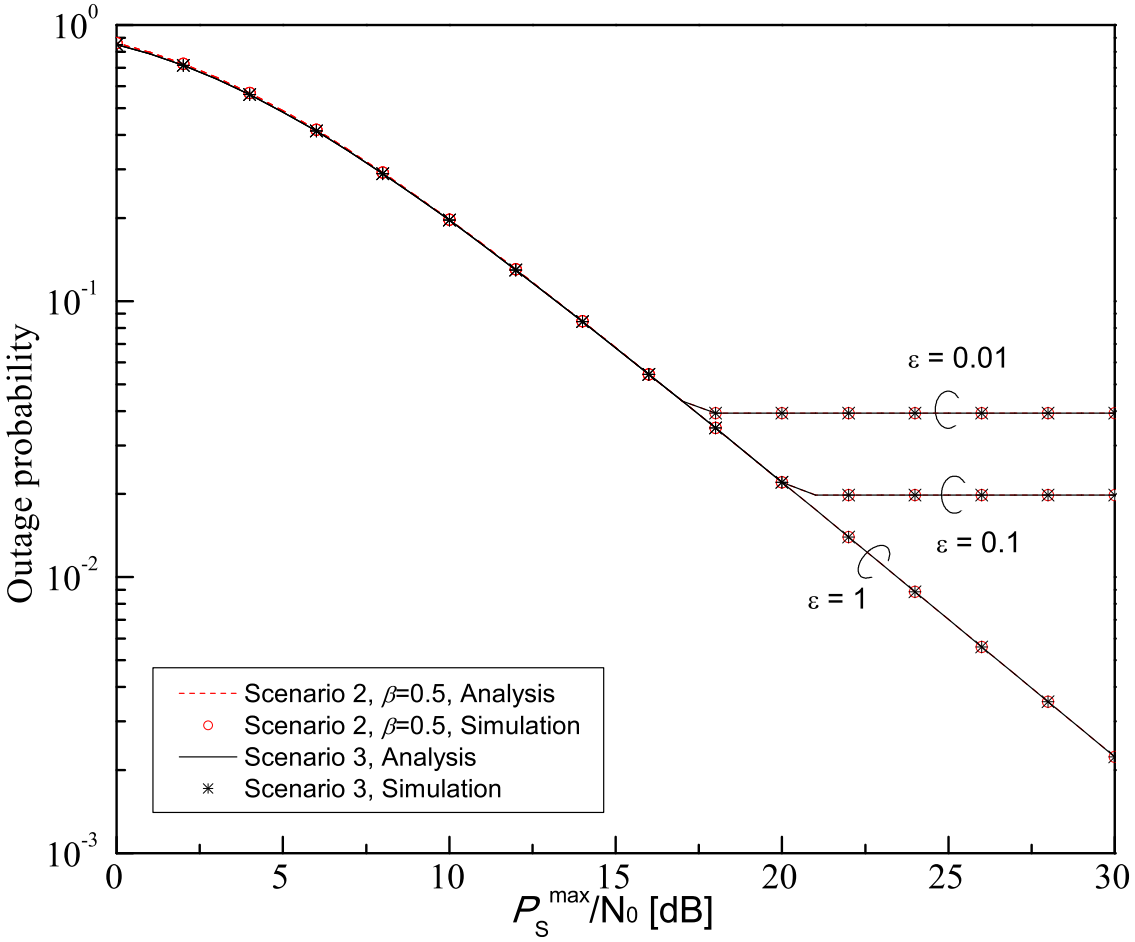

Figure 3.14. Outage probability of the single-hop secondary network with the interference threshold $\bar{I}/N_0 = 5$dB, the transmit SNR of the PUs P_{PS}/N_0=20dB, the distance between the primary network and secondary network $d = 3$, and various tolerable probability thresholds.

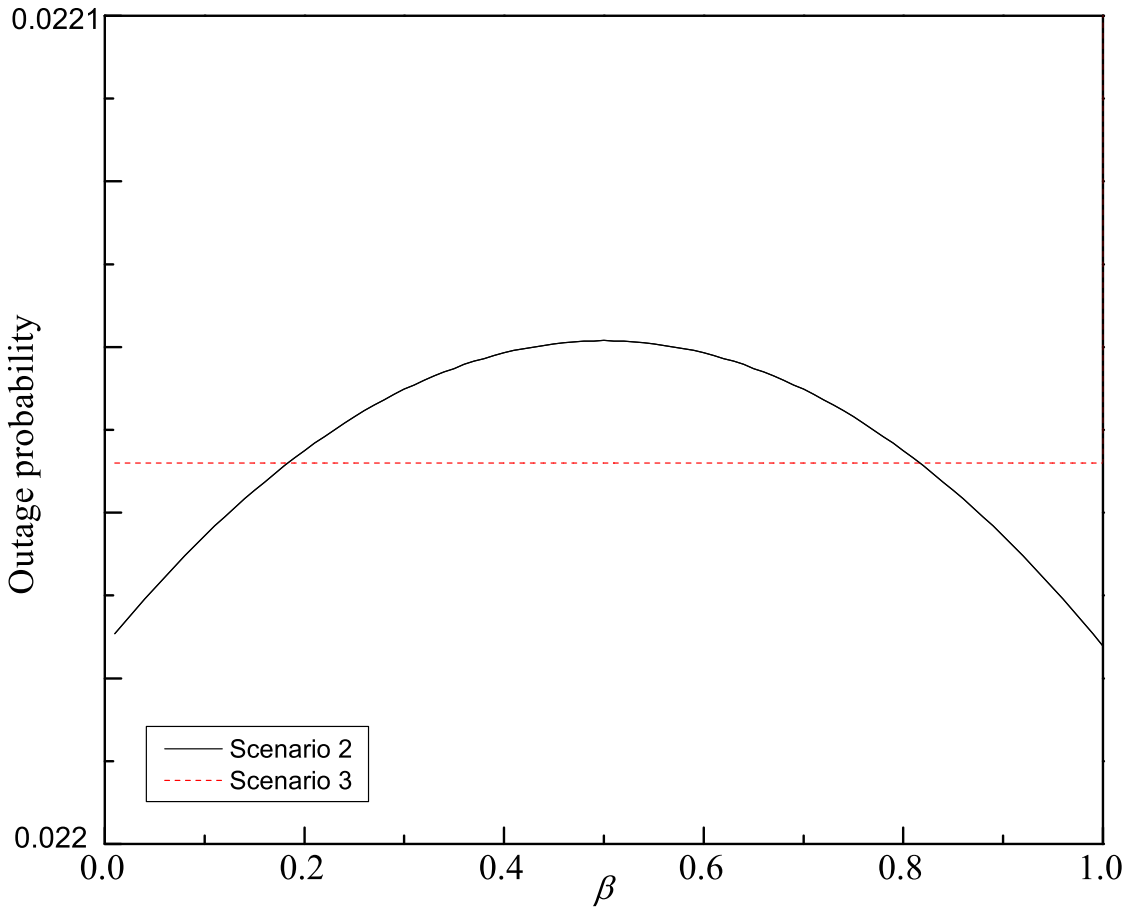

Figure 3.15. Outage probability of the single-hop secondary network according to β with the interference threshold $\bar{I}/N_0 = 5$dB, the transmit SNR of the PSs P_{PS}/N_0=20dB, the maximum transmit SNR of the SU $P_S^{\max}/N_0 = 10$dB the tolerable probability threshold $\epsilon = 0.1$, and the distance between the primary network and secondary network $d = 3$.

the tolerable probability threshold $\epsilon = 0.1$, and various distances between the primary network and secondary network. It is shown that as the distance between the primary network and secondary network increases, the slope of the outage probability curve increases, the floor level decreases, and the outage probability approaches the non-cognitive radio network that monopolize the spectrum bands.

Figure 3.14 shows the outage probability of the single-hop secondary network with the interference threshold $\bar{I}/N_0 = 5$dB, the transmit SNR of the PUs P_{PS}/N_0=20dB, the distance between the primary network and secondary network $d = 3$, and various tolerable probability thresholds. It is shown that as the tolerable probability threshold increases, the floor level decreases. Moreover, there is no floor for $\epsilon = 1$. It is also shown that the tolerable probability threshold rarely affects the slope of the outage probability curve.

Figure 3.15 shows the outage probability of the single-hop secondary network according to β with the interference threshold $\bar{I}/N_0 = 5$dB, the transmit SNR of the PSs P_{PS}/N_0=20dB, the maximum transmit SNR of the SU $P_S^{\max}/N_0 = 10$dB the tolerable probability threshold $\epsilon = 0.1$, and the distance between the primary network and secondary network $d = 3$. It is shown that the outage probability is maximized at $\beta = 0.5$ and minimized at $\beta = 1$. That is, the outage probability of the single-hop communication becomes worse as the secondary network becomes asynchronous with the primary network.

Throughout the Figures 3.11-3.15, the analytical results perfectly match the simulation results. Compared to the Figures 3.5-3.10, it is shown that the effects of system parameters on the outage probability of single-hop secondary network and dual-hop secondary network are almost same.

3.6 Summary

In this chapter, we investigate the spectrum-sharing CR network. We suppose the dual-hop relaying system as the secondary network where the both interferences from and to the primary network exist. We consider three network scenarios according to the relation of the primary network and secondary network: first, one that the primary network and secondary network are synchronized, second, one that the primary network and secondary network are not synchronized with same frame length, and third, one that the frame lengths of the primary network and secondary network are different. For each scenario, we propose the power allocation and relay selection of the secondary network. Also, we analyze the outage probability of the secondary network for each scenario. Especially, we derive the outage probability in the closed-form for the scenarios 1 and 2. Numerical results verify the validity of theoretical analysis by comparison with Monte Carlo simulation results. It is shown that there is the floor of outage probability curve due to the interference to the primary network. It is shown that the slope increases and the floor level decreases as the number of relay increases or the transmit SNR of the PUs decreases. It is also shown that the floor level decreases but the slope is nearly invariant as the interference threshold increases or the tolerable probability threshold increases. In addition, it is shown that as the distance between the primary network and secondary network increases, the slope of the outage probability curve increases, the floor level decreases, and the outage probability approaches the non-cognitive radio network that monopolize the spectrum bands. It is shown that the outage probability of one path becomes worse but the better relay is selected as the secondary network becomes asynchronous with the primary network. However, it is also shown that the effect of asynchronous transmission on the outage probability is not critical. It is shown that the outage probability of scenarios 2 and

3 is close to that of scenario 1 for the SNR lower than the SNR that the floor is appeared. However, it is also shown that the floor level of scenario 1 is much lower than that of scenarios 2 and 3.

Chapter 4

Conclusions

In this dissertation, we have investigated the relay communication in the wireless network.

In Chapter 1, we introduce the basic idea, history, and related issues of the relay communication. We also describe the outline of this dissertation. In addition, we present some notations, abbreviations, and mathematical definitions and functions used in this dissertation.

In Chapter 2, we propose a novel DF protocol for a multi-hop network. In the proposed protocol, multiple terminals transmit simultaneously to minimize the outage probability. We analyze the outage probability of the proposed protocol. Also, we propose an optimization algorithm that minimize the outage probability. The optimization algorithm includes the power allocation and the selection of the number of hops and phases. Also, we propose the reduced complexity selection of the number of hops and phases by using some approximations and mathematical manipulations. Some examples show that the reduced complexity selection reduces the computational complexity significantly. Numerical results verify the validity of theoretical analysis

by comparison with Monte Carlo simulation results. It is shown that the proposed multi-hop protocol provides lower outage probability than the conventional multi-hop protocol as well as single-hop protocol. Especially, the proposed multi-hop protocol is more attractive in the case of low signal-to-noise ratio (SNR) and that of high path-loss exponent. It is also shown that the reduced complexity selection provides almost same outage probability to the exhaustive search in most regions. In addition, we extend the concept of the proposed DF protocol to the AF protocol.

In Chapter 3, In this chapter, we investigate the spectrum-sharing CR network. We suppose the dual-hop relaying system as the secondary network where the both interferences from and to the primary network exist. We consider three network scenarios according to the relation of the primary network and secondary network: first, one that the primary network and secondary network are synchronized, second, one that the primary network and secondary network are not synchronized with same frame length, and third, one that the frame lengths of the primary network and secondary network are different. For each scenario, we propose the power allocation and relay selection of the secondary network. Also, we analyze the outage probability of the secondary network for each scenario. Especially, we derive the outage probability in the closed-form for the scenarios 1 and 2. Numerical results verify the validity of theoretical analysis by comparison with Monte Carlo simulation results. It is shown that there is the floor of outage probability curve due to the interference to the primary network. It is shown that the slope increases and the floor level decreases as the number of relay increases or the transmit SNR of the PUs decreases. It is also shown that the floor level decreases but the slope is nearly invariant as the interference threshold increases or the tolerable probability threshold increases. In addition, it is shown that as the distance between the primary network and secondary network

increases, the slope of the outage probability curve increases, the floor level decreases, and the outage probability approaches the non-cognitive radio network that monopolize the spectrum bands. It is shown that the outage probability of one path becomes worse but the better relay is selected as the secondary network becomes asynchronous with the primary network. However, it is also shown that the effect of asynchronous transmission on the outage probability is not critical. It is shown that the outage probability of scenarios 2 and 3 is close to that of scenario 1 for the SNR lower than the SNR that the floor is appeared. However, it is also shown that the floor level of scenario 1 is much lower than that of scenarios 2 and 3.

Appendix A

Proof of Theorem 2

The joint PDF of Y_1, Y_2, and Y_3 is given by

$$f_{Y_1,Y_2,Y_3}(y_1,y_2,y_3) = \frac{1}{\lambda_1\lambda_2\lambda_3}\exp\left(-\frac{y_1}{\lambda_1}-\frac{y_2}{\lambda_2}-\frac{y_3}{\lambda_3}\right). \tag{A.1}$$

The CDF of Z_1 is given by

$$\begin{aligned} F_{Z_1}(z) &= \Pr\left[\frac{Y_1\min\left\{\frac{c_1}{Y_2},c_2\right\}}{c_3Y_3+1}<z\right] \\ &= \int_0^\infty\int_0^{c_1/c_2}\int_0^{\frac{z(c_3y_3+1)}{c_2}} f_{Y_1,Y_2,Y_3}(y_1,y_2,y_3)dy_1dy_2dy_3 \\ &\quad + \int_0^\infty\int_{c_1/c_2}^\infty\int_0^{\frac{zy_2(c_3y_3+1)}{c_1}} f_{Y_1,Y_2,Y_3}(y_1,y_2,y_3)dy_1dy_2dy_3. \end{aligned} \tag{A.2}$$

The first term of right-hand side of (A.2) is calculated as

$$\begin{aligned} &\int_0^\infty\int_0^{c_1/c_2}\int_0^{\frac{z(c_3y_3+1)}{c_2}} \frac{1}{\lambda_1\lambda_2\lambda_3}\exp\left(-\frac{y_1}{\lambda_1}-\frac{y_2}{\lambda_2}-\frac{y_3}{\lambda_3}\right)dy_1dy_2dy_3 \\ &= \int_0^\infty\int_0^{c_1/c_2}\frac{1}{\lambda_2\lambda_3}\exp\left(-\frac{y_2}{\lambda_2}-\frac{y_3}{\lambda_3}\right)\left\{1-\exp\left(-\frac{z(c_3y_3+1)}{c_2\lambda_1}\right)\right\}dy_2dy_3 \\ &= \int_0^\infty\frac{1}{\lambda_3}\exp\left(-\frac{y_3}{\lambda_3}\right)\left\{1-\exp\left(-\frac{c_1}{c_2\lambda_2}\right)\right\}\left\{1-\exp\left(-\frac{z(c_3y_3+1)}{c_2\lambda_1}\right)\right\}dy_3 \\ &= \left\{1-\exp\left(-\frac{c_1}{c_2\lambda_2}\right)\right\}\left\{1-\frac{c_2\lambda_1}{c_2\lambda_1+c_3\lambda_3z}\exp\left(-\frac{z}{c_2\lambda_1}\right)\right\}. \end{aligned} \tag{A.3}$$

The second term of right-hand side of (A.2) is calculated as

$$\begin{aligned}
&\int_0^\infty \int_{c_1/c_2}^\infty \int_0^{\frac{zy_2(c_3y_3+1)}{c_1}} \frac{1}{\lambda_1\lambda_2\lambda_3} \exp\left(-\frac{y_1}{\lambda_1} - \frac{y_2}{\lambda_2} - \frac{y_3}{\lambda_3}\right) dy_1 dy_2 dy_3 \\
&\quad = \int_0^\infty \int_{c_1/c_2}^\infty \frac{1}{\lambda_2\lambda_3} \exp\left(-\frac{y_2}{\lambda_2} - \frac{y_3}{\lambda_3}\right) \left\{1 - \exp\left(-\frac{zy_2(c_3y_3+1)}{c_1\lambda_1}\right)\right\} dy_2 dy_3 \\
&\quad = \int_0^\infty \frac{1}{\lambda_3} \exp\left(-\frac{y_3}{\lambda_3} - \frac{c_1}{c_2\lambda_2}\right) \\
&\qquad\qquad \times \left\{1 - \frac{c_1\lambda_1}{c_1\lambda_1 + \lambda_2 z(c_3y_3+1)} \exp\left(-\frac{z(c_3y_3+1)}{c_2\lambda_1}\right)\right\} dy_3 \\
&\quad = \exp\left(-\frac{c_1}{c_2\lambda_2}\right) - \frac{c_1\lambda_1}{c_3\lambda_2\lambda_3 z} \exp\left\{\frac{1}{c_3\lambda_3}\left(\frac{c_1\lambda_1}{\lambda_2 z} + 1\right)\right\} \\
&\qquad\qquad \times E_1\left[\frac{1}{c_3\lambda_3}\left(\frac{c_1\lambda_1}{\lambda_2 z} + 1\right) + \frac{1}{c_2}\left(\frac{c_1}{\lambda_2} + \frac{z}{\lambda_1}\right)\right]. \qquad \text{(A.4)}
\end{aligned}$$

Substituting (A.3) and (A.4) into (A.2), the CDF becomes (3.38).

Appendix B

Proof of Theorem 3

Let

$$Z_2 = 2\beta|h_{PS_1,R_k}|^2 P_{PS} + (1-2\beta)|h_{PS_2,R_k}|^2 P_{PS}. \tag{B.1}$$

Using *Corollary* 1, the PDF of Z_2 is given by

$$f_{Z_2}(z) = \frac{1}{(4\beta-1)P_{PS}\lambda_{PS,R}} \times \left\{ \exp\left(-\frac{z}{2\beta P_{PS}\lambda_{PS,R}}\right) - \exp\left(-\frac{z}{(1-2\beta)P_{PS}\lambda_{PS,R}}\right)\right\}. \tag{B.2}$$

The probability that the relay R_k is in the decoding set $\mathcal{D}$ is given by

$$\begin{aligned}
\Pr\left[R_k \in \mathcal{D}\right] &= \Pr\left[\frac{X_{S,R_k}}{Z_2+1} \geq \gamma_{th}\right] \\
&= \int_0^\infty \left\{1 - F_{X_{S,R_k}}\left(\gamma_{th}(\gamma+1)\right)\right\} f_{Z_2}(\gamma) d\gamma \\
&= \frac{1}{(4\beta-1)P_{PS}\lambda_{PS,R}} \exp\left(-\frac{\gamma_{th}}{P_S\lambda_{S,R}}\right) \\
&\quad \times \left\{ \left(\frac{\gamma_{th}}{P_S\lambda_{S,R}} + \frac{1}{2\beta P_{PS}\lambda_{PS,R}}\right)^{-1} \right. \\
&\qquad \left. -\left(\frac{\gamma_{th}}{P_S\lambda_{S,R}} + \frac{1}{(1-2\beta)P_{PS}\lambda_{PS,R}}\right)^{-1} \right\} \\
&= \eta_1.
\end{aligned} \tag{B.3}$$

Then, the probability of decoding set is given by

$$\Pr\left[\mathcal{D}\right] = \prod_{R_k \in \mathcal{D}} \Pr\left[R_k \in \mathcal{D}\right] \prod_{R_k \notin \mathcal{D}} \Pr\left[R_k \notin \mathcal{D}\right] = \eta_1^{|\mathcal{D}|}(1-\eta_1)^{K-|\mathcal{D}|}. \tag{B.4}$$

The probability that the outage event occurs for the decoding set $\mathcal{D}$ is given by

$$\begin{aligned}
\Pr\left[\gamma_{R^*,D} < \gamma_{th} | \mathcal{D}\right] &= \sum_{R_k \in \mathcal{D}} \Pr\left[R_k = R^* | \mathcal{D}\right] \Pr\left[\gamma_{R_k,D} < \gamma_{th} | \mathcal{D}\right] \\
&= \sum_{R_k \in \mathcal{D}} \int_0^{\gamma_{th}} \prod_{R_l \in \mathcal{D}-\{R_k\}} F_{X_{R_l,D}}(\gamma) f_{X_{R_k,D}}(\gamma) d\gamma \\
&\quad + \sum_{R_k \in \mathcal{D}} \int_{\gamma_{th}}^{\infty} \left\{1 - F_{X_{PS_2,D}}\left(\frac{\gamma}{\gamma_{th}} - 1\right)\right\} \\
&\qquad \times \prod_{R_l \in \mathcal{D}-\{R_k\}} F_{X_{R_l,D}}(\gamma) f_{X_{R_k,D}}(\gamma) d\gamma \\
&= \left\{F_{X_{R,D}}(\gamma_{th})\right\}^{|\mathcal{D}|} \\
&\quad + \sum_{R_k \in \mathcal{D}} \int_{\gamma_{th}}^{\infty} \exp\left(-\frac{\gamma/\gamma_{th} - 1}{P_{PS}\lambda_{PS,D}}\right) \left\{1 - \exp\left(-\frac{\gamma}{P_R\lambda_{R,D}}\right)\right\}^{|\mathcal{D}|-1} \\
&\qquad \times \frac{1}{P_R\lambda_{R,D}} \exp\left(-\frac{\gamma}{P_R\lambda_{R,D}}\right) d\gamma \\
&= \left\{1 - \exp\left(-\frac{\gamma_{th}}{P_R\lambda_{R,D}}\right)\right\}^{|\mathcal{D}|} \\
&\quad + \frac{\gamma_{th}}{P_R\lambda_{R,D}} \exp\left(-\frac{\gamma_{th}}{P_R\lambda_{R,D}}\right) \\
&\qquad \times \sum_{R_k \in \mathcal{D}} \int_0^{\infty} \exp\left\{-\left(\frac{1}{P_{PS}\lambda_{PS,D}} + \frac{\gamma_{th}}{P_R\lambda_{R,D}}\right)\gamma\right\} \\
&\qquad \times \left\{1 - \exp\left(-\frac{\gamma_{th}}{P_R\lambda_{R,D}}\right) \exp\left(-\frac{\gamma_{th}\gamma}{P_R\lambda_{R,D}}\right)\right\}^{|\mathcal{D}|-1} d\gamma \\
&= \left\{1 - \exp\left(-\frac{\gamma_{th}}{P_R\lambda_{R,D}}\right)\right\}^{|\mathcal{D}|} \\
&\quad + |\mathcal{D}| \exp\left(\frac{1}{P_{PS}\lambda_{PS,D}}\right) \\
&\qquad \times B_{\exp\left(-\frac{\gamma_{th}}{P_R\lambda_{R,D}}\right)}\left(1 + \frac{P_R\lambda_{R,D}}{P_{PS}\lambda_{PS,D}\gamma_{th}}, |\mathcal{D}|\right).
\end{aligned} \tag{B.5}$$

The last equality comes from

$$\int_0^\infty \exp\left(-\mu x\right)\left\{1-\tau\exp\left(-\frac{x}{\rho}\right)\right\}^{\nu-1}dx = \int_0^\tau t^{\rho\mu-1}(1-t)^{\nu-1}\tau^{-\rho\mu}\rho dt$$
$$= \tau^{-\rho\mu}\rho B_\tau\left(\rho\mu,\nu\right) \tag{B.6}$$

where the first equality is obtained by the replacement

$$t = \tau\exp\left(-\frac{x}{\rho}\right). \tag{B.7}$$

Substituting (B.4) and (B.5) into

$$\begin{aligned} P_{out} &= \Pr\left[\gamma_{R^*,D} < \gamma_{th}\right] \\ &= \Pr\left[\mathcal{D}=\phi\right] + \sum_{\mathcal{D}\neq\phi}\Pr\left[\mathcal{D}\right]\Pr\left[\gamma_{R^*,D} < \gamma_{th}|\mathcal{D}\right], \end{aligned} \tag{B.8}$$

we obtain (3.41).

Appendix C

Proof of Theorem 4

For $\beta = 1/4$, the random variable Z_2 in B.1 becomes

$$Z_2 = \frac{1}{2}|h_{PS_1,R_k}|^2 P_{PS} + \frac{1}{2}|h_{PS_2,R_k}|^2 P_{PS}. \tag{C.1}$$

Using *Corollary* 2, its PDF is given by

$$f_{Z_2}(z) = \frac{4z}{\left(P_{PS}\lambda_{PS,R}\right)^2} \exp\left(-\frac{2z}{P_{PS}\lambda_{PS,R}}\right). \tag{C.2}$$

The probability that the relay R_k is in the decoding set $\mathcal{D}$ is given by

$$\begin{aligned}
\Pr\left[R_k \in \mathcal{D}\right] &= \Pr\left[\frac{X_{S,R_k}}{Z_2 + 1} \geq \gamma_{th}\right] \\
&= \int_0^\infty \left\{1 - F_{X_{S,R_k}}\left(\gamma_{th}(\gamma+1)\right)\right\} f_{Z_2}(\gamma) d\gamma \\
&= \frac{4}{\left(P_{PS}\lambda_{PS,R}\right)^2} \exp\left(-\frac{\gamma_{th}}{P_S\lambda_{S,R}}\right)\left(\frac{\gamma_{th}}{P_S\lambda_{S,R}} + \frac{2}{P_{PS}\lambda_{PS,R}}\right)^{-2} \\
&= \eta_2.
\end{aligned} \tag{C.3}$$

Then, the probability of decoding set is given by

$$\begin{aligned}
\Pr\left[\mathcal{D}\right] &= \prod_{R_k \in \mathcal{D}} \Pr\left[R_k \in \mathcal{D}\right] \prod_{R_k \notin \mathcal{D}} \Pr\left[R_k \notin \mathcal{D}\right] \\
&= \eta_2^{|\mathcal{D}|}(1-\eta_2)^{K-|\mathcal{D}|}.
\end{aligned} \tag{C.4}$$

The probability that the outage event occurs for the decoding set $\mathcal{D}$ is given by (B.5). Substituting (B.5) and (C.4) into (B.8), we obtain (3.43).

Appendix D

Proof of Theorem 5

The probability that the relay R_k is in the decoding set $\mathcal{D}$ is given by

$$\begin{aligned}\Pr\left[R_k \in \mathcal{D}\right] &= \Pr\left[\frac{X_{S,R_k}}{X_{PS_1,R_k}+1} \geq \gamma_{th}\right] \\ &= \int_0^\infty \left\{1 - F_{X_{S,R_k}}\left(\gamma_{th}(\gamma+1)\right)\right\} f_{X_{PS_1,R_k}}(\gamma) d\gamma \\ &= \exp\left(-\frac{\gamma_{th}}{P_S\lambda_{S,R}}\right)\left(1+\frac{P_{PS}\lambda_{S,R}}{P_S\lambda_{S,R}}\gamma_{th}\right)^{-1} \\ &= \eta_3. \end{aligned} \tag{D.1}$$

Then, the probability of decoding set is given by

$$\begin{aligned}\Pr\left[\mathcal{D}\right] &= \prod_{R_k\in\mathcal{D}} \Pr\left[R_k \in \mathcal{D}\right] \prod_{R_k\notin\mathcal{D}} \Pr\left[R_k \notin \mathcal{D}\right] \\ &= \eta_3^{|\mathcal{D}|}(1-\eta_3)^{K-|\mathcal{D}|}. \end{aligned} \tag{D.2}$$

Let

$$Z_3 = (2\beta-1)|h_{PS_1,D}|^2 P_{PS} + 2(1-\beta)|h_{PS_2,D}|^2 P_{PS}. \tag{D.3}$$

Using *Corollary* 1, the CDF of Z_3 is given by

$$F_{Z_3}(z) = 1 - \frac{2\beta-1}{4\beta-3}\exp\left(-\frac{z}{(2\beta-1)P_{PS}\lambda_{PS,D}}\right) + \frac{2(1-\beta)}{4\beta-3}\exp\left(-\frac{z}{2(1-\beta)P_{PS}\lambda_{PS,D}}\right). \tag{D.4}$$

The probability that the outage event occurs for the decoding set $\mathcal{D}$ is given by

$$\begin{aligned}
\Pr\left[\gamma_{R^*,D} < \gamma_{th}|\mathcal{D}\right] &= \sum_{R_k\in\mathcal{D}} \Pr\left[R_k = R^*|\mathcal{D}\right]\Pr\left[\gamma_{R_k,D} < \gamma_{th}|\mathcal{D}\right] \\
&= \sum_{R_k\in\mathcal{D}}\int_0^{\gamma_{th}} \prod_{R_l\in\mathcal{D}-\{R_k\}} F_{X_{R_l,D}}(\gamma) f_{X_{R_k,D}}(\gamma)d\gamma \\
&\quad + \sum_{R_k\in\mathcal{D}}\int_{\gamma_{th}}^{\infty}\left\{1 - F_{Z_3}\left(\frac{\gamma}{\gamma_{th}} - 1\right)\right\} \\
&\qquad \times \prod_{R_l\in\mathcal{D}-\{R_k\}} F_{X_{R_l,D}}(\gamma) f_{X_{R_k,D}}(\gamma)d\gamma \\
&= \left\{F_{X_{R,D}}(\gamma_{th})\right\}^{|\mathcal{D}|} \\
&\quad + \sum_{R_k\in\mathcal{D}}\int_{\gamma_{th}}^{\infty}\frac{2\beta-1}{4\beta-3}\exp\left(-\frac{\gamma/\gamma_{th}-1}{(2\beta-1)P_{PS}\lambda_{PS,D}}\right) \\
&\qquad \times\left\{1-\exp\left(-\frac{\gamma}{P_R\lambda_{R,D}}\right)\right\}^{|\mathcal{D}|-1}\frac{1}{P_R\lambda_{R,D}}\exp\left(-\frac{\gamma}{P_R\lambda_{R,D}}\right)d\gamma \\
&\quad - \sum_{R_k\in\mathcal{D}}\int_{\gamma_{th}}^{\infty}\frac{2(1-\beta)}{4\beta-3}\exp\left(-\frac{\gamma/\gamma_{th}-1}{2(1-\beta)P_{PS}\lambda_{PS,D}}\right) \\
&\qquad \times\left\{1-\exp\left(-\frac{\gamma}{P_R\lambda_{R,D}}\right)\right\}^{|\mathcal{D}|-1}\frac{1}{P_R\lambda_{R,D}}\exp\left(-\frac{\gamma}{P_R\lambda_{R,D}}\right)d\gamma.
\end{aligned} \tag{D.5}$$

Similar to (B.5), using (B.6), this is calculated as

$$\begin{aligned}\Pr\left[\gamma_{R^*,D} < \gamma_{th} | \mathcal{D}\right] = & \left\{1 - \exp\left(-\frac{\gamma_{th}}{P_R \lambda_{R,D}}\right)\right\}^{|\mathcal{D}|} \\ & + |\mathcal{D}| \frac{2\beta - 1}{4\beta - 3} \exp\left(\frac{1}{(2\beta - 1) P_{PS} \lambda_{PS,D}}\right) \\ & \times B_{\exp\left(-\frac{\gamma_{th}}{P_R \lambda_{R,D}}\right)}\left(1 + \frac{P_R \lambda_{R,D}}{(2\beta - 1) P_{PS} \lambda_{PS,D} \gamma_{th}}, |\mathcal{D}|\right) \\ & - |\mathcal{D}| \frac{2(1 - \beta)}{4\beta - 3} \exp\left(\frac{1}{2(1 - \beta) P_{PS} \lambda_{PS,D}}\right) \\ & \times B_{\exp\left(-\frac{\gamma_{th}}{P_R \lambda_{R,D}}\right)}\left(1 + \frac{P_R \lambda_{R,D}}{2(1 - \beta) P_{PS} \lambda_{PS,D} \gamma_{th}}, |\mathcal{D}|\right). \quad \text{(D.6)}\end{aligned}$$

Substituting (D.2) and (D.6) into (B.8), we obtain (3.45).

Appendix E

Proof of Theorem 6

The probability of decoding set is given by (D.2). For $\beta = 3/4$, the random variable Z_3 in (D.3) becomes

$$Z_3 = \frac{1}{2}|h_{PS_1,D}|^2 P_{PS} + \frac{1}{2}|h_{PS_2,D}|^2 P_{PS}. \tag{E.1}$$

Using *Corollary* 2, its CDF is given by

$$F_{Z_3}(z) = 1 - \exp\left(-\frac{2z}{P_{PS}\lambda_{PS,D}}\right) - \frac{2z}{P_{PS}\lambda_{PS,D}} \exp\left(-\frac{2z}{P_{PS}\lambda_{PS,D}}\right). \tag{E.2}$$

The probability that the outage event occurs for the decoding set $\mathcal{D}$ is given by

$$\begin{aligned}
\Pr\left[\gamma_{R^*,D} < \gamma_{th} | \mathcal{D}\right] &= \sum_{R_k \in \mathcal{D}} \Pr\left[R_k = R^* | \mathcal{D}\right] \Pr\left[\gamma_{R_k,D} < \gamma_{th} | \mathcal{D}\right] \\
&= \sum_{R_k \in \mathcal{D}} \int_0^{\gamma_{th}} \prod_{R_l \in \mathcal{D} - \{R_k\}} F_{X_{R_l,D}}(\gamma) f_{X_{R_k,D}}(\gamma) d\gamma \\
&\quad + \sum_{R_k \in \mathcal{D}} \int_{\gamma_{th}}^{\infty} \left\{1 - F_{Z_3}\left(\frac{\gamma}{\gamma_{th}} - 1\right)\right\} \\
&\qquad \times \prod_{R_l \in \mathcal{D} - \{R_k\}} F_{X_{R_l,D}}(\gamma) f_{X_{R_k,D}}(\gamma) d\gamma \\
&= \left\{1 - \exp\left(-\frac{\gamma_{th}}{P_R \lambda_{R,D}}\right)\right\}^{|\mathcal{D}|} \\
&\quad + \sum_{R_k \in \mathcal{D}} \int_{\gamma_{th}}^{\infty} \exp\left(-\frac{2\gamma/\gamma_{th} - 2}{P_{PS} \lambda_{PS,D}}\right) \\
&\qquad \times \left\{1 - \exp\left(-\frac{\gamma}{P_R \lambda_{R,D}}\right)\right\}^{|\mathcal{D}|-1} \frac{1}{P_R \lambda_{R,D}} \exp\left(-\frac{\gamma}{P_R \lambda_{R,D}}\right) d\gamma \\
&\quad + \sum_{R_k \in \mathcal{D}} \int_{\gamma_{th}}^{\infty} \frac{2\gamma/\gamma_{th} - 2}{P_{PS} \lambda_{PS,D}} \exp\left(-\frac{2\gamma/\gamma_{th} - 2}{P_{PS} \lambda_{PS,D}}\right) \\
&\qquad \times \left\{1 - \exp\left(-\frac{\gamma}{P_R \lambda_{R,D}}\right)\right\}^{|\mathcal{D}|-1} \frac{1}{P_R \lambda_{R,D}} \exp\left(-\frac{\gamma}{P_R \lambda_{R,D}}\right) d\gamma.
\end{aligned} \tag{E.3}$$

Similar to (B.5), using (B.6), the second term of right-hand side of (E.3) is calculated as

$$|\mathcal{D}| \exp\left(\frac{2}{P_{PS} \lambda_{PS,D}}\right) B_{\exp\left(-\frac{\gamma_{th}}{P_R \lambda_{R,D}}\right)}\left(1 + \frac{2 P_R \lambda_{R,D}}{P_{PS} \lambda_{PS,D} \gamma_{th}}, |\mathcal{D}|\right). \tag{E.4}$$

Using the formula

$$\begin{aligned}
&\int_0^\infty x\left\{1-\tau\exp\left(-\frac{x}{\rho}\right)\right\}^{\nu-1}\exp\left(-\mu x\right)dx \\
&\qquad=\sum_{n=0}^{\nu-1}\binom{v-1}{n}(-\tau)^n\int_0^\infty x\exp\left\{-\left(\frac{n}{\rho}+\mu\right)x\right\}dx \\
&\qquad=\sum_{n=0}^{\nu-1}\binom{v-1}{n}(-\tau)^n\left(\frac{n}{\rho}+\mu\right)^{-2} \\
&\qquad=\frac{{}_3F_2\left(\rho\mu,\rho\mu,1-\nu;1+\rho\mu,1+\rho\mu;\tau\right)}{\mu^2},
\end{aligned}\tag{E.5}$$

the third term of right-hand side of (E.3) is calculated as

$$\begin{aligned}
&\frac{2\left|\mathcal{D}\right|\gamma_{th}}{P_{PS}\lambda_{PS,D}P_R\lambda_{R,D}}\exp\left(-\frac{\gamma_{th}}{P_R\lambda_{R,D}}\right)\left(\frac{2}{P_{PS}\lambda_{PS,D}}+\frac{\gamma_{th}}{P_R\lambda_{R,D}}\right)^{-2} \\
&\quad\times{}_3F_2\left[\frac{2P_R\lambda_{R,D}}{P_{PS}\lambda_{PS,D}\gamma_{th}}+1,\frac{2P_R\lambda_{R,D}}{P_{PS}\lambda_{PS,D}\gamma_{th}}+1,1-\left|\mathcal{D}\right|;\right. \\
&\qquad\left.\frac{2P_R\lambda_{R,D}}{P_{PS}\lambda_{PS,D}\gamma_{th}}+2,\frac{2P_R\lambda_{R,D}}{P_{PS}\lambda_{PS,D}\gamma_{th}}+2;\exp\left(-\frac{\gamma_{th}}{P_R\lambda_{R,D}}\right)\right].
\end{aligned}\tag{E.6}$$

Substituting (D.2), (E.4), and (E.6) into (B.8), we obtain (3.47).

Appendix F

Proof of Corollary 3

Consider $0 < \beta < 1/4$ or $1/4 < \beta < 2/4$. The outage probability can be obtained in two different ways.

First, it is obtained using

$$P_{out} = 1 - \Pr\left[\gamma_{S,R_1} \geq \gamma_{th}\right] \times \Pr\left[\gamma_{R_1,D} \geq \gamma_{th}\right]. \tag{F.1}$$

Then, $\Pr\left[\gamma_{S,R_1} \geq \gamma_{th}\right]$ is given by (B.3). Also, we have

$$\begin{aligned}
\Pr\left[\gamma_{R_1,D} \geq \gamma_{th}\right] &= \Pr\left[\frac{X_{R,D}}{X_{PS,D}+1} \geq \gamma_{th}\right] \\
&= \int_0^\infty \left\{1 - F_{X_{R,D}}\left(\gamma_{th}(\gamma+1)\right)\right\} f_{X_{PS,D}}(\gamma) d\gamma \\
&= \int_0^\infty \exp\left(-\frac{\gamma_{th}(\gamma+1)}{P_R\lambda_{R,D}}\right) \frac{1}{P_{PS}\lambda_{PS,D}} \exp\left(-\frac{\gamma}{P_{PS}\lambda_{PS,D}}\right) d\gamma \\
&= \exp\left(-\frac{\gamma_{th}}{P_R\lambda_{R,D}}\right)\left(\frac{P_{PS}\lambda_{PS,D}}{P_R\lambda_{R,D}}\gamma_{th}+1\right)^{-1}.
\end{aligned} \tag{F.2}$$

Substituting (B.3) and (F.2) into (F.1), the outage probability is given by (3.49).

Second, the outage probability is obtained by substituting $K = 1$ into (3.41).

Then, it becomes

$$P_{out} = 1 - \eta_1 \exp\left(-\frac{\gamma_{th}}{P_R \lambda_{R,D}}\right) + \eta_1 \exp\left(\frac{1}{P_{PS}\lambda_{PS,D}}\right) B_{\exp\left(-\frac{\gamma_{th}}{P_R \lambda_{R,D}}\right)}\left(1 + \frac{P_R \lambda_{R,D}}{P_{PS}\lambda_{PS,D}\gamma_{th}}, 1\right). \quad \text{(F.3)}$$

After some manipulations using the formula

$$B_x(p,1) = \int_0^x t^{p-1} dt = p^{-1} x^p, \quad \text{(F.4)}$$

it becomes (3.49).

Note that the two different ways eventually reach the same result. The other outage probabilities in (3.50)-(3.53) are obtained similarly.

Appendix G

Proof of Theorem 8

Let

$$Z_4 = \beta|h_{PS_1,D}|^2 P_{PS} + (1-\beta)|h_{PS_2,D}|^2 P_{PS}. \tag{G.1}$$

First, consider $0 < \beta < 1/2$ or $1/2 < \beta < 1$. Using *Corollary* 1, the PDF of Z_4 is given by

$$\begin{aligned} f_{Z_4}(z) = & \frac{1}{(2\beta-1)P_{PS}\lambda_{PS,R}} \\ & \times \left\{ \exp\left(-\frac{z}{\beta P_{PS}\lambda_{PS,D}}\right) - \exp\left(-\frac{z}{(1-\beta)P_{PS}\lambda_{PS,D}}\right) \right\}. \end{aligned} \tag{G.2}$$

The outage probability is given by

$$\begin{aligned} P_{out,0<\beta<\frac{1}{2}} = P_{out,\frac{1}{2}<\beta<1} &= \Pr\left[\frac{X_{S,D}}{Z_4+1} < \gamma_{th}\right] \\ &= 1 - \int_0^\infty \left\{1 - F_{X_{S,D}}\left(\gamma_{th}(\gamma+1)\right)\right\} f_{Z_4}(\gamma) d\gamma \\ &= 1 - \frac{1}{(2\beta-1)P_{PS}\lambda_{PS,D}} \exp\left(-\frac{\gamma_{th}}{P_S\lambda_{S,D}}\right) \\ &\quad \times \left\{ \left(\frac{\gamma_{th}}{P_S\lambda_{S,D}} + \frac{1}{\beta P_{PS}\lambda_{PS,D}}\right)^{-1} \right. \\ &\quad \left. - \left(\frac{\gamma_{th}}{P_S\lambda_{S,D}} + \frac{1}{(1-\beta)P_{PS}\lambda_{PS,D}}\right)^{-1} \right\}. \end{aligned} \tag{G.3}$$

Second, consider $\beta = 1/2$. Using *Corollary* 2, the PDF of Z_4 is given by

$$f_{Z_4}(z) = \frac{4z}{\left(P_{PS}\lambda_{PS,D}\right)^2} \exp\left(-\frac{2z}{P_{PS}\lambda_{PS,D}}\right). \tag{G.4}$$

The outage probability is given by

$$\begin{aligned} P_{out,\beta=\frac{1}{2}} &= \Pr\left[\frac{X_{S,D}}{Z_4+1} < \gamma_{th}\right] \\ &= 1 - \int_0^\infty \left\{1 - F_{X_{S,D}}\left(\gamma_{th}(\gamma+1)\right)\right\} f_{Z_4}(\gamma) d\gamma \\ &= 1 - \frac{4}{\left(P_{PS}\lambda_{PS,D}\right)^2} \exp\left(-\frac{\gamma_{th}}{P_S\lambda_{S,D}}\right)\left(\frac{\gamma_{th}}{P_S\lambda_{S,D}} + \frac{2}{P_{PS}\lambda_{PS,D}}\right)^{-2}. \end{aligned} \tag{G.5}$$

Third, consider $\beta = 1$. Similar to (F.2), the outage probability is given by

$$\begin{aligned} P_{out,\beta=1} &= \Pr\left[\frac{X_{S,D}}{X_{PS,D}+1} < \gamma_{th}\right] \\ &= 1 - \exp\left(-\frac{\gamma_{th}}{P_S\lambda_{S,D}}\right)\left(\frac{P_{PS}\lambda_{PS,D}}{P_S\lambda_{S,D}}\gamma_{th} + 1\right)^{-1}. \end{aligned} \tag{G.6}$$

Bibliography

[1] R. Pabst, B. H. Walke, D. C. Schultz, P. Herhold, H. Yanikomeroglu, S. Mukherjee, H Viswanathan, M. Lott, W. Zirwas, M. Dohler, AH. Aghvami, D. D. Falconer, and G. P. Fettweis, "Relay-based deployment consepts for wireless and mobile broadband radio," *IEEE Commun. Mag.*, vol. 42, no. 9, pp. 80-89, Sep. 2004.

[2] A. Nostratinia, T. E. Hunter, and A. Hedayat, "Cooperative communication in wirless networks," *IEEE Commun. Mag.*, vol. 42, no. 10, pp. 74-80, Oct. 2004.

[3] L. Le and E. Hossain, "Multihop cellular network: Potential gains, research challenges, and a resource allocation framework," *IEEE Commun. Mag.*, vol. 45, no. 9, pp. 66-73, Sep. 2007.

[4] Ö. Oyman, J. Laneman, and S. Sandhu, "Multihop relaying for broadband wireless mesh networks: From theory to practice," *IEEE Commun. Mag.*, vol. 45, no. 11, pp. 116-122, Nov. 2007.

[5] Y. Yang, H. Hu, J. Xu, and G. Mao, "Relay technologies for WiMAX and LET-Advanced mobile systems," *IEEE Commun. Mag.*, vol. 47, no. 10, pp. 100-105, Oct. 2009.

[6] K. Loa, C.-C. Wu, S.-T. SHeu, Y. Yuan, M. Chion, D. Huo, and L. Xu, "IMT-Advanced relay standards," *IEEE Commun. Mag.*, vol. 48, no. 8, pp. 40-48, Aug. 2010.

[7] X. Tao, X. Xu, and Q. Cui, "An overview of cooperative communications," *IEEE Commun. Mag.*, vol. 50, no. 6, pp. 65-71, June 2012.

[8] M. O. Hasna and M.-S. Alouini, "Outage probability of multihop transmission over Nakagami fading channels," *IEEE Commun. Lett.*, vol. 7, no. 5, pp. 216-218, May 2003.

[9] M. O. Hasna and M.-S. Alouini, "A performance study of dual-hop transmissions with fixed gain relays," *IEEE Trans. Wireless Commun.*, vol. 3, no. 6, pp. 1963-1968, Nov. 2004.

[10] E. C. V. D. Meulen, "Three-terminal communication channels," *Applied Probability Trust, Advances in Applied Probability*, vol. 3, no. 1, pp. 120-154, Spr. 1971.

[11] T. M. Cover and A. A. El Gamal, "Capacity theorems for the relay channel," *IEEE Trans. Inf. Theory*, vol. 25, pp. 572-584, Sep. 1979.

[12] D. Lee, *Performance analysis of multi-hop relaying systems in the presence of cochannel interference*, Ph.D. dissertation, Seoul Nat'l Univ., Seoul, Korea, Aug. 2011.

[13] A. Sendonaris, E. Erkip, and B. Aazhang, "Increasing uplink capacity via user cooperation diversity," in *Proc. IEEE Int. Symp. Inf. Theory (ISIT) 1998*, Cambridge, MA, Aug. 1998.

[14] A. Sendonaris, E. Erkip, and B. Aazhang, "User cooperation diversity - Part I: System description," *IEEE Trans. Commun.*, vol. 51, no. 11, pp. 1927-1938, Nov. 2003.

[15] A. Sendonaris, E. Erkip, and B. Aazhang, "User cooperation diversity - Part II: Implementation aspects and performacne analysis," *IEEE Trans. Commun.*, vol. 51, no. 11, pp. 1939-1948, Nov. 2003.

[16] M. Gastpar and M. Vetterli, "On the capacity of wireless networks: The relay case," in *Proc. IEEE Int. Conf. Comput. Commun. (INFOCOM) 2002*, New York, NY, June 2002.

[17] J. N. Laneman and G. W. Wornell, "Distributed space-time-coded protocols for exploiting cooperative diversity in wireless networks," *IEEE Trans. Inf. Theory*, vol. 49, no. 10, pp. 2415-2425, Oct. 2003.

[18] J. N. Laneman, D. N. C. Tse, and G. W. Wornell, "Cooperative diversity in wireless networks: Efficient protocols and outage behavior," *IEEE Trans. Inf. Theory*, vol. 50, no. 12, pp. 3062-3080, Dec. 2004.

[19] G. Korkmaz, E. Ekici, F. Özgüner, and Ü. Özgüner, "Urban multi-hop broadcast protocol for inter-vehicle communication systems," in *Proc. 1st ACM Wksp. VANET*, Philadelphia, PA, Oct. 2004.

[20] S. Yousefi, E. Altman, R. El-Azouzi, and M. Fathy, "Analytical model for connectivity in vehicular ad hoc networks," *IEEE Trans. Veh. Technol.*, vol. 57, no. 6, pp. 3341-3356, Nov. 2008.

[21] C. Jang and J. H. Lee, "Path selection algorithms for muti-hop VANETs," in *Proc. Veh. Technol. Conf. (VTC) 2010-SPring*, Ottawa, Canada, Sep. 2010.

[22] M. Seyfi, S. Muhiaday, J. Liang, and M. Uysal, "Relay selection in dual-hop vehicular networks," *IEEE Signal Process. Lett.*, vol. 18, no. 2, pp. 134-137, Feb. 2011.

[23] R. Zhang and L. Hanjo, "Interleave division multiplexing aided space-time coding for high-throughput uplink," in *Proc. Wireless Commun. Netw. Conf. (WCNC) 2008*, Las Vegas, NV, Apr. 2008.

[24] Z. Fang, L. Liangbin, and Z. Wang, "An interleaver-based asynchronous cooperative diversity scheme for wireless relay networks," in *Proc. Int. Conf. Commun. (ICC) 2008*, Beijing, China, May 2008.

[25] C. Jang and J. H. Lee, "IDMA system with relays," in *Proc. Int. Conf. Wireless Commun. Veh. Technol. Inf. Theory Aerosp. Electron. Syst. Technol. (VITAE) 2009*, Aalborg, Denmark, May 2009.

[26] *IEEE standard for local and metropolitan area networks Part 16: Air interface for broadband wireless access systems, Amendment 1- Multiple relay specification*, IEEE Std 802.16j-2009, June 2009.

[27] J. Boyer, D. D. Falconer, and H. Yanikomeroglu, "Multihop diversity in wireless relaying channels," *IEEE Trans. Commun.*, vol. 52, no. 10, pp. 1820-1830, Oct. 2004.

[28] A. Stefanov and E. Erkip, "Cooperative space-time coding for wireless networks," *IEEE Trans. Commun.*, vol. 53, no. 11, pp. 1804-1809, Nov. 2005.

[29] A. Bletsas, A. Khisti, D. P. Reed, and A. Lippman, "A simple cooperative diversity method based on network path selection," *IEEE J. Sel. Areas Commun.*, vol. 24, no. 3, pp. 659-672, Mar. 2006.

[30] A. Bletsas, H. Shin, and M. Z. Win, "Cooperative communications with outage-optimal opportunistic relaying," *IEEE Trans. Wireless Commun.*, vol. 6, no. 9, pp. 3450-3460, Sep. 2007.

[31] T. Issariyakul and E. Hossain, "Performance modeling and analysis of a class of ARQ protocols in multi-hop wireless networks," *IEEE Trans. Wireless Commun.*, vol. 5, no. 12, pp. 3460-3468, Dec. 2006.

[32] L. Le and E. Hossain, "An analytical model for ARQ cooperative diversity in multi-hop wireless networks," *IEEE Trans. Wireless Commun.*, vol. 7, no. 5, pp. 1786-1791, May 2008.

[33] B. Gui, L. Dai, and L. J. Cimini, JR., "Routing strategies in multihop cooperative network," *IEEE Trans. Wireless Commun.*, vol. 8, no. 2, pp. 843-855, Feb. 2009.

[34] Z. Yi and I.-M. Kim, "Relay ordering in a multi-hop cooperative diversity network," *IEEE Trans. Commun.*, vol. 57, no. 9, pp. 2590-2596, Sep. 2009.

[35] E. Beres and R. adve, "Selection cooperation in multi-source cooperative networks," *IEEE Trans. Wireless Commun.*, vol. 7, no. 1, pp. 118-127, Jan. 2008.

[36] B. Rankov and A. Wittneben, "Spectral efficient protocols for half-duplex fading relay channels," *IEEE J. Sel. Areas Commun.*, vol. 25, no. 2, pp. 379-389, Feb. 2007.

[37] Y. Hu, K. H. Li, and K. C. Teh, "An efficient successive relaying protocol for multiple-relay cooperative networks," *IEEE Trans. Wireless Commun.*, vol. 11, no. 5, pp. 1892-1899, Sep. 2012.

[38] A. Ikhlef, J. Kim, and R. Schober, "Mimicking full-duplex relaying using half-duplex relays with buffers," *IEEE Trans. Veh. Technol.*, vol. 61, no. 7, pp. 3025-3037, Sep. 2012.

[39] T. Riihonen and S. Werver, "Hybrid full-duplex/half-duplex relaying with transmit power adaptation," *IEEE Trans. Wireless Commun.*, vol. 10, no. 9, pp. 3074-3085, Sep. 2011.

[40] D. W. K. Ng, E. S. Lo, and R. Schober, "Dynamic resource allocation in MIMO-OFDMA systems with full-duplex and hybrid relaying," *IEEE Trans. Wireless Commun.*, vol. 11, no. 12, pp. 4381-4393, Dec. 2012.

[41] I. Krikidis, H. A. Suraweera, P. J. Smith, and C. Yuen, "Full-duplex relay selection for amplify-and-forward cooperative networks," *IEEE Trans. Wireless Commun.*, vol. 11, no. 12, pp. 4381-4393, Dec. 2012.

[42] I. Krikidis, H. A. Suraweera, S. Yang, K. Berberidis, "Full-duplex relaying over block fading channel: A diversity perspective," *IEEE Trans. Wireless Commun.*, vol. 11, no. 12, pp. 4524-4534, Dec. 2012.

[43] F. Xue and S. Sandhu, "Cooperation in a half-duplex Gaussian diamond relay channel," *IEEE Trans. Inf. Theory*, vol. 53, no. 10, pp. 3806-3814, Oct. 2007.

[44] C. Jang and J. H. Lee, "Outage analysis and optimization of DF-based multi-hop transmission for fading channels with large path-loss exponent," *IEEE Trans. Veh. Technol.*, vol. 61, no. 9, pp. 4183-1389, Nov. 2012.

[45] FCC, *Spectrum policy task force*. ET Docket 02-135, Nov. 2002.

[46] M. McHenry, *NSF spectrum occupancy measurements project summary*, Shared spectrum co. report, Aug. 2005.

[47] M. McHenry, E. Livsics, T. Nguyen, and N. Majumdar, "XG dynamic spectrum access field test results," *IEEE Commun. Mag.*, vol. 45, no. 6, pp. 51-57, June 2007.

[48] K. B. Letaief and W. Zhang, "Cooperative communications for cognitive radio networks," *Proc. IEEE*, vol. 97, no. 5, pp. 878-893, May 2009.

[49] I. J. Mitola, "Software radios: Survey, critical evaluation, and future directions," *IEEE Aerosp. Electron. Syst. Mag.*, vol. 8, no. 4, pp. 25-36, Apr. 1993.

[50] I. J. Mitola and G. Q. Maguire, Jr., "Cognitive radio: Making software radio more personal," *IEEE Pers. Commun.*, vol. 6, no. 4, pp. 13-18, Aug. 1999.

[51] S. Haykin, "Cognitive radio: Brain-empowered wireless communications," *IEEE J. Sel. Areas Commun.*, vol. 23, no. 2, pp. 201-220, Feb. 2005.

[52] A. Ghasemi and E. S. Sousa, "Spectrum sensing in cognitive radio networks: Requirements, challengers and design trade-offs," *IEEE Commun. Mag.*, vol. 46, no. 4, pp. 32-39, Apr. 2008.

[53] G. Ganesan and Y. G. Li, "Coopeative spectrum sensing in cognitive radio, Part I: Two user networks," *IEEE Trans. Wireless Commun.*, vol. 6, no. 6, pp. 2204-2213, June 2007.

[54] G. Ganesan and Y. G. Li, "Coopeative spectrum sensing in cognitive radio, Part II: Multiuser networks," *IEEE Trans. Wireless Commun.*, vol. 6, no. 6, pp. 2214-2222, June 2007.

[55] J. Ma, G. Zhao, and Y. G. Li, "Soft combination for cooperative spectrum sensing in cognitive radio networks," *IEEE Trans. Wireless Commun.*, vol. 7, no. 11, pp. 4502-4507, Nov. 2008.

[56] D. Duan, L Yang, J. C. Principe, "Coopeative diversity of spectrum sensing for cognitive radio systems," *IEEE Trans. Signal Process.*, vol. 58, no. 6, pp. 3218-3227, June 2010.

[57] C. Jang and J. H. Lee, "Sum of discrete i.i.d. random variables and its application to cooperative spectrum sensing," *IEEE Trans. Veh. Technol.*, vol. 62, no. 3, pp. 1383-1389, Mar. 2013.

[58] Y. Zou, Y.-D. Yao, and B. Zheng, "Outage probability analysis of cognitive transmission: Impact of spectrum sensing overhead," *IEEE Trans. Wireless Commun.*, vol. 9, no. 8, pp. 2676-2688, Aug. 2010.

[59] Y. Zou, Y.-D. Yao, and B. Zheng, "Cognitive transmissions with multiple relays in cognitive radio networks," *IEEE Trans. Wireless Commun.*, vol. 10, no. 2, pp. 648-659, Feb. 2011.

[60] Y. Zou, Y.-D. Yao, and B. Zheng, "A cooperative sensing based cognitive relay transmission scheme without a dedicated sensing relay channel in cognitive radio networks," *IEEE Trans. Signal Process.*, vol. 59, no. 2, pp. 854-858, Feb. 2011.

[61] J. M. Peha, "Approaches to spectrum sensing," *IEEE Commun. Mag.*, vol. 43, no. 2, pp. 10-12, Feb. 2005.

[62] Y. Zou, J. Zhu, B. Zheng, and Y.-D. Yao, "An adaptive cooperation diversity scheme with best-relay selection in cognitive radio networks," *IEEE Trans. Signal Process.*, vol. 58, no. 10, pp. 5438-5445, Oct. 2010.

[63] J. Lee, H. Wang, J. G. Andrews, and D. Hong, "Outage probability of cognitive relay networks with interference constraints," *IEEE Trans. Wireless Commun.*, vol. 10, no. 2, pp. 390-395, Feb. 2011.

[64] D. Li, "Outage probability of cognitive relay networks with relay selection," *IET Commun.*, vol. 5, no. 18, pp. 2730-2735, Dec. 2011.

[65] W. Xu, J. Zhang, P. Zhang, and C. Tellambura, "Outage probability of decode-and-forward cognitive relay in presence of primary user's interference," *IEEE Commun. Lett.*, vol. 16, no. 8, pp. 1252-1255, Aug. 2012.

[66] R. M. Corless, G. H. Gonnet, D. E. G. Hare, D. J. Jeffrey, and D. E. Knuth, "On the Labert W function," *Adv. Comp. Math.*, vol. 5, pp. 329-359, 1996.

[67] F. Chapeau-Blondeau and A. Monir, "Numerical evaluation of the Lambert W function and application to generation of generalized Gaussian noise with exponent 1/2," *IEEE Trans. Signal Process.*, vol. 50, no. 9, pp. 2160-2165, Sep. 2002.

[68] I. S. Gradshteyn and I. M Ryzhik, *Table of Integrals, Series and Products*. NY: Academic, 2007.

[69] A. Erdelyi, *Higher Transcendental Functions*, vol. 2. NY: McGraw-Hill, 1953.

[70] A. Erdelyi, *Higher Transcendental Functions*, vol. 1. NY: McGraw-Hill, 1953.

[71] D. Zhou and T.-H. Lai, "An accurate and scalable clock synchronization protocol for IEEE 802.11-based multihop ad hoc networks," *IEEE Trans. Parallel Distrib. Syst.*, vol. 18, no. 12, pp. 1797-1808, Dec. 2007.

[72] A. Marco, R. Casas, J. L. S. Ramos, V. Coarasa, A. Asensio, and M. S. Obaidat, "Synchronization of multihop wireless sensor networks at the application layer," *IEEE Wireless Commun.*, vol. 18, no. 1, pp. 82-88, Feb. 2011.

[73] A. L.-Garcia, *Probability and Random Processes for Electrical Engineering*. Reading, MA: Addison-Wesley Publishing, 1994.

[74] H. Shin and M. Z. Win, "MIMO diversity in the presence of double scattering," *IEEE Trans. Inf. Theory*, vol. 54, no. 7, pp. 2976-2996, July 2008.

[75] D. Lee and J. H. Lee, "Outage Probability for Dual-Hop Relaying Systems With Multiple Interferers Over Rayleigh Fading Channels," *IEEE Trans. Veh. Technol.*, vol. 60, no. 1, pp. 333-338, Jan. 2011.

[76] D. Bharadia, G. Bansal, P. Kaligineedi, and V. K. Bhargava, "Relay and power allocation schemes for OFDM-based cognitive radio systems," *IEEE Trans. Wireless Commun.*, vol. 10, no. 9, pp. 2812-2817, Sep. 2011.

[77] R. J. Schilling and S. L. Harris, *Applied numerical methods for engineers using Matlab and C*, Pacific Grove, CA: Brooks/Cole, 2000.

[78] T. Chrysikos and S. Kotsopoulos, "Impact of channel-dependent variation of path loss exponent on wireless information-theoretic security," in *Proc. Wireless Telecommun. Symp. (WTS) 2009*, Prague, Czech Rep., Apr. 2009.

[79] A. Fort, J. Ryckaert, C. Desset, P. D. Doncker, P. Wambacq, and L. V. Biesen, "Ultra-wideband channel model for communication around the human body," *IEEE J. Sel. Areas Commun.*, vol. 24, no. 4, pp. 927-933, Apr. 2006.

[80] B. Braem, B. Latre, I. Moerman, C. Blondia, E. Reusens, W. Joseph, L. Martens, and P. Demeester, "The need for copperation and relaying in short-rango high path loss sensor networks," in *Proc. Int. Conf. Seonser Technol. Appl. (SENSORCOMM) 2007*, Valencia, Spain, Oct. 2007.

[81] M. O. Hasna and M.-S. Alouini, "End-toend performance of transmission systems with relays over Rayleigh-faing channels," *IEEE Trans. Wireless Commun.*, vol. 2, no. 6, pp. 1126-1131, Nov. 2003.

[82] H. Rosenthal and J. Binia, "On the epsilon entropy of mixed random variables," *IEEE Trans. Inf. Theory*, vol. 34, no. 5, pp. 1110-1114, Sep. 1988.

[83] D. Li, "Performance analysis of uplink cognitive cellular networks with opportunistic scheduling," *IEEE Commun. Lett.*, vol. 14, no. 9, pp. 827-829, Sep. 2010.

[84] K. Tourki, K. A. Qaraqe, and M.-S. Alouni, "Outage analysis for underlay cognitive networks using incremental regenerative relaying," *IEEE Trans. Veh. Technol.*, vol. 62, no. 2, pp. 721-734, Feb. 2013.

Korean Abstract

중계 기술은 차세대 무선통신 시스템에서 요구되는 데이터 전송률 및 신뢰도를 비롯한 서비스품질 향상 달성을 위한 가장 중요한 기술 중의 하나이다. 중계 기술의 장점으로 인해 많은 관심을 받고 폭넓게 연구되어 왔으며, IEEE 802.16j 등의 통신 표준에 반영되기도 하였다. 그러나 더 효율적인 다중 홉 포로토콜 설계 및 무선 인지 네트워크에의 응용 등의 분야에 연구가 미흡한 실정이다.

본 논문에서는 중계 기술 연구에 있어 다음과 같은 결과를 보인다. 첫째, 다중 홉 네트워크를 위한 새로운 복호후재전송 프로토콜을 제안한다. 제안한 프로토콜은 불능 확률 최소화를 위해 몇몇 단말기들이 동일은 채널을 사용한다. 이를 위해, 제안한 프로토콜의 불능 확률을 닫힌 형태로 유도하며, 불능 확률 최소화를 위한 최적화 기법을 제안한다. 최적화 기법은 전송 전력 할당, 홉 수 및 시간 분할 수 선택 방법을 포함한다. 또한, 수학적 기법을 이용하여 홉 수 및 시간 분할 수 선택 방법의 복잡도를 줄이는 방법을 제안한다. 모의실험을 통해 얻어진 불능 확률이 유도한 값과 일치함을 확인한다. 또한 제안된 다중 홉 통신 프로토콜이 기존 다중 홉 통신 프로토콜 및 직접 전송 프로토콜보다 낮은 불능 확률을 달정함을 보이며, 특히 신호대잡음비가 낮거나 감쇄 경로 지수가 클 수록 효과적임을 보인다. 또한 홉 수 및 시간 불할 수 선택과정의 복잡도를 줄여도 거의 동일한 불능 확률을 달성함을 확인한다.

둘째, 스펙트럼 공유 무선 인지 네트워크의 성능을 조사한다. 일차 네트워크 및

이차 네크워크의 관계에 따라 두 네트워크가 동기화 된 시나리오, 두 네트워크의 프레임 길이는 동일하지만 동기화 되지 않은 시나리오 및 프레임 길이가 다른 시나리오의 세 가지를 고려한다. 각 시나리오에 대하여 이차 네트워크의 전송 전력 할당 및 중계기 선택 기법을 제안하고, 불능 확률을 유도한다. 모의실험을 통해 얻어진 불능 확률이 유도한 값과 일치함을 확인한다. 일차 네트워크로의 간섭으로 인해 전송 전력이 제약을 받기 때문에 불능 확률 마루가 생김을 확인할 수 있으며, 각 시나리오의 성능이 불능 확률 곡선의 기울기는 비슷하지만 불능 확률 마루가 다름을 확인할 수 있다. 또한 동기화, 중계기 수, 일차네트워크의 송신 신호대잡음비, 간섭 문턱값, 간섭 허용 확률 문턱값 및 일차네트워크와 이차네트워크 간 거리가 불능 확률에 미치는 영향을 확인한다.

주요어: 중계 기술, 다중 홉 네트워크, 무선 인지 네트워크, 스펙트럼 공유, 불능 확률, 최적화 기법, 무선 통신.

학번: 2008-30241